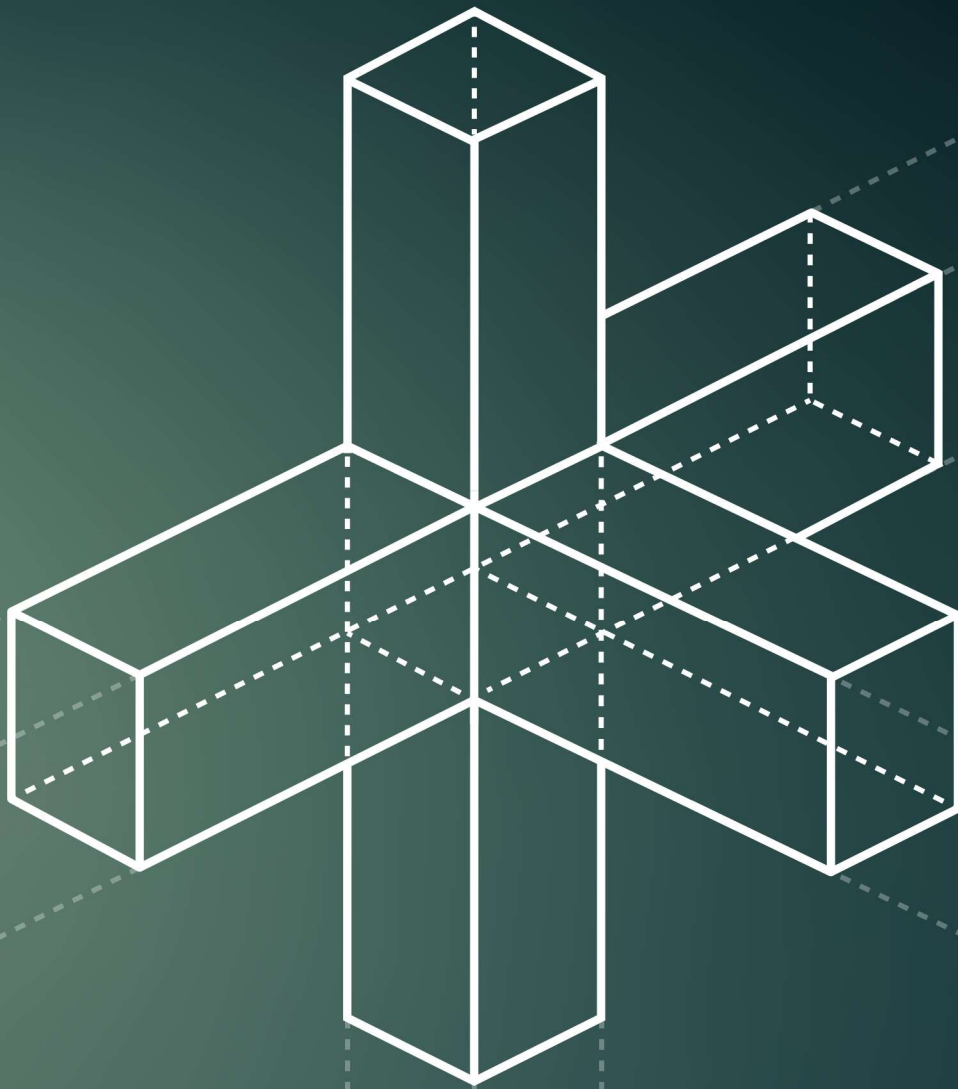


MASTER THESIS

Timber Joints

A parametric study on the dimensional interaction
between joints and members in timber frame structures



Jornt Bieze

 **TU Delft**

 **LÜNING**
Ingenieurs in houtconstructies

Timber Joints

A parametric study on the dimensional interaction
between joints and members in timber frame structures

by

Jornt Bieze

in partial fulfillment of the requirements for the degree of Master of Science in

Civil Engineering

with a specialisation in Building Engineering - Structural Design

at the Delft University of Technology,
to be defended publicly on Thursday January 12, 2023 at 16:00.

| | | |
|-------------------|--------------------------------|----------------------|
| Student number: | 4740718 | |
| Project duration: | November, 2021 – January, 2023 | |
| Thesis committee: | Dr. ir. G.J.P. Ravenhorst, | TU Delft, Chair |
| | Ass. Prof. Dr. M.A. Popescu, | TU Delft, Supervisor |
| | Ir. R. Crielaard, | TU Delft, Supervisor |
| | Ir. M.P. Felicita, | TU Delft, Supervisor |
| | Ir. J. Lauppe, | Lüning, Supervisor |

An electronic version of this thesis is available at <http://repository.tudelft.nl/>.

Abstract

The demand for timber structures has significantly increased over the last decades due to this material's potential to reduce the environmental footprint of a structure. In timber structures, a widely used structural system is a frame structure. In general, frame structures consist of columns, beams, and stability members, such as bracing or shear walls, placed on a regular grid to form a load bearing structure. To complete a structural system, joints are necessary to connect the different types of members.

The importance of joints in timber structures is strongly emphasized in the existing literature (Blaß & Sandhaas, 2017; McLain, 1998). In the current building design industry, the design of joints mostly takes place in a relatively late phase of the project. In this phase, the general global design decisions have already been made, and the costs of changes are high. Considering the design consequences of a joint in an early phase of the design process may prevent significant changes in a later design phase, thereby decreasing the risk of cost underestimation and deviations from the original design. The aim of this project is to provide insight into whether the cross-sectional sizes of the member are dictated by the dimensional sizes of the laterally loaded dowel-type connection or the strength and stiffness requirements of the member itself. The results of this study may help structural engineers to make well-argued decisions in determining the cross-section of timber members in a frame structure that take into account the effect of joints in the early design phase. Moreover, the insight gained in this study adds knowledge to the existing literature on timber structures, offering a new perspective on the importance of joints in timber structures. The following research question guides this study:

"What is the dimensional interaction between laterally loaded dowel-type connections and structural members in timber frame structures?"

In order to answer this question, a parametric study is performed. The parameters in this study represent the global frame structure and the laterally loaded dowel-type connections. Together, these parameters form a parametric model that lays the foundation for the tool that is constructed in this study. This tool is built in order to generate a number of unique configurations that fulfill the design verification provided by the Eurocode for the selected joint and member in the frame structure. Using the tool, two analyses are performed. In analysis 1, the effect of different distances between the secondary beams is examined. In analysis 2, the effect of different grid sizes of the column in the frame structure is studied. In both analyses, two member sizes are first selected based on the criteria 'lowest cross-sectional area' (LCA) and 'lowest height beam' (LHB). These two member sizes form the starting point for generating different configurations of laterally loaded dowel-type connections. In both analyses, the connection is separated into two steel parts, parts A and B. Moreover, two joints are analysed - the joint between a primary beam and a column (joint 1) and the joint between two secondary beams and a primary beam (joint 2).

In this research project, three factors are found to contribute to the largest reduction in the number of unique configurations for all constructed cases examined in analysis 1 and 2. These three factors are small column widths combined with high shear forces, the effect of a 'compact' member, and the effect of 'brittle' failure mechanisms on the LCA-members, which was selected as a design constraint in this study. These factors may be relevant for engineers to take into account when designing the structural members.

However, in this study, no constructed case is found in which the member needs to be redesigned in order to fit the connection. With regard to this study's main research question, this means that one can conclude that the dimensional size of the structural member is dictated by the strength and stiffness requirements of the member itself. Before the start of this study, one of the imagined outcomes was the identification of certain turning points between the cross-sectional size being dictated by the member or being dictated by the connection, forcing the engineer to redesign the member. The fact that these

turning points do not appear in the data adds a new perspective to the existing literature on timber structures regarding the importance of joints in these structures. Important to note is that, although a large number of parameters was incorporated into this study, not all potentially relevant parameters were taken into account. When incorporating factors such as the horizontal forces in the connection, the effect of shrinkage and swelling, the level of difficulty in terms of assembling the joints on site, and adjustments to guarantee a certain level of fire resistance, certain turning points in the dimensional interaction between joints and members may be found. Ultimately, the findings of this study are specific to timber frame structures that only transfer vertical loads and to the selected parameters.

Finally, beyond allowing for the dimensional interaction between joints and members to be studied, the tool constructed in this study is also valuable to practical engineering. The large amount of data that is generated by the tool allows the engineer to explore the different possible configurations in the process of designing joints. By connecting the output of the tool to the Design Explorer interface, the engineer has the opportunity to search through all the individual characteristics or a specific range and examine different possible connections in an efficient manner. One of the main contributions of this research project, therefore, lies in the tool itself.

Acknowledgements

This thesis on the dimensional interaction between joints and members in timber frame structures is the final step in my educational journey. This journey has been long, yet unforgettable. Ten years ago, I started with an HBO bachelor in Built Environment at the Hanze University of Applied Science in Groningen. Subsequently, I moved to Delft and started with a bridging program, which eventually led me to my final destination: graduating with a master's degree in Civil Engineering. Over the past years, my interest in timber has grown strongly, and I will definitely continue with designing structures with this beautiful material in my future career. I would like to acknowledge and express my gratitude to the people who have supported me in the process of writing my thesis.

First, I would like to thank Lüning for giving me the opportunity to perform this research project. Many thanks to all my colleagues at Lüning, who were always open to having discussions and providing feedback. Special thanks to Joost Lauppe, for the time and effort to supervise my work. I enjoyed all the useful talks we had and would like to thank you for helping me to stay on track and put things into perspective.

I would like to thank my graduation committee, Geert Ravenhorst, Marinana Popescu, Roy Crielaard, and Maria Felicita for all the feedback and critical questions during our meetings. You shared valuable knowledge about the design of joints in timber structures and the potential of parametric design and stimulated me to incorporate the point of view of the engineer into this research project.

Thanks to my fellow students at TU Delft for always being available for questions and for the fun moments in working together in different projects during the master's program.

I would like to thank my parents for enabling me to study in Delft and for the infinite support you gave in order to achieve this milestone.

Finally, I would like to thank my girlfriend, Luka, for always being there to keep me motivated in hard times, for inspiring me, for making me laugh, and for the enormous support in reading the different sections of my report over and over.

*Jornt Bieze
Maarssen, December 2022*

Contents

| | |
|---|------------|
| Abstract | iii |
| Acknowledgements | v |
| 1 Introduction | 1 |
| 1.1 Research Context | 1 |
| 1.2 Problem Definition | 3 |
| 1.3 Objective | 3 |
| 1.4 Research Questions and Outline | 4 |
| 1.5 Methodology | 5 |
| 1.6 Scope | 5 |
| 2 Literature Review | 7 |
| 2.1 Wood and Timber. | 7 |
| 2.2 Engineered Wood Products | 9 |
| 2.2.1 Glued Laminated Timber. | 9 |
| 2.2.2 Laminated Veneer Lumber. | 10 |
| 2.2.3 EWP Selection | 11 |
| 2.2.4 Cross Laminated Timber. | 11 |
| 2.3 Joints and Connections | 12 |
| 2.3.1 Applied Connections in Practice | 12 |
| 2.3.2 Load Transfer Connections | 20 |
| 2.3.3 Fastener Types | 21 |
| 2.4 The Components of Mechanical Connections | 22 |
| 2.4.1 Load Carrying Capacity of the Fasteners | 22 |
| 2.4.2 Rope Effect | 22 |
| 2.4.3 Embedment Strength. | 23 |
| 2.4.4 Failure Mechanisms | 24 |
| 2.4.5 Ductile Behavior | 28 |
| 2.5 Conclusions. | 29 |
| 3 Parametric Model | 31 |
| 3.1 Design Parameters | 31 |
| 3.1.1 Frame structure. | 31 |
| 3.1.2 Joints | 33 |
| 3.1.3 Reduction Parameters | 35 |
| 3.1.4 Members | 36 |
| 3.2 System Loads | 37 |
| 3.2.1 Vertical Loads. | 37 |
| 3.2.2 Load Combination | 38 |
| 3.2.3 Additional Load Columns. | 38 |
| 3.3 Design Constraints | 38 |
| 3.3.1 Verification Members | 39 |
| 3.3.2 Verification Connections | 39 |
| 3.4 Constructed Cases | 39 |
| 3.4.1 Grid Dimensions Columns | 40 |
| 3.4.2 Analysis 1: Variable Distance Between Secondary Beams | 41 |
| 3.4.3 Analysis 2: Different Grid Sizes Columns | 41 |
| 3.5 Design Assumptions | 42 |
| 3.6 Conclusions. | 43 |

| | | |
|----------|--|------------|
| 4 | Development Tool | 45 |
| 4.1 | Set-up Tool | 45 |
| 4.2 | Workflow | 46 |
| 4.3 | Development Components. | 48 |
| 4.3.1 | Component III - Layout Fastener Group. | 48 |
| 4.3.2 | Component V - Forces Fasteners | 49 |
| 4.3.3 | Component VI - Load Capacity Steel Part A | 51 |
| 4.3.4 | Component VII - Load Capacity Steel Part B | 51 |
| 4.4 | Brute Force Method | 52 |
| 4.5 | Output Tool | 52 |
| 4.6 | Design Implications. | 54 |
| 4.6.1 | Visualization Output Tool. | 54 |
| 4.6.2 | Different Scenarios in Joint Design Phase | 56 |
| 4.7 | Conclusions. | 59 |
| 5 | Results and Discussion | 61 |
| 5.1 | Results and Observations | 61 |
| 5.1.1 | Graph Interpretation Corresponding Parameters | 61 |
| 5.2 | Analysis 1: Variable Distances Between Secondary Beams | 62 |
| 5.2.1 | Graphs 1a: Corresponding Parameters | 62 |
| 5.2.2 | Graph 1b: Number of Unique Configurations | 69 |
| 5.2.3 | Graphs 1c: Steel Mass Ratio Unique Configurations. | 70 |
| 5.3 | Analysis 2: Different Grid Sizes Columns | 74 |
| 5.3.1 | Graphs 2a: Corresponding Parameters | 74 |
| 5.3.2 | Graph 2b: Number of Unique Configurations | 81 |
| 5.3.3 | Graphs 2c: Mass Ratio Unique Configurations | 82 |
| 5.4 | Discussion | 85 |
| 5.4.1 | Corresponding parameters. | 85 |
| 5.4.2 | Number of Unique Configurations Steel Part A and B | 90 |
| 5.4.3 | Steel Mass Ratio Steel Part A and B | 91 |
| 6 | Conclusions and Recommendations | 93 |
| 6.1 | Conclusions. | 93 |
| 6.2 | Recommendations | 95 |
| | References | 97 |
| A | Appendix Verification Members | 101 |
| B | Appendix Verification Connections | 105 |
| C | Appendix CLT-verification | 109 |
| C.1 | Part 1: Forces and Deflection | 109 |
| C.2 | Part 2: Vibration | 121 |
| D | Appendix Minimum Values of Spacing and Edge and End Distances | 123 |
| E | Appendix Failure Mechanisms Steel-to-timber Connections | 125 |
| F | Appendix Database Tool | 129 |

Introduction

1.1. Research Context

Timber as Construction Material

The Intergovernmental Panel on Climate Change (IPCC) published the sixth climate report in the summer of 2021. In this report, the panel advised to reduce greenhouse gas emission rapidly in order to prevent a sea level rise of 44 to 76 centimeters by 2100 (Masson-Delmotte et al., 2021). Carbon dioxide (CO₂) is one of the greenhouse gases that drive climate change. The building industry has a significant contribution of 38% of the total CO₂ emission (United Nations Environment Programme & Construction, 2020). The materials used as structural material in the building industry, such as steel, reinforced concrete, and wood, show significant differences in the amount of CO₂ that is released during production¹. Soft wood from sustainable sources produces approximately 5 times less CO_{2;eq} per m³ compared to reinforced concrete and approximately 138 times less CO_{2;eq} per m³ than steel (van der Lugt, P., 2020). In these comparisons, the effect of locking the CO₂ temporarily into the timber products during their useful lives is not considered. Considering these observations, using timber as structural material in the building industry holds the potential to reduce greenhouse gas emission in the future. Herein lies the main reason why this research project focuses on timber structures for buildings.

Timber Frame Structure

A frame structure is a widely used structural system in timber constructions. This system is characterized by extensive design freedom in the interior and the facade, since the enclosing walls and structural frame are independent of each other (Kolb, 2008). Frame structures consist of columns, beams, and stability elements, such as bracing or shear walls, placed on a regular grid to form a load bearing structure. This so-called primary structure supports the floors, which form the secondary structure. Different types of floors are suitable, such as individual joists, prefabricated elements, or solid panels. Figure 1.1 illustrates a typical timber frame structure.

In general, a frame structure is a collection of different structural members, as discussed above. In terms of load transfers, a frame structure needs to transfer vertical loads (e.g. self weight, permanent load, and imposed load) and horizontal loads (e.g. wind load and earthquake load). The vertical loads are transferred from the floor elements, beams, and columns into the foundation. The horizontal forces are mainly transferred from the floor elements, which include diaphragm action or horizontal bracing, into the vertical stability elements, such as bracing and shear walls. To narrow down the research, this project will focus the vertical load transfer of a frame system. The examined frame structure consists of primary beams, secondary beams, and columns that are loaded solely with vertical loads.

¹Green House Gas (GHG) emission of a product during manufacturing ('cradle to gate')

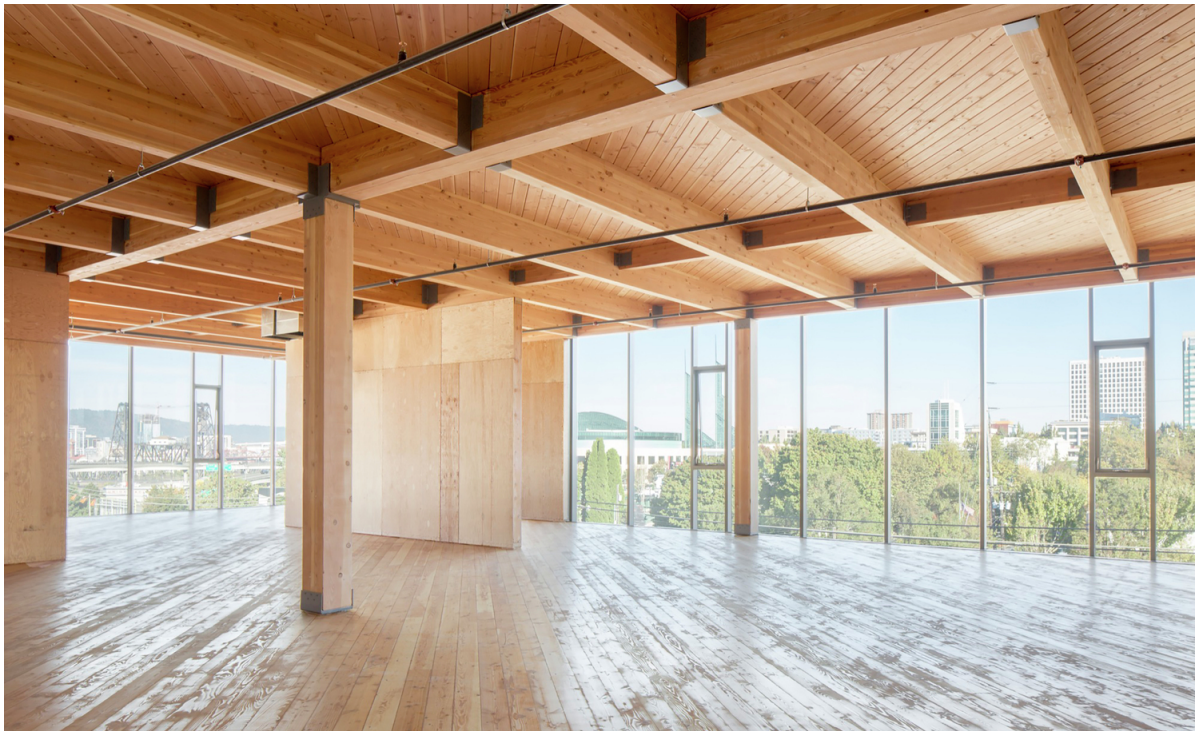


Figure 1.1: Timber frame structure

Timber Joints

To complete a structural system, joints are necessary to connect the different types of members. The joints transfer the inner forces caused by external action from one member to another (Thelandersson & Larsen, 2003). In timber structures, the main joints are categorized in carpentry joints, glued joints, and joints that include different metal fasteners (Blaß & Sandhaas, 2017).

Carpentry joints have been used since the start of traditional joinery and have been developed over the centuries. There is a large number of historical timber buildings that consists of these types of joints. The forces in the joints are mainly transmitted by contact which creates internal compression and shear surface forces (Blaß & Sandhaas, 2017).

Glued joints are not often applied in timber structures. The glued joint that is used more frequently in frames is the large finger joint (Blass et al., 1995b). This joint requires a controlled environment in production, since many glues are affected by moisture content and temperature differences (Borgström, 2016).

Based on the type of force transmission between the members of a structure, the traditional metal fasteners can be divided into two main groups. The first group is formed by dowel-type fasteners, which include nails, bolts, screws, and dowels. In dowel-type fasteners, bending and tensile stresses occur in the fasteners and embedment and shear stresses occur in the timber along the shank. The second group includes 'surface-type' fasteners, in which the force is transmitted on the surface area of the member. Fasteners such as split rings, toothed-plates connectors, and punched metal plates are examples of surface-type fasteners (Blaß & Sandhaas, 2017).

The joints that include different metal fasteners are the most commonly applied joint in timber structures (Borgström, 2016). In contrast to the other joint types, metal fasteners, such as bolts and dowels, improve the disassembly characteristics of building structures. Moreover, applying metal fasteners increases the ductile behaviour of the joints, which enlarges the safety of the structure in case of failure (Borgström, 2016). Additionally, with pre-drilled holes in the timber members and metal fasteners such as bolts and dowels, the complexity and the time needed to assemble the members decreases. Finally, the current European building standard code for timber structures, Eurocode 5, is mainly focused on metal fasteners (NEN-EN-1995-1-1, 2004). Within the category of metal fasteners, screws, dowels, and bolts are the most commonly used fastener types, according to a questionnaire filled out by 412 respondents from 28 European countries and five non-European countries. The majority of the

respondents were structural engineers working at an engineering firm, followed by engineers working in academia and the construction industry. (Stepinac et al., 2018). Considering these findings and the limited scope of this research project, these types of mechanical dowel-type fasteners will be focused on. Still, various configurations of this connection type can be constructed, such as the shape of the steel-to-timber connection, the type of fastener, the steel quality of the fastener type, the size of the fasteners, and the number of fasteners.

1.2. Problem Definition

The importance of joints in timber structures is strongly emphasized in the existing literature (Blaß & Sandhaas, 2017; Jockwer et al., 2021). McLain (1998) demonstrated the importance of joints by stating that "a structure is a constructed assembly of joints separated by members". Joints are critical factors in timber structures, since they determine the overall strength and stiffness of the global structure (Ottensmeyer et al., 2021). The dimensional sizes of the integrated connection in a joint may even determine the cross-section dimensions of the members rather than the strength and stiffness requirements of the member itself (Claisse & Davis, 1998; Gečys & Daniūnas, 2017).

The following characteristics of timber support the idea that having an adequate section size for joints in timber structure is important. First, timber is an anisotropic material. This means that the characteristics of each fiber direction, such as strength, shrinkage, and swelling, are different. These differences lead to relatively low tensile and compressive strength perpendicular to the grain direction of the element. Second, large spacing between the fasteners themselves and the distance between the fasteners and the edge and end of the beam are required to avoid splitting of the member (Thelandersson & Larsen, 2003). Third, the effect of swelling and shrinkage caused by varying moisture levels may lead to crack forming between the member and the connection components. These cracks may lead to strength and stiffness reduction of the member and the joint (Sjödín & Johansson, 2007).

Moreover, the importance of joints in timber structures has been reflected in a analysis of structural failures in timber structures examined by Frühwald Hansson (2011). This research shows that joints were involved in 23 percent of cases of failure in a study of 127 failures in timber structures. Out of these joint failures², 57 percent were dowel-type connections. However, as dowel-type connections are frequently used, this number may be biased. Still, this highlights the importance of carefully considering the connections within timber structures.

All of these aspects illustrate that joints are critical in the design of timber structures. In the current building design industry, the design of joints mostly takes place in a relatively late phase of the project. In this phase, the general global design decisions have already been made and the costs of changes are high. Considering the design consequences of a joint in an early phase of the design process may prevent significant changes in a later design phase, thereby decreasing the risk of cost underestimation and deviations from the original design.

1.3. Objective

This research project focuses on the dimensional interaction between the joints and the members in different frame structures. The main objective of this research project is to determine the influences of laterally loaded dowel-type connections on the cross-section of the members in different frame structures. In order to reach this goal, a parametric study is performed. The results of this study can provide additional knowledge to the existing literature that emphasizes the importance of joints in timber structures. In particular, this study can provide insight into whether the cross-sectional sizes of the members are dictated by the dimensional size of the laterally loaded dowel-type connection or the strength and stiffness requirements of the member itself. Additionally, the results can help structural engineers to make well-argued decisions in determining the cross-section of timber members in a frame structure that take into account the effect of joints in the early design phase.

²No distinction is made between strength or stiffness failures

Sub-Objectives

In order to achieve the main objective of this research project, the following sub-objectives are set:

- Gaining a deeper understanding of the theoretical fundamentals of mechanical connections in timber structures.
- Developing a parametric model of a timber frame structure that provides input for a tool that helps to analyse the dimensional interaction between the joints and the members in different frame structures.
- Constructing a tool that designs, verifies, and visualizes different configurations of laterally loaded dowel-type connections based on different frame structures. This tool allows one to study the influences of laterally loaded dowel-type connections on the cross-section of the members in different frame structures in a parametric manner.

1.4. Research Questions and Outline

In order to reach the goals that have been set out in the previous chapter, a set of sub-research questions is formulated. Each chapter or set of chapters provides an answer to individual research questions which will provide sufficient insight to answer the following main research question.

"What is the dimensional interaction between laterally loaded dowel-type connections and structural members in timber frame structures?"

Part I - Literature Review

This part consist of a literature study on engineered wood products and mechanical connections. The main goal of this part is to collect sufficient information to determine the most suitable mechanical connection and engineered wood product to apply in the parametric study.

- *"What is the most suitable mechanical connection type and engineered wood product to apply on frame structures?"*
 - Chapter 2: Literature Review

Part II - Parametric Study

This part focus on the development of the parametric model for the frame structure and the tool that designed and verified different configurations of the connection.

- *"Which parameters and constraints will define the parametric model of the frame structure and the joints?"*
 - Chapter 3: Parametric Model and Constructed Cases
- *"How can the calculation of the structural members and connections be developed and integrated into the tool?"*
 - Chapter 4: Development Tool

Part III - Research Outcome

This part summarizes the findings of the research project and discuss relevant observations from the collected data.

- *"How do the different geometrical designs of a timber frame structure influence the configuration of a laterally loaded dowel-type connection?"*
 - Chapter 5: Results and Discussion
 - Chapter 6: Conclusions and Recommendations

1.5. Methodology

For each part a methodology has been defined that aims to provide the answer to the sub-questions.

Literature Review

In the literature review, engineered wood products are examined to provide sufficient insight to select the product for the structural members in the frame structure. Moreover, mechanical connections are studied to provide an indication of the availability in mechanical connections for different joints. In addition to that the characteristics related to loading capacity are analyzed for the different connections types. For the selected connection type the related components that determine the loading capacity are examined. These components are potential parameters that defines the parametric model of the investigated connection.

Development Tool

Once all the relevant information is collected from the literature reviews, the set-up of the tool is determined. The tool is divided into two parts, which is the analysis of the frame structure and the analysis of the joints. In this chapter the interaction and the workflow of the different parts are determined and software that suits the workflow are selected. Moreover, the key components that are integrated into the tool are outlined.

Parametric Model

The development of the tool and the set-up of the parametric model are running parallel, since the parametric model of the frame structure and the connection is part of the tool. In this chapter, the parameters defined in the literature review are reduced to decrease the complexity of the model. The output of the parametric model are different configurations of the connection that includes the type of fastener, the fastener quality, the diameter of the fastener, the position of the steel plate(s) and the thickness of the steel plate(s). For the purposes of this investigation, the design constraints are the member resistance in terms of strength and deflection and the connection resistance in terms of strength.

Constructed Cases

In order to collect sufficient data to analyse the dimensional interaction between laterally loaded dowel-type connections and structural members, different constructed cases for the frame structure are determined. These constructed cases consist of frame structures that includes different column grids and different distances between the secondary beams.

1.6. Scope

Scope limitations will help to narrow down the research focus of this master's thesis. The following limitations are set to the research scope.

Fire Resistance

Examining the fire limit state is beyond the scope of this research project due to time limits. Integrating fire resistance into the tool may be a valuable direction for future research.

Floor Panels

The floor panels are set to Cross Laminated Timber (CLT) panels in this research project. The dimensional size (height) of the floor panels is determined according to the maximum span of the constructed cases. This approach is not the most efficient way of designing the floor elements, however the core of this research project is to analyse the effect of differences in the geometry of the frame structure rather than the influences of different loads caused by different panel sizes.

Lateral-Torsional Buckling

Slender bending beams that are mainly subjected to bending and have a large height-width ratio are in general sensitive to lateral-torsional buckling. In this research project it is assumed that the CLT

floor panels provide lateral support to the secondary beams and the secondary beams provide lateral support to the primary beams.

Floor Vibration

Besides that floor panels transfer the external loading to the remaining structural members, the floors are subjected to user activities. These activities can cause vibrations, which can lead to uncomfortable experience for the users. CLT panels are in general more sensitive to human induced vibrations due to its low density and stiffness. The magnitude of vibrations are primarily determined by the mass, span, and width of the floor panel. In order to simplify the scope of this investigation, the design of the floor panel is based on the simplified analytical method described in the "Vibration Design of Floors" guideline written by HIVOSS (Human Induced Vibrations of Steel Structures).

2

Literature Review

This chapter consists of a literature study on engineered wood products and mechanical connections. In this chapter, the focus lies on reviewing the existing literature on mechanical connections and engineered wood products applied in practice. In this literature review, the characteristics in terms of strength and stiffness of the different engineered wood products and mechanical connections are examined. The main goal of this chapter is to collect sufficient information to determine the most suitable mechanical connection and engineered wood product to apply in the parametric study. Overall, this chapter focuses on answering the following research question:

- "What is the most suitable mechanical connection type and engineered wood product to apply on frame structures?"

2.1. Wood and Timber

Wood is a natural material and a collective term for a large number of species worldwide. In general, wood can be divided into two groups, softwood and hardwood. The division between these two groups is primarily made based on their physical structures. This research project does not zoom in on the explanation of wood at a microscopic level, as this is not required for a structural design.

Wood is anisotropic, which means that it has different properties in different directions. The longitudinal, radial, and tangential directions are the three main directions, as shown in figure 2.1. Due to the different properties in different directions, it is essential to keep track of the loading direction. The properties in radial and tangential directions are often assumed equally and are defined as perpendicular-to-grain (σ_{90} or σ_{\perp}). The axial direction is defined as parallel-to-grain (σ_0 or σ_{\parallel}) and is the stronger axis in terms of strength and stiffness due to the tube structure of wood (Borgström, 2016).

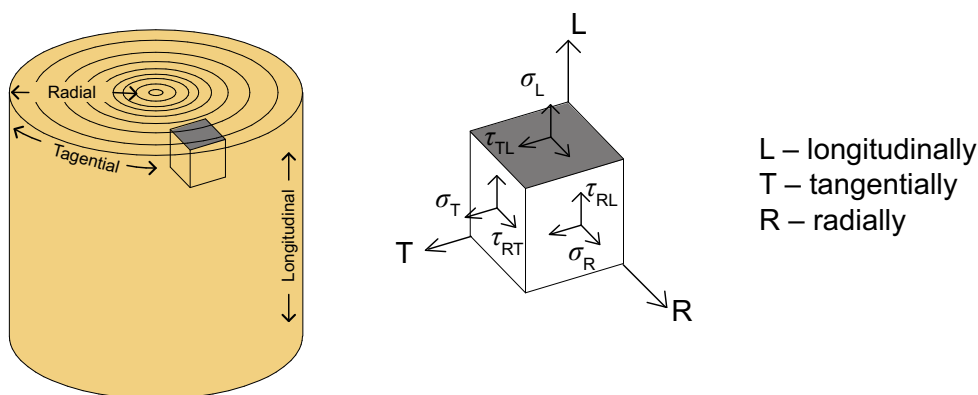


Figure 2.1: Definition of normal- (□) and shear- (□) stresses in different directions in wood (Borgström, 2016).

Wood is hygroscopic, which means that the moisture content in the material constantly changes with the relative humidity of the surrounding environment. Moisture content (MC) is one of the main contributing factors that change the mechanical properties of wood. An increase in MC generally leads to a decrease in strength and stiffness and an increase in creep deformation and risk of fungal infection (Blaß & Sandhaas, 2017). Moreover, changes in MC cause shrinkage and swelling, which influence the size of wood. The moisture coefficient in expansion and contraction is different for each direction. The longitudinal shrinkage and swelling is significantly small compared to the tangential and radial direction. The shrinkage in tangential direction is approximately two times higher than the radial direction (Borgström, 2016). Figure 6.1 illustrates the shrinkage and swelling in percentages for the tangential and radial direction as a result of the moisture content differences between winter and summer indoors. The figure displays a movement of approximately 1.6% in tangential direction, assuming that the moisture content in wood changes by around 6% from summer to winter.

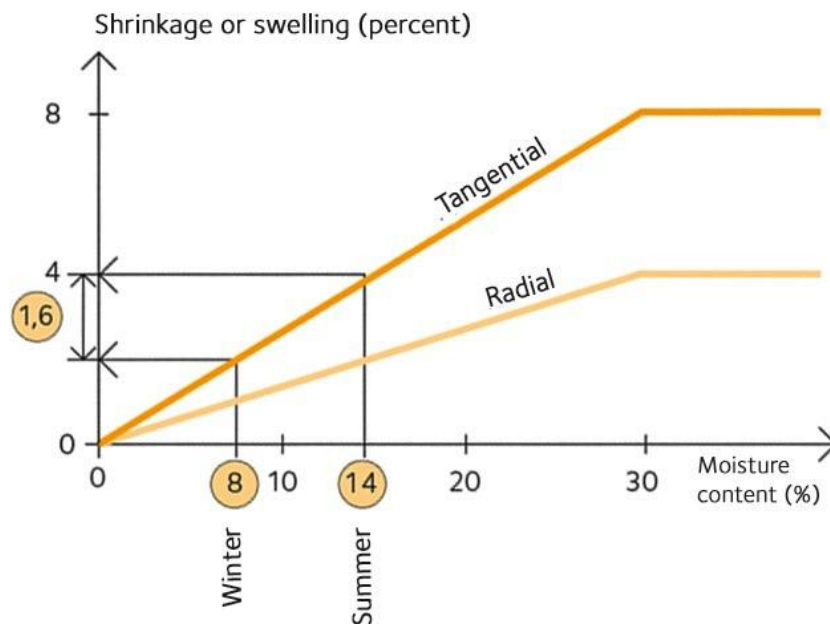


Figure 2.2: The wood's movement indoors over the year, from summer to winter (Swedish-Wood, n.d.)

Timber is wood that is manufactured to be used in structural applications. Timber has been applied for centuries as a building material in the construction industry. The natural characteristics of wood, such as knots, have a negative influence on the mechanical properties of timber. Visual or machine grading processes determine the strength class of sawn timber based on the size, number, shape, and location of the knots. Moreover, other imperfections, such as spiral grain and cracks, are grading criteria that are relevant in determining the strength class (Blaß & Sandhaas, 2017).

Another aspect that plays an important role in timber is an increase of deflection due to sustained loading over time. The tendency of a material to deform under sustained loading is called creep. In structures, the permanent load on the structure is most often the sustained loading under which creep will occur. External factors, such as temperature and moisture content, influence the magnitude of creep. These factors are covered by the use of the creep coefficient (k_{def}) that is included in NEN-EN-1995-1-1 (2004). The creep coefficient needs to be considered within the verification of deflection in the service limit state (SLS).

2.2. Engineered Wood Products

The sizes of sawn timber are limited due to the size of trees and the industrial processes. For instance, in Sweden, the maximum depth and length of sawn timber is 245 mm and 5.50 m (Borgström, 2016). In the last century, a wide variety of engineered wood products (EWPs) have been invented to achieve shapes and sizes that cannot be achieved with sawn timber. In general, EWPs are a composition of sawn timber pieces that are glued together and are oriented in one direction or in different directions in different layers. Constructing new compositions allows one to remove defects and create elements that are more homogeneous and reach higher mechanical properties in one specific direction or increase the mechanical properties in weak directions by applying specific processes.

In this research project, the frame structure consists of primary beams, secondary beams, and columns, as discussed in section 1.1. Glued Laminated Timber, commonly known as GLT or Glulam, and Laminated Veneer Lumber, also known as LVL, are the most commonly used EWPs to apply on frame structures. Another type of EWP is I-beams, also known as I-joists, which are build up with flanges of sawn timber or LVL and webs of board material, such as plywood or Oriented Strand Board (OSB). These light-frame elements are commonly used as secondary beams with a center to center distance of 300-600 mm in combination with plywood or OSB panels. Figure 2.3 illustrates the composition of the three different EWPs.

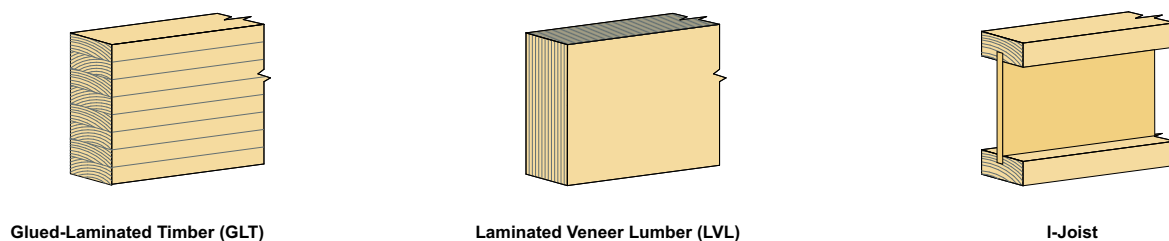


Figure 2.3: Timber Engineered Products

2.2.1. Glued Laminated Timber

Glued Laminated Timber (GLT) consists of timber boards, also known as lamellae, with a thickness of approximately 40-50 mm. In order to extend the length of the lamellae, the boards are finger-jointed together (Thelandersson & Larsen, 2003). All the individual lamellae with the grain in longitudinal direction are glued together over the entire contact surface with adhesives. The adhesives harden under a certain pressure and in a specified temperature. Figure 2.4 demonstrates the entire manufacturing process of GLT. The width of regular glued laminated timber is limited by the width of sawn timber. In order to extend the standard width, the timber pieces are glued in horizontal direction, which is called block-glued glulam. The application and timber species used for block-glued glulam are equal to the production of regular glulam (Blaß & Sandhaas, 2017).

The composition of the beams can be homogeneous (h) or combined (c). All the lamellae in the homogeneous compositions contain the same strength quality, whereas the combined composition matches with the design stress levels in the beam with higher strength quality in the outer lamellae (Borgström, 2016). Weak spots, such as knots, have less effect on the strength and stiffness of GLT. This can be explained in terms of the smearing-out-effect. Since the sawn timber is cut into smaller pieces, the low-strength defects are more uniformly distributed over the entire beam (Thelandersson & Larsen, 2003). Moreover, each defect is less important, since the lamellae above and below consist of clear wood (without defects) (Blaß & Sandhaas, 2017). This process of constructing beams limits the variability in strength, which results in higher mechanical properties of the GLTs compared to sawn timber.

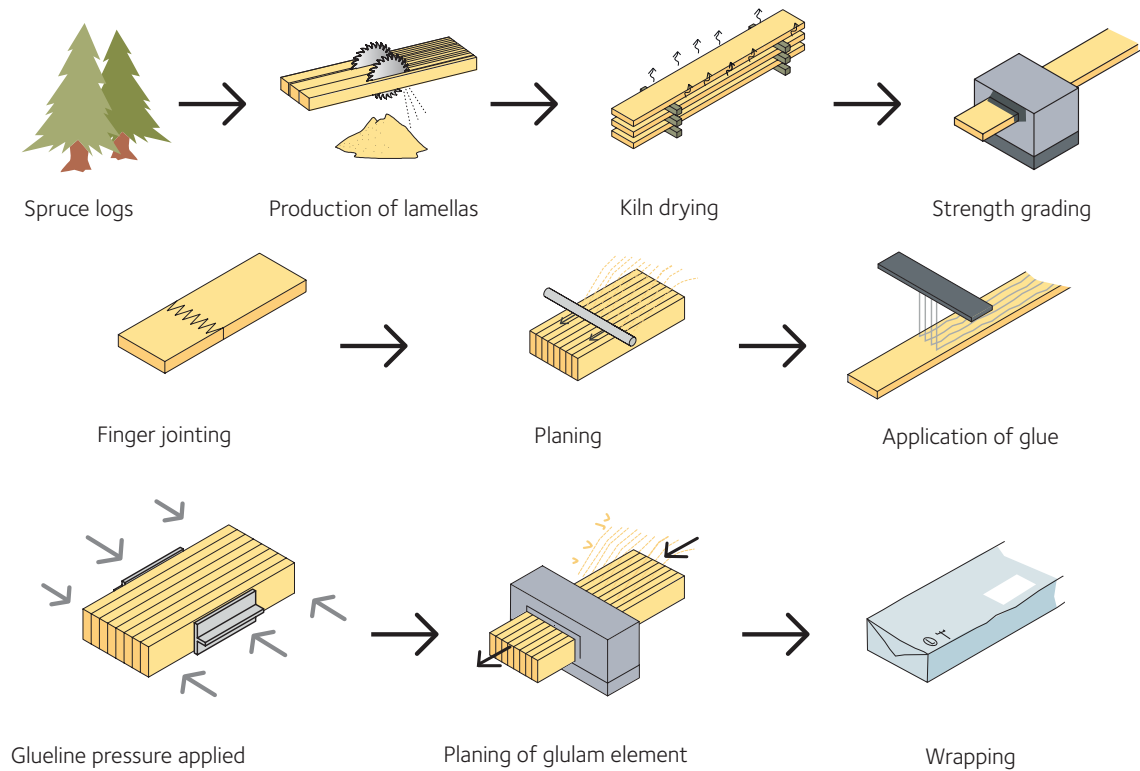


Figure 2.4: Manufacturing process for glued laminated beams (Borgström, 2016)

2.2.2. Laminated Veneer Lumber

Besides laminating boards, veneering is another efficient manner for processing logs to be used as input for timber products. Veneers are thin layers of wood, approximately 2-4 mm. The logs are debarked and steamed in hot water before being rotary peeled. After peeling, the veneers are dried to the target moisture content and often strength graded before being used as EWP (Borgström, 2016). Laminated Veneer Lumber (LVL) consists of multiple veneer sheets glued together to form thick panels. Figure 2.5 illustrates the entire manufacturing process of LVL products by Metsä wood.

The direction of the grains depends on the intended use of the element. In general, the grains for beam elements are placed in longitudinal direction and for panels the layers are placed crosswise. Similar to the production of GLT, this process produces elements with higher reliability and lower variability through elimination and distribution of defects. Moreover, the standard width of elements is limited to 90 mm, although multiple elements can be glued together up to 400 mm (Borgström, 2016).

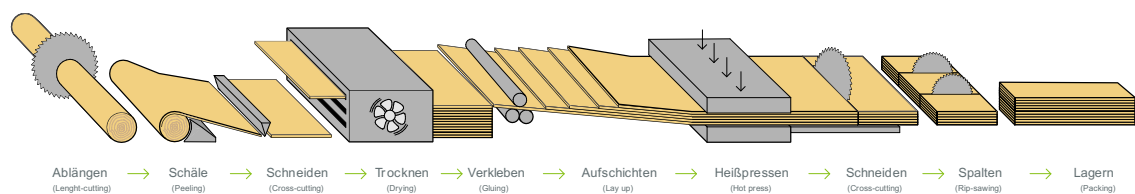


Figure 2.5: Manufacturing process for Laminated Veneer Lumber (Metsä-Wood, 2016)

2.2.3. EWP Selection

I-joint demonstrates to be a suitable alternative for sawn timber in terms of saving material. This product is commonly used for secondary beams and is limited for larger structures, as discussed. Moreover, the specific composition of this product limits the possibility to apply all types of connections. For instance, applying a slotted-in steel plate connection to this product is unfeasible.

GLT and LVL both have higher mechanical properties than sawn timber due to the elimination of defects. Moreover, the manufacturing process allows one to produce cross-sectional sizes that are significantly larger than those for sawn timber. When considering the width of the members, GLT produces larger standard widths compared to LVL. In order to produce a member with equal widths, LVL needs additional processes (e.g. gluing multiple lamellae) to construct the member. Moreover, GLT is already often used in frame structures, such as Palazzo Meridia, Treet, and Circl Pavilion of ABN AMRO. Based on these observations, in this research project, Glued Laminated Timber is selected as EWP for all structural members of the frame structure. Table 2.1 illustrates the mechanical properties for some commonly used homogeneous GLT classes according to NEN-EN-14080 (2013).

| Property | Symbol | GL24h | GL28h | GL30h |
|------------------------|-----------------|-------|-------|-------|
| Bending strength | $f_{m,g,k}$ | 24 | 28 | 30 |
| Tensile strength | $f_{t,0,g,k}$ | 19.2 | 22.3 | 24 |
| | $f_{t,90,g,k}$ | 0.5 | 0.5 | 0.5 |
| Compression strength | $f_{c,0,g,k}$ | 24 | 28 | 30 |
| | $f_{c,90,k}$ | 2.5 | 2.5 | 2.5 |
| Shear strength | $f_{v,g,k}$ | 3.5 | 3.5 | 3.5 |
| Rolling shear strength | $f_{r,g,k}$ | 1.2 | 1.2 | 1.2 |
| Modulus of elasticity | $E_{0,g,mean}$ | 11500 | 12600 | 13600 |
| | $E_{0,g,05}$ | 9600 | 10500 | 11300 |
| | $E_{90,g,mean}$ | 300 | 300 | 300 |
| | $E_{90,g,05}$ | 250 | 250 | 250 |
| Shear modulus | $G_{g,mean}$ | 650 | 650 | 650 |
| | $G_{g,05}$ | 540 | 540 | 540 |
| Rolling shear modulus | $G_{r,g,mean}$ | 65 | 65 | 65 |
| | $G_{r,g,05}$ | 54 | 54 | 54 |
| Density | $\rho_{g,k}$ | 385 | 425 | 430 |
| | $\rho_{g,mean}$ | 420 | 460 | 480 |

Table 2.1: Glued Laminated Timber mechanical properties (NEN-EN-14080, 2013)

2.2.4. Cross Laminated Timber

Cross Laminated Timber (CLT) is constructed in a similar way as GLT, although the lamellae in each layer are placed perpendicular to the layer above and below, as illustrated in figure 2.6. This way of stacking provides more strength and stiffness in both plate directions. In general, CLT panels are often used as load-bearing vertical walls and as horizontal floor diaphragms. As discussed in section 1.6, the floor panels are set to CLT-panels in this research project. The calculation of the applied CLT-panel in this research project can be found in Appendix C.

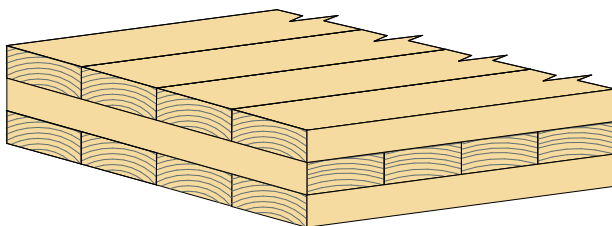


Figure 2.6: Composition Cross Laminated Timber

2.3. Joints and Connections

The definitions of joints and connections used in the context of this thesis are illustrated in figure 2.7. The joint defines the relation between the different structural elements, and the connection defines the components, such as fasteners, steel brackets, and slotted steel plates, that are required to connect the different structural elements. In this research project the focus lies on the mechanical dowel-type connection as discussed in section 1.1. Still, various of different type of connections and fasteners are available to examine.

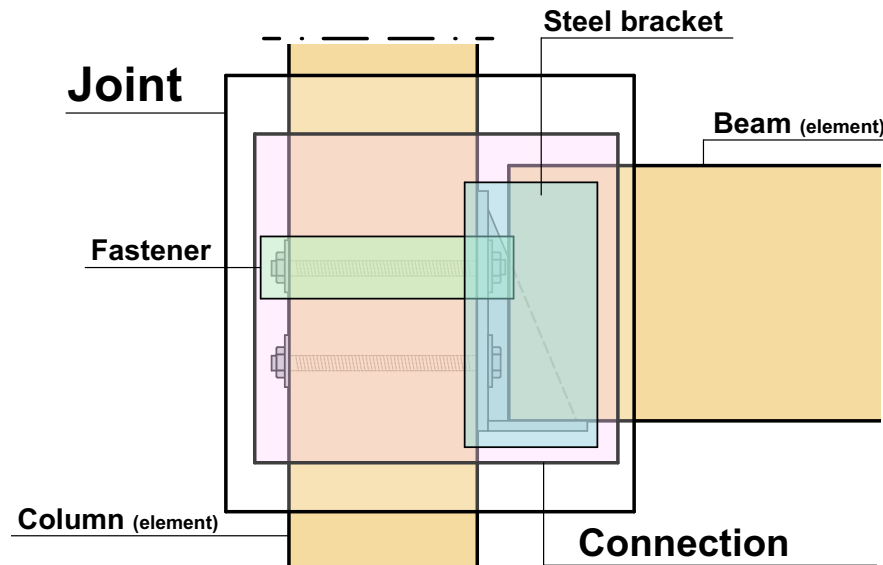


Figure 2.7: The definition of joint and connection

2.3.1. Applied Connections in Practice

The connections that are suitable for joints in frame structures will be examined in this section. Since frame structures include different types of elements, such as secondary beams, primary beams and columns, the joints will be categorized in beam to beam joints and beam to column joints. This categorization is illustrated in 2.8. In this paragraph the standard connections of glulam timber appliers such as Heko Spanten and DeGroot Vroomshoop are examined (DeGroot-Vroomshoop, n.d.; Heko-spanten, n.d.).

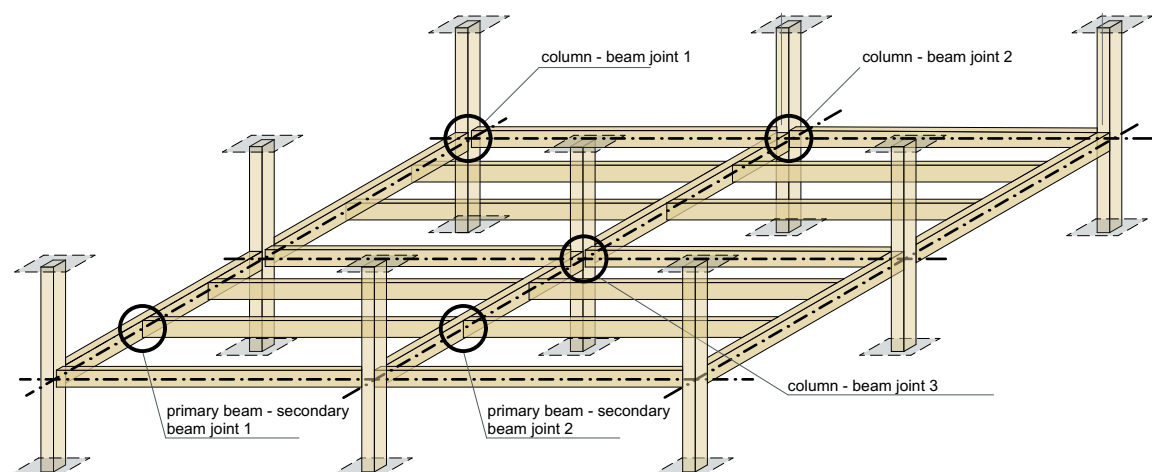


Figure 2.8: Joints in the global timber structures

Beam to beam joint - joint between a secondary and primary beam

Timber suppliers offers standard connections for joints between secondary beams and primary beams. Figure 2.9 illustrates some examples of standard details of DeGroot Vroomshoop.

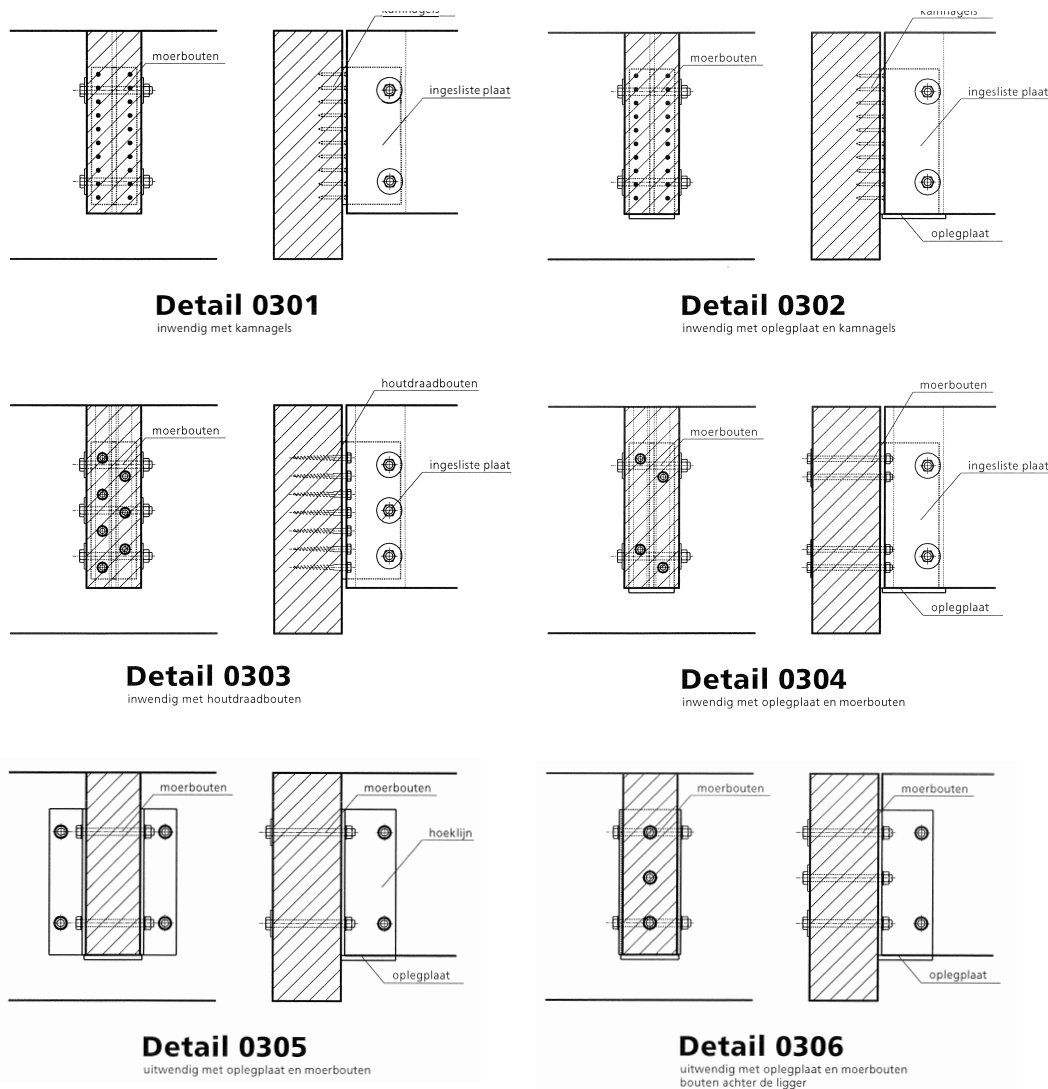


Figure 2.9: Standard details of a joint between column and beam retrieved from (DeGroot-Vroomshoop, n.d.).

In order to analyse the standard details properly, the joint is separated into two connection parts. The first connection part is the connection on the secondary beam. The second connection part is the connection on the primary beam. The connection on the secondary beam can be categorized into two groups based on their load transfer.

The first group, which consists the details 0301 and 0303 transfers their forces by lateral loading of the mechanical fasteners mounted at the beam. In these details the fastener type are bolts, however dowels can be applied as well (Blass et al., 1995b). The combination of the fasteners and the integrated slotted-in steel plate or the outer steel plates allows the transfer of the forces from the secondary beam to the primary beam.

The second group, which consists of the remaining standard details transfer the forces by direct contact between the secondary beam and the bearing steel plate. Additionally to the bearing steel plate the details still have a slotted-in steel plate (detail 0302 and 0304) or outer steel plates (detail 0305 and 0306) to prevent the secondary beam to slipping off the bearing plate. The two type of connection discussed above, requires different approaches in terms of design verification. In section 2.3.2 the difference parameters that involves the design verification are discussed and which connection type is

used for further analysis within this research project.

The connections part on the primary beam shows the different fasteners that are applied to transfer the forces from the slotted-in steel plate or bearing plate to the primary beam. In details 0301, 0302 and 0303 nails and screws are applied, which penetrate the primary beam with a certain length. Details 0304, 0305 and 0306 are executed in bolts, which penetrates the full primary beam and is completed with a washer and nut. Moreover, the position and the number of columns of the fasteners in the primary beam differs in the standard details. In most details the fasteners are placed within the thickness of the secondary beam, except from detail 0305, in which the steel plate on the primary beam is wider than the thickness of the secondary beam and the bolts are placed with a larger center to center distance.

In more detail figure 2.10 shows the possible steel components, such as a steel bracket or joist hanger to connect a secondary- and primary beam. The configurations 1b, 1c, and 1d are part of the group connection that transfer the forces by direct contact. Joist hanger 1d is developed in case two secondary beam cross the continuous primary beam in the same line. The transfer of the forces takes place by compression perpendicular to the grain for the secondary beam as well as the primary beam.

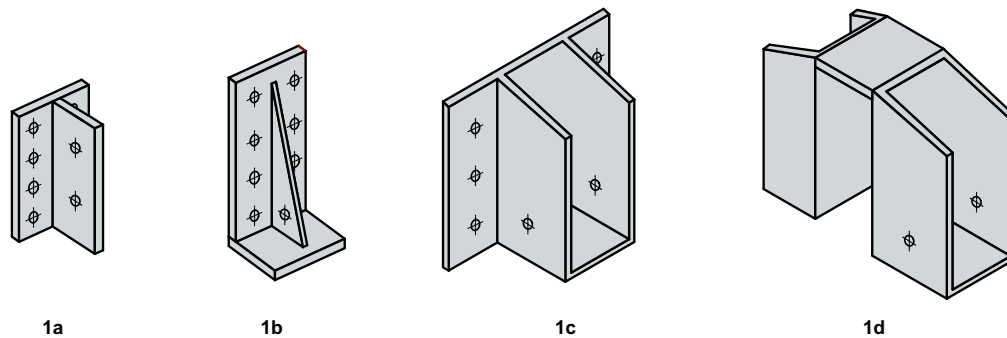


Figure 2.10: Configuration steel brackets/joist hanger

The fasteners that connect the steel component at the secondary beam to the primary beam can be executed as nails, screws or bolts as illustrated in the standard details of DeGroot Vroomshoop. The main difference between these fasteners is that bolts penetrate the full beam compared to the nails and screws, which have certain penetration length as shown in figure 2.9. Moreover, the fastener types have different characteristics in terms of axial resistance and bending moment capacity. In section 2.4.1 the fasteners types will be discussed in more detail.

All connection types shown in figure 2.9 generates a additional moment due to the eccentricity between the two elements. The eccentricity of load bearing connections are defined as the difference between the center line of the primary beam and the line of loading of the bearing plate (left), as shown in figure 2.11. For the connections that transfer the forces by lateral loading of the mechanical fasteners the eccentricity is defined as the difference between the center line of the primary beam and the centroid of the fasteners group (right) as shown in figure 2.11.

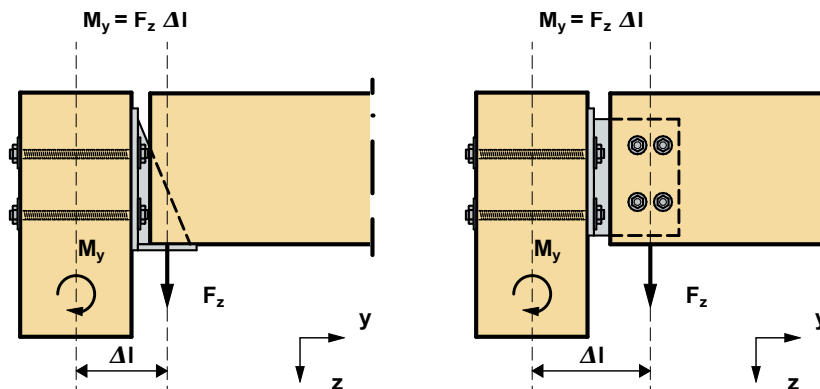


Figure 2.11: Determining eccentricity moment

The additional moment occurs in joints between secondary beams and primary beams as well in joints between primary beams and columns. In the following paragraph the example of a joints between a secondary beam and primary beam is demonstrated.

There are two ways to solve the additional moment caused by the eccentricity. The first approach is to transfer the additional moment to the primary beam, which generates a tensile force at the top fastener and compression force at the bottom fastener (left), as shown in figure 2.12. NEN-EN-1995-1-1:concept (20XX) demonstrates a methodology to calculate the resistance of a joist hanger that is based on this approach. In this approach the primary beam is subjected to torsion including the corresponding joints.

The second approach is to take up the eccentricity moment in the fastener group of the secondary beam itself (right) as shown in figure 2.12. With this approach, the primary beam is not loaded with torsion. In this research project, the latter approach is chosen to relieve the primary beam from torsional moment. Moreover, if the primary beam does not contains a torsional moment, the connection of the joint between the primary beam and the column does not have to design for torsional moment. Finally, applying the first approach to joints between columns and high loaded primary beams causes high locally compressive and tensile stresses in the column at joint level. From practical engineering the eccentricity between the two members is determined by the distance between the centroid of the fastener group or the line of loading for bearing plates until the edge of the joint member. This approach is discussed in section 4.3.2 in more detail. The additional moment caused by the remaining eccentricity (e.g. the half of the member size) is carried by the member itself.

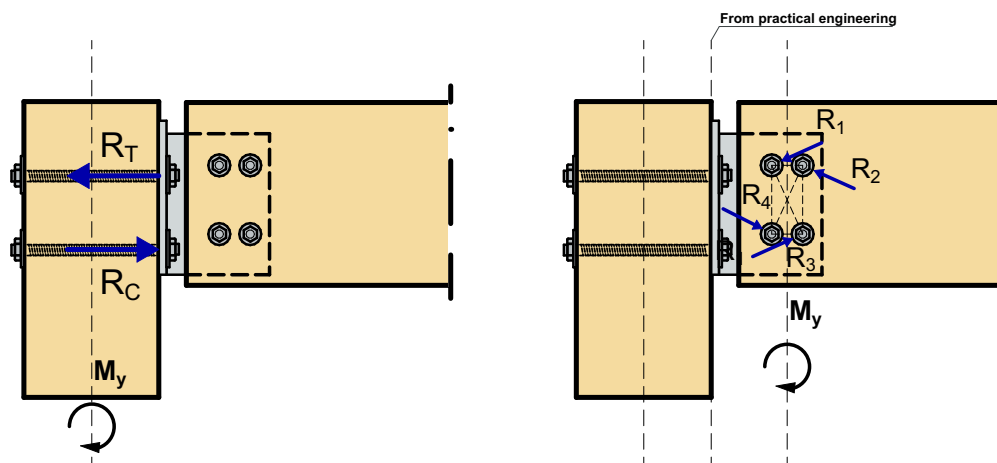


Figure 2.12: Two options to resist the eccentricity moment

Beam to column joint - joint between column and beam

Another joint that is part of the frame structure is the joint between a beam and column. Timber supplier De Groot Vroomshopp offers the following standard connections between a beam and column, as shown in figure 2.13. These connection are primarily applicable for specific frame structures such as a roof system wherein the column does not continues. Moreover, these connections are suitable for end beams, as shown in figure 2.13, and beams that continues. In detail 0401 and 0402 the beam is positioned on top of the column, which indicates that the forces are transferred by direct contact between the two elements. Two prevent the beam to slipping off and in some cases to lifting up the column detail 0401 has an slotted-in steel plate mounted at both elements and detail 0402 has an double external steel plate. By applying this type of connection, no eccentricity moment between the column and beam will occur, since the center lines of each element are placed in the same line.

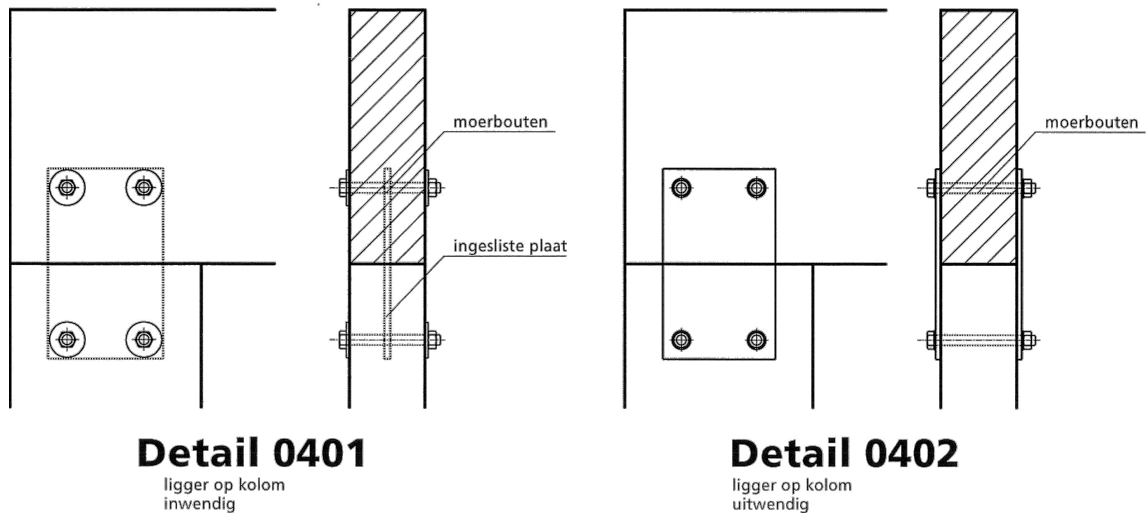


Figure 2.13: Standard details of a joint between primary beam and column from DeGroot Vroomshoop

The details shown in figure 2.13 are commonly not suitable for intermediate floors, wherein another column with high normal forces is placed on top of the beam. Generally the main issue in having a system wherein the column is positioned on top of the beam is that the beam is loaded with high normal forces from the column perpendicular to the grain. As discussed in section 2.1 timber has a low compressive strength capacity perpendicular to the grain. Additional steel components can be applied in these connections to avoid that the normal forces from the column will transfer through the beam as shown in figure 2.14.



Figure 2.14: Additional steel components applied to transfer the normal forces from one column to the other

Another option to avoid forces that runs through the beam perpendicular to the grain, is to have a continuous column with an attached beam. This detail has similarities to the details of the joints between the primary beam and the secondary beam, discussed in section 2.9. Figure 2.15 shows different connection configurations of the joint between a continuous column and a beam.

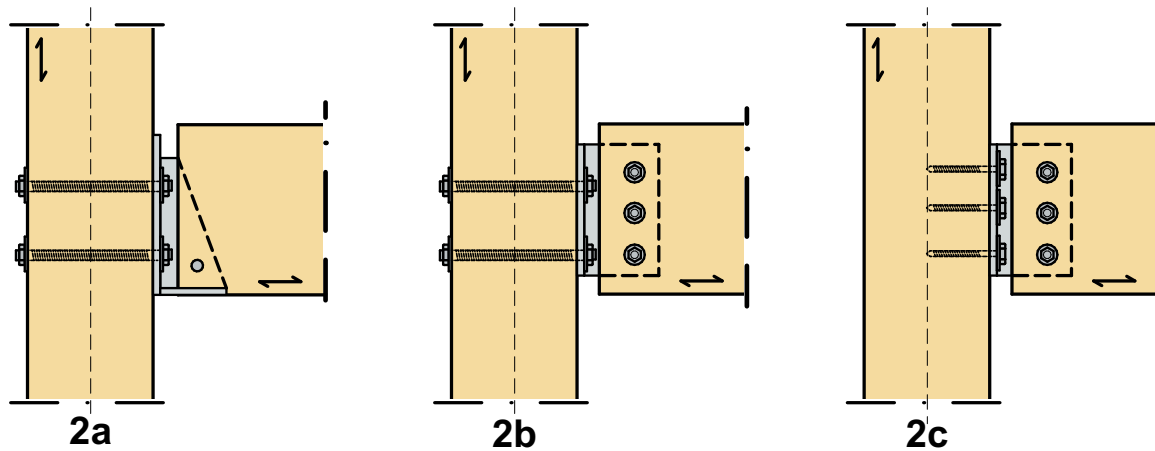


Figure 2.15: Example of a connections between continuous column and beam

Connection type 2a is similar to details 0302 and 0304, as shown in figure 2.9, wherein the forces are transferred by a combination of direct contact between the beam and the bearing plate and lateral loading of the bolts mounted at the column.

Connection type 2b shows an alternative to connection type 2a, wherein the steel bearing plate is replaced by a slotted-in steel plate. This connection type refers to details 0301 and 0303, as shown in figure 2.9, in which the forces are transferred by lateral loading of the mechanical fastener mounted at the column and beam. The grain orientation of the column and beam are most often different (90 degrees), compared to the grain orientation in the connection between the primary beam secondary beam (0 degrees). The effect on the embedment strength of the member caused by the different grain directions will be discussed in more depth in section 2.4.3.

Connection type 2c is similar to connection type 2b, although the fastener type in the column is replaced by lag screws, which refers to detail 0301, 0302 and 0303 as shown in figure 2.9.

All connection types shown in figure 2.15, are subjected to an eccentricity moment, since the center line of the column and the beam are not in the same line. Similar to the connection types illustrated in figure 2.9 the moment is determined by the distance between the center lines of the elements and the shear force in the joint. In a system of secondary and primary beams, the primary beams commonly transfer higher shear forces. The higher shear forces combined with the eccentricity causes higher eccentricity moments. These eccentricity moments are taken by the fastener group of the beam, which is a similar approach as the joints between the primary- and secondary beam.

The examining of joints between a column and beam illustrates that different connection types are possible to apply to the joints. The configuration of having a continuous column or two disrupted columns has a significant impact on the configuration of the connection. In case of disrupted column and high normal forces, additional steel components need to be incorporated to prevent that the forces will transfer through the beam. This connection adds more complexity to the joint compared with a continuous column. Since the continuous column has no unlimited length a connection as shown in figure 2.16 can be applied between two columns. In this thesis the joint configuration of a continuous column with attached beam(s) will be focused on.

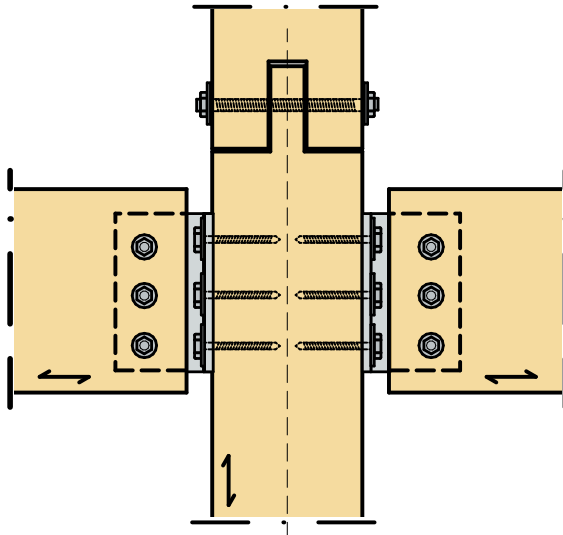


Figure 2.16: Connection for joint between two columns

Beam to column joint - joint between column and multiple beams

The investigated frame structure discussed in section 2.3.1 consists of joints that connects a column with multiple beams, as shown in figure 2.8. For these joints a selection of the connection types discussed in the previous paragraph can be applied. Figure 2.17 shows two examples of connections between a continuous column and two secondary beams. Option 3a shows a slotted-in steel plate in combinations with full penetrated bolts. Option 3b consist of L-shaped steel bracket in combination with screws. In case the column is attached with multiple beams in two direction, the possibility that the fasteners can intersect with each other need to be considered during the design of the joint.

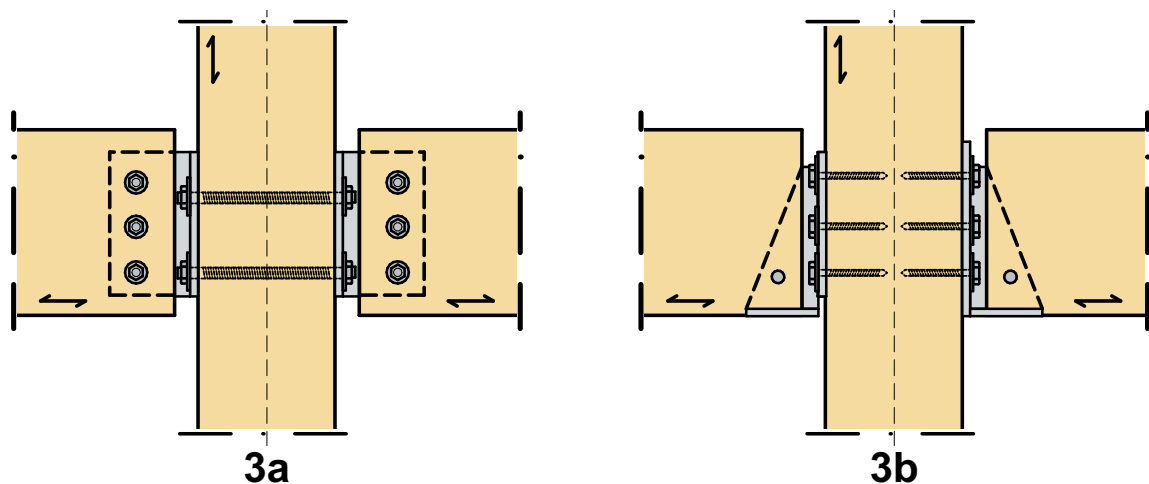


Figure 2.17: Example of connections between column and multiple beams

The following project Askim Torg build in Göteborg illustrates a (braced) frame structure with continuous columns attached with multiple beams.



Figure 2.18: Askims Torg at Göteborg ©Sören Hakanlind (Swedish-Wood, n.d.)

2.3.2. Load Transfer Connections

There are two different types of connections when it comes to the transfer of forces as discussed in section 2.3.1. The first connection type transfers its forces by direct bearing contact (type 1), such as joist hangers and steel brackets. The second connection type transfers its forces by lateral loading of the fasteners (type 2). One or more slotted-in steel plate(s) or one or more steel plate(s) on the outer side of the beam in combination with fasteners are examples of this type of connection. These two connection types have different design parameters regarding the design verification.

The configuration of connection type 1 (direct bearing contact) is mainly determined by the compressive stress at the contact area of the timber element. The angle between the grain orientation of the element and the direction of the load strongly determines the compressive strength of the timber elements. Table 2.2 illustrates the difference between the compressive strength perpendicular to the grain and parallel to the grain of glued laminated timber with a strength class GL28h.

| Strength class | $f_{c,0,k}$ [N/mm ²] | $f_{c,90,k}$ [N/mm ²] |
|----------------|----------------------------------|-----------------------------------|
| GL28h | 28 | 2.5 |

Table 2.2: Compression strength parallel to the grain vs perpendicular to the grain

The wood grain in glued laminated beams generally runs in one direction, parallel to the long axis of the beam (Ong, 2015). This way, the load acts perpendicular to the grain of the secondary beam. The compressive strength perpendicular to the grain is governing for the calculation of the bearing resistance. The two parameters that determine the contact area are the thickness of the secondary beam and the contact length on the steel plate. With the expression 2.1 the verification of compression perpendicular to the grain of the timber element can be computed (NEN-EN-1995-1-1, 2004). The discussed connection types rest at the end of the beams on the bearing plate, which means that the $k_{c,90}$ ¹ is taken as 1.

$$\sigma_{c,90,d} \leq k_{c,90} f_{c,90,d} \quad (2.1)$$

Where:

| | | |
|-------------------|---|-------------------|
| $\sigma_{c,90,d}$ | compressive stress in the contact area perp. to grain | N/mm ² |
| $f_{c,90,d}$ | design compressive strength perp. to grain | N/mm ² |
| $k_{c,90}$ | factor ¹ | |

Connection type 2 (lateral loading of fasteners) consists of different components that determine the configuration. These components are separated into two groups. Group one consists of the components that determine the carrying capacity of a fastener per shear plane, such as the load carrying capacity of the fasteners, the embedment strength of the timber element, and the configuration of the steel plate(s). Group two represents the (design) components, such as the number of fasteners (in rows and columns) and the number of steel plates. Within these components, a large number of sub-parameters influences the eventual capacity of the connection type. For instance, the embedment strength of the timber element depends on the density of the wood, the diameter of the fastener and the angle between the load and the grain. In section 2.4, the components are examined in more detail. The number of parameters that are involved when determining the capacity of connection type 2 is higher compared to connection type 1.

Another aspect that is analyzed when comparing the two connection types is the compressive strength (related to the direct bearing contact) and the embedment strength (related to the lateral loading of the fasteners). In both cases, the strength parallel and perpendicular to the grain are determined, as shown in table 2.3, based on the example of glued laminated timber with a timber strength of GL28h. The embedment strength is calculated according to the equations 2.6 and 2.7. Moreover, a fastener with a diameter of 12 mm is assumed. Table 2.3 shows that perpendicular to the grain the compressive strength is significantly lower than the embedment strength.

The difference in strength is the effect of membrane action that occurs by loading round dowels. The stress distribution of embedment stress is a combination of compressive stress parallel and perpendicular to the grain, and small tensile stresses at the bottom of the dowel, as shown in figure 2.19.

¹factor taking into account the load configurations possibility of splitting and degree of compressive deformation

| | ρ_k [kg/m^3] | $f_{c,0,k}$ [N/mm^2] | $f_{c,90,k}$ [N/mm^2] | $D_{fast.}$ [mm] | reduction[%] |
|----------------------|-----------------------|--------------------------|---------------------------|------------------|--------------|
| Compressive strength | 425 | 28,0 | 2,5 | | 91 |
| Embedment strength | 425 | 30,7 | 20,0 | 12 | 35 |

Table 2.3: Compression strength vs embedment strength - parallel and perpendicular to the grain

More information about the embedment strength can be found in section 2.4.3. The comparison that is made between the compressive strength and the embedment strength perpendicular to the grain does not imply that connection type 2 generally has a higher resistance capacity than connection type 1. Still, other components of connection type 2, which are discussed above, influence the connection capacity.

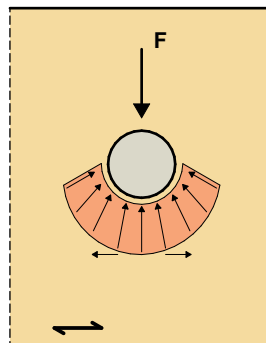


Figure 2.19: Embedment stress distribution

Connection type 2, which transfers the forces by lateral loading of the fasteners, will be examined further in this research project. This choice was made because the high number of parameters that determine the capacity of connection type 2 matched with the parametric and computational approach of this research project. Moreover, the high variety of parameters of connection type 2 offers a wide range of possible configurations that resist the forces in the joint.

2.3.3. Fastener Types

In the section 'Applied connection in practice' 2.3.1, different types of fasteners are applied in the standard details, such as nails, screws, and bolts. A fastener type that is not addressed in this section are dowels, which are smooth cylinders without a head. Since this type of fastener does not have a head, it cannot hold the joint together (Blaß & Sandhaas, 2017). That is why dowels are commonly used for mechanical connections that include slotted-in steel plate(s). The fasteners applied in the connections that are examined in this research project are primarily loaded on shear. Fastener types with larger diameters are more efficient in terms of the number of fasteners that are needed to fulfill the shear capacity compared to fasteners with a smaller diameter. In this research project, the fastener types with a minimal diameter of 8 mm are chosen. The fastener types bolts and dowels meet this requirement. For screws, only lag screws have a larger diameter of 8 mm. Moreover, all nail types have a smaller diameter than 8 mm. Therefore, they will be neglected in this research project. The discussed fastener types require pre-drilling in case of mounting. Lag screws in particular need pre-drilling to prevent splitting of the timber member.

To avoid a splitting failure of the primary beam, the tensile stresses perpendicular to the grain caused by the shear forces of the secondary beam should be limited. To limit these stresses, the connector of the secondary beam should be placed as high as possible. Moreover, from practice based knowledge, if the connector covers the primary beam from 70% to 80%, the tensile stresses perpendicular to the grain are not governing in the design (Blass et al., 1995b). However, by increasing the height of the connector, the probability of causing cracks due to shrinkage will enlarge.

2.4. The Components of Mechanical Connections

All the components that are related to laterally loaded dowel-type mechanical connections, such as the load carrying capacity of the fasteners, the rope effect, embedment strength, failure mechanisms, and ductile behavior are examined in this chapter to understand the principles of the mechanical connections. These principles will lay the foundation for the tool that is developed in chapter 4.

2.4.1. Load Carrying Capacity of the Fasteners

As shown in figure 2.7, fasteners are part of a connection. In a connection, fasteners contribute to the transfer of forces from one element to another. In the case of shear forces, the forces are transferred through lateral loading of the mechanical fasteners. In this paragraph, the shear capacity and the yield moment of the fastener types steel dowels and bolts are examined. These fastener types are also known as dowel-type connectors in the literature, since the fasteners have similar characteristics (Borgström, 2016). In case the fastener is perpendicularly loaded, a pressure load against the surrounding timber member occur. As a result, the timber member will create an embedment pressure against the fastener. The embedment pressure will function as a distributed load on the fastener, which act as a beam. In case the fastener is thick, it will not bend. However, if the fastener is more slender, it will deform by bending, as shown in figure 2.20. Eventually, the fastener will create one or more plastic hinges and at certain position along the dowel the timber is crushed. Once the fastener is deformed, a tensile action in the fastener can occur as a result of the shear action. The tensile action can be increased by using bolts with a head and nut including washers to achieve anchorage. Since dowels are smooth and do not have a head and nut, the tensile action of dowels is zero (Borgström, 2016).

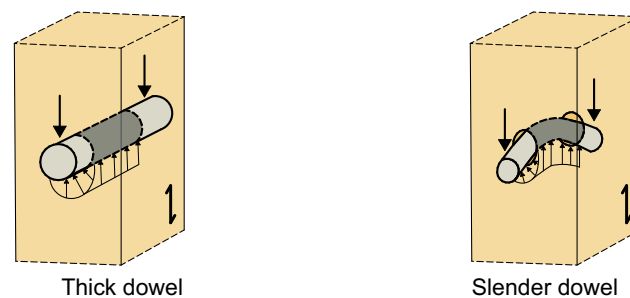


Figure 2.20: Lateral loading of a thick dowel compared to a slender dowel

The slenderness and the ultimate steel strength of the fastener determine the number of plastic hinges that could occur in the fastener. The yield moment that is required to produce the plastic hinge(s) in the fasteners is determined using a test for different types of fasteners according to SS-EN 408. The characteristic value of the yield moment $M_{y,Rk}$ of fasteners depends on the diameter (d) in mm of the fastener and the steel strength f_u in N/mm^2 of the fastener. The following empirical expression according to NEN-EN-1995-1-1 (2004) shows the yield moment for all fasteners with $d > 8$ mm.

$$M_{y,Rk} = 0,3f_u d^{2,6} \quad (2.2)$$

Where:

| | | |
|------------|--|-----------------|
| $M_{y,Rk}$ | characteristic value of the yield moment | Nmm |
| f_u | ultimate steel strength | N/mm^2 |
| d | diameter fastener | mm |

2.4.2. Rope Effect

Once the fasteners is deformed a tensile action in the fastener can occur as discussed in section 2.4.1. Fastener type such as bolts and screws has the ability to restrain these tensile forces, which gives these fastener an additional shear capacity. For bolts, the withdrawal capacity depends on the anchorage capacity of the washer and nuts and the tensile capacity of the bolt itself. For screws, the

withdrawal capacity depends on the threading and the penetration length of this threaded part in the timber (Borgström, 2016).

The anchorage capacity of the washer can be determined by using the equation 2.3, according to (NEN-EN-1995-1-1, 2004).

$$F_{ax,washer,Rk} = 3f_{c,90,k}A_{washer} \quad (2.3)$$

Where:

| | | |
|-----------------|--|-------------------|
| $F_{ax,washer}$ | characteristic value of withdrawal capacity washer | N |
| $f_{c90,k}$ | charac. compressive strength perp. to the grain | N/mm ² |
| A_{washer} | area washer | mm ² |

The withdrawal capacity of lag screws can be determined by using the equation 2.4, according to (NEN-EN-1995-1-1, 2004)

$$F_{ax,\alpha,Rk} = \frac{n_{ef}f_{ax,k}dl_{ef}k_d}{1,2\cos^2\alpha + \sin^2\alpha} \quad (2.4)$$

$$f_{ax,k} = 0,52d^{-0,5}l_{ef}^{-0,1}\rho_k^{0,8}$$

Where:

| | | |
|--------------------|--|-------------------|
| $F_{ax,\alpha,Rk}$ | char. withdrawal capacity of the connection at an angle to the grain | N |
| $f_{ax,k}$ | char. withdrawal strenght perp. to the grain | N/mm ² |
| n_{ef} | effective number of screws | - |
| d | outer diameter measured on the threaded part | mm |
| l_{ef} | penetration length of the threaded part | mm |
| ρ_k | characteristic density wood | kg/m ³ |
| α | the angle between screw shaft and the grain | rad or ° |

The rope effect is taken into account by adding 25% of the withdrawal capacity to the shear capacity of of a single dowel. The contribution from the rope effect is limited to given percentage of the shear capacity (table E.4-E.6) as illustrated in table 2.4, according to (NEN-EN-1995-1-1, 2004).

| Fastener type | Percentage [%] |
|---------------|----------------|
| Bolts | 25 |
| Screws | 100 |
| Dowels | 0 |

Table 2.4: Maximum contribution from rope effect in relation to the shear capacity of a fastener type

2.4.3. Embedment Strength

The maximum allowable pressure of the timber around the fastener is defined as the embedment strength f_h . This strength is determined through tests, wherein a thick dowel is pressed perpendicular to the grain of the timber element, according to NEN-EN-383 (2007).

The embedment strength of timber is related to the following parameters according to Blaß (2003). First, in case the fastener diameter d increases, the embedment strength decreases. Second, a higher density results in a higher embedment strength. Third, the effect of the angle α between the grain and load direction shows that the highest embedment strength is achieved in compression parallel to the grain and the lowest perpendicular to the grain. Fourth, the moisture content in wood has a negative effect on the embedment strength if it is high and a positively effect on the embedment strength if the moisture content is low. Fifth, in case holes are pre-drilled, the majority of the load will be carried by compression parallel to the grain, whereas holes that are not pre-drilled will result in a load situation in which the embedment strength is a combination of compression parallel and perpendicular to the grain.

According to NEN-EN-1995-1-1 (2004), the empirical expressions for the determination of the characteristic embedment strength under loading parallel to the grain for softwood is illustrated in the equation 2.5 for fasteners without pre-drilling ($d < 8$ mm) and the equation 2.6 with pre-drilling for all diameters.

$$f_{h,0,k} = 0,082\rho_k d^{-0,3} \quad (2.5)$$

$$f_{h,0,k} = 0,082(1 - 0,01d)\rho_k \quad (2.6)$$

Where:

| | | |
|-------------|--|-------------------|
| $f_{h,0,k}$ | embedment strength parallel to the grain | N/mm ² |
| ρ_k | characteristic density wood | kg/m ³ |
| d | diameter fastener | mm |

As mentioned above, the angle between the grain and load direction has an effect on the embedment strength. The reduction that needs to be considered can be determined by using Hankinson's formula if loading takes place at an angle to the grain. The formula is defined in the equation 2.7, which k_{90} is related to softwood (NEN-EN-1995-1-1, 2004).

$$f_{h,\alpha,k} = \frac{f_{h,0,k}}{k_{90} \sin^2 \alpha + \cos^2 \alpha} \quad (2.7)$$

$$k_{90} = 1,35 + 0,015d$$

Where:

| | | |
|------------------|--|-------------------|
| $f_{h,\alpha,k}$ | embedment strength under load direction in an angle to the grain | N/mm ² |
| k_{90} | softwood correction factor | - |
| α | angle of the load to the grain | rad or ° |

2.4.4. Failure Mechanisms

In case a dowel-type fastener is loaded in shear, it can fail in a number of failure modes. These failure mechanisms are based on the European Yield Model (EYM) proposed by Johansen (1949). This model illustrates that the load-bearing behaviour of the dowel-type fastener mainly depends on the embedment properties of timber, the yield moment of the dowel-type fastener, and the thickness and configurations of the timber members. Moreover, the EYM forms the basis of the design of dowel-type connections contained in the NEN-EN-1995-1-1 (2004). The dowel-type connections are categorized into timber-to-timber, panel-to-timber and steel-to-timber connections (NEN-EN-1995-1-1, 2004). The dowel-type connections examined in section 2.3.1 consist of steel plate(s) and timber, which means that the failure mechanisms of steel-to-timber connections is the relevant category to explore in this thesis. The consequence of applying a steel plate as one of the members in a dowel-type connection is that theoretically the plastic hinge occurs at the interface between the steel and timber member. This increases the capacity of the connection compared to timber-to-timber connections (Borgström, 2016).

Moreover, the thickness of the steel plate determines the way in which the plastic hinge is generated. In case the thickness of the steel plate is larger or equal to the diameter of the dowel-type fastener, the steel plate is rigid enough to force a plastic hinge in the dowel. In case the thickness of the steel plate is smaller or equal to half of the diameter of the dowel, the steel plate can be defined as a pinned support, in which the dowel will solely rotate without generating a plastic hinge (Borgström, 2016).

Dowel-type joints with slotted-in steel plates are derived in the same manner as described for steel-to-timber connections. The plastic hinges occur at the interface between the steel and timber member. Additionally, the thickness of the (slotted) steel plate must be thick enough to prevent failure mechanisms such as shearing out of the steel plate part and hole ovalisation of the steel plate.

NEN-EN-1995-1-1 (2004) outlines a number of failure mechanisms for steel-to-timber joints. These failure mechanisms are supported by expressions that illustrate the resistance per fastener per shear plane, as shown in figure 2.21. In case the connection consists of two shear planes, the value of the expression must be multiplied by 2. The steel-to-timber joints are categorized into single shear steel-to-timber joints with steel plates $t_{steel} \geq d$ (table E.1), single shear steel-to-timber joints with $t_{steel} \leq 0,5d$ (table E.2), slotted-in steel plates (table E.3), double shear steel-to-timber joints with steel plates $t_{steel} \geq d$ (table E.5), and double shear steel-to-timber joints with $t_{steel} \leq 0,5d$ (table E.4).

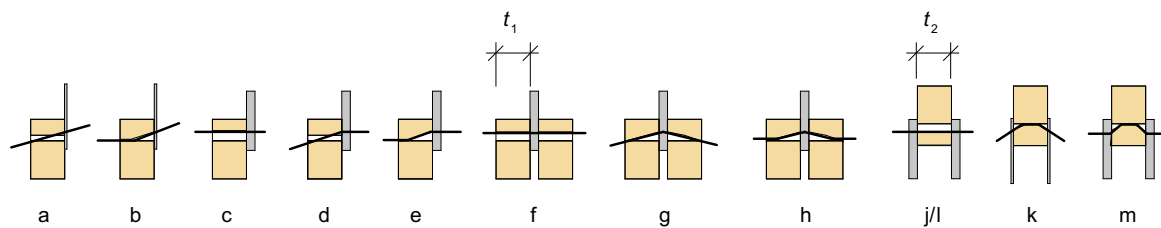


Figure 2.21: Failure mechanisms for steel-to-timber connections

Multiple Slotted-in Steel Plates

In general, the load-carrying capacity of a connection increases with the extension of the number of slotted-in steel plates. By having more slotted-in steel plates in a timber element, the dowel-spans are shorter compared to a similar connection with a lower number of slotted-in steel plates. The shorter spans lead to a decrease in the bending moment for a given external load (Rossi et al., 2016).

The failure mechanisms of slotted-in steel plates with more than one plate (more than 2 shear planes) are not explicitly given in the Eurocode 5 (NEN-EN-1995-1-1, 2004). However, the load-bearing capacity of a multi-shear connection can be determined as a combination of different shear plane configurations. In case of two slotted-in steel plates, which is a four shear connection, the load-bearing capacity can be calculated as the sum of a single-shear connection and a two-shear connection (Phong, 2020). Moreover, different models that examine the failure mechanisms of multi-shear connections can be found in the literature. For instance, Pedersen (2002) and Sawata et al. (2006) developed a method based on the EYM, which proposed equations to determine the load capacity of a connection that consists of four and six shear planes (double slotted-in steel plate and three slotted-in steel plate) and considered a ductile behavior for all mechanisms. Moreover, Phong (2020) examined the most optimal position of a double slotted-in steel plate in terms of bearing capacity by comparing the calculation models of Pedersen (2002) and Sawata et al. (2006) with the Eurocode 5 standards (NEN-EN-1995-1-1, 2004). In this study, each calculation method shows different plastic failure mechanisms and bearing capacities. Moreover, in this study, the positions of the slotted-in steel plates are represented in a t_2/t_1 ratio, in which the t_2 illustrates the timber thickness from the edge of the timber member to the slotted-in steel plate and t_1 is the distance between the two slotted-in steel plates. Regarding the position of the slotted-in steel plates, the NEN-EN-1995-1-1 (2004) model shows a t_2/t_1 ratio of 0.89, Pedersen (2002) model illustrates a ratio of 6.67 and Sawata et al. (2006) shows a ratio of 1.67. Moreover, Phong (2020) stated that the resulted failure mechanisms of NEN-EN-1995-1-1 (2004) obtained the most proper Stress - Deformation state compared to the calculation models of Pedersen (2002) and Sawata et al. (2006). From this study can be concluded that t_1 and t_2 are approximately equal to get the highest bearing capacity of the connection.

Phong (2020) verified the accuracy of the methods developed by Pedersen (2002) and Sawata et al. (2006) for a double slotted-in steel plate with the experimental test performed by Rossi et al. (2016). Both methods show excellent correspondence with the test results, although the method of Pedersen (2002) shows slightly more accuracy. Based on these observations, the method developed by Pedersen (2002) is used for the double slotted-in steel plate calculation in this research project.

Moreover, Phong (2020) examined the bearing capacity of 1 slotted-in steel plate until 10 slotted-in steel plates by applying the discussed calculation models. This analysis shows that the methods discussed above become less accurate as the number of steel-plates increases, since the differences between the loading capacity that is calculated by the three models grow with the number of steel plates. Based on this observation, the number of slotted-in steel plates is limited to a maximum of 2 steel plates.

Comparing Failure Mechanisms

The joints types discussed in section 2.3.1 consist of different type of failure mechanisms. For instance the joints between a primary and secondary beam as illustrated in detail 0303 in figure 2.9. At the secondary beam side of the joint a steel plate is integrated in the beam. In case this is single slotted-in steel plate, failure mechanisms E,F, and G illustrated in figure 2.21 are the mechanisms to verify. An alternative connection for the slotted-in steel plate is a double steel plate placed outside the timber element. In this case the failure mechanism depends on the thickness of the steel plate. For a thin steel plate the mechanisms J and K are the corresponding failure mechanisms and in case a thick steel plate is applied, the mechanism L and M are the ones to verify.

At the primary side of the joint all details illustrated in figure 2.3.1 are connected with a single shear steel plate. Depending on the thickness of the steel plate, mechanisms a and b (thin) or c,d, and e (thick) are the mechanisms to verify.

As discussed in the previous paragraph, the connection in the secondary beam can be applied with a slotted-in steel plate or a steel plate positioned at the outer side of the timber element. In this paragraph the load bearing capacity of these two configuration is analyzed, in which the slotted-in steel plate is limited to two plates. The shear resistance is determined according to the formulas found in the tables E.3, E.5, E.4, and E.6. The timber thickness of the element is the variable parameter with a range between 60 and 240 mm in steps of 20 mm. The minimum timber thickness of the double slotted-in steel plate is 140 mm, to guarantee a minimum thickness of 40 mm for t_1 . The following parameters are set for the example:

- Fastener diameter: $d = 8$ mm
- GL28h timber: $\rho_k = 410$ kg/m³
- Steel 8.8 $f_u = 800$ N/mm²
- Slotted-in steel plate: $t = 8$ mm

Moreover, the embedment strength is calculated under a load direction of 90° (perpendicular to the grain) and the rope effect for bolts is limited to 25% of the Johanson part, according to NEN-EN-1995-1-1 (2004). This example is applied to all failure mechanisms of the double shear steel-to-timber joints with $t_{steel} \geq d$, as shown in graph 2.22a, the double shear steel-to-timber joints with $t_{steel} \leq 0,5d$, as shown in graph 2.22b, the single slotted-in steel plate, as shown in graph 2.23a, and the double slotted-in steel plates, as shown in graph 2.23b.

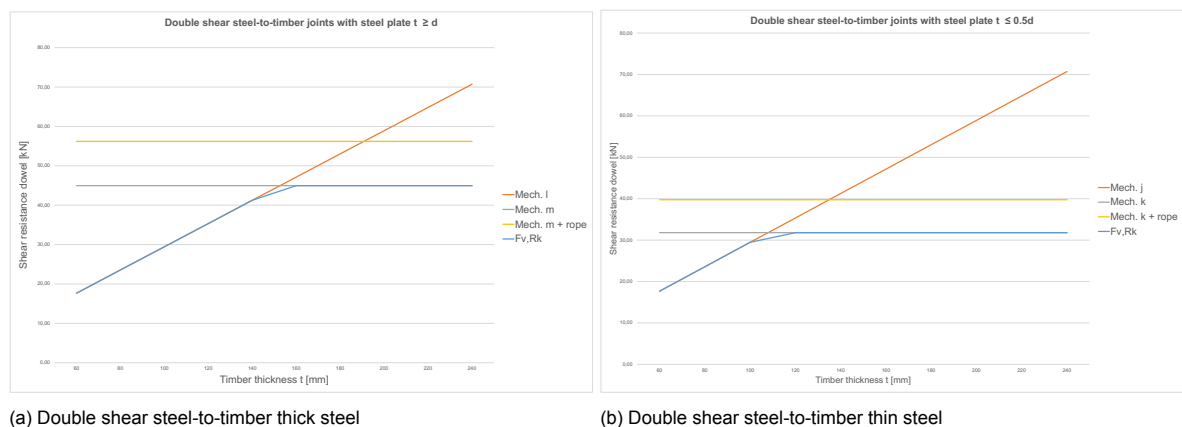


Figure 2.22: Resistance and failure mechanism for a double shear steel-to-timber connection with thin and thick steel plate

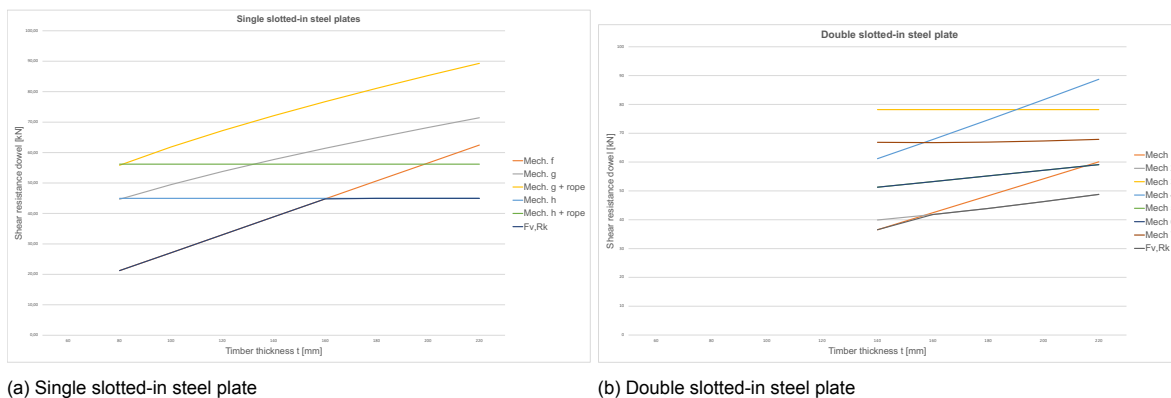


Figure 2.23: Resistance and failure mechanism for a single and double slotted-in steel plate connection

In the following graph 2.24, the governing fail mechanism for each connection type is shown.

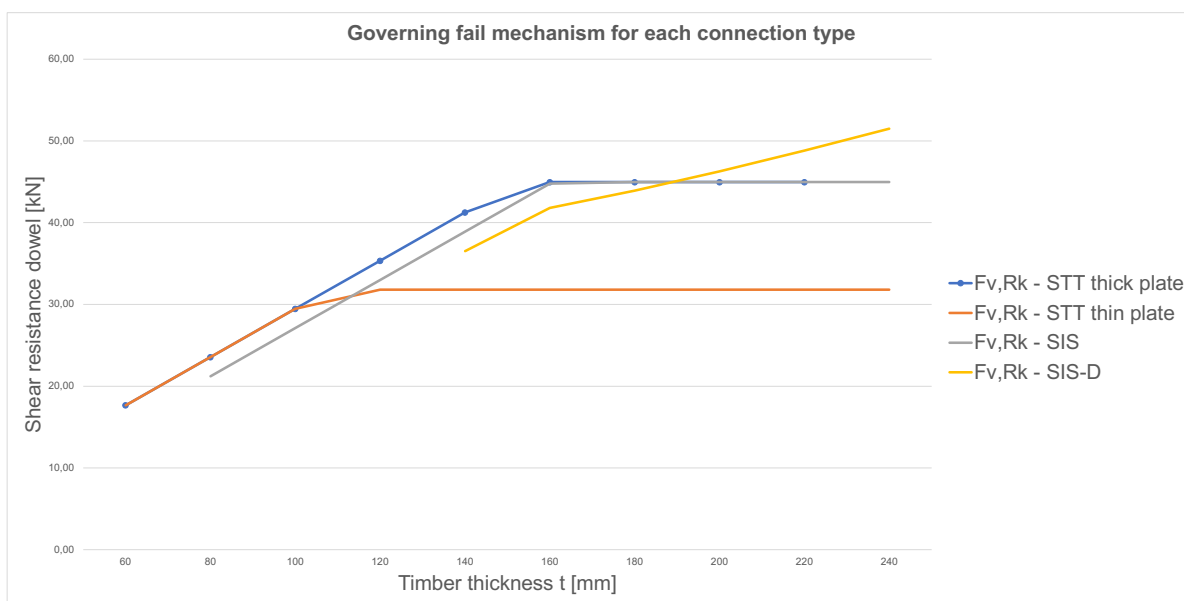


Figure 2.24: The governing fail mechanism and corresponding shear resistance for each connection type

The following observations can be made:

- With a timber thickness between 60 mm and 100 mm, a double shear steel-to-timber connections (STT) that contain a thick or a thin plate are the most effective connections in terms of shear resistance per dowel.
- With a timber thickness between 100 mm and approximately 190 mm, the double shear steel-to-timber connection (STT) with a thick steel plate and the single slotted-in steel plate (SIS) are the most effective connections.
- In case the timber thickness is larger than approximately 190 mm, the double slotted-in steel plate (SIS-D) is the most effective connection.
- With a timber thickness larger than approximately 160 mm a single slotted-in steel plate (SIS) has a equal shear resistance per dowel with the double shear steel-to-timber thick steel plate.

Considering these observations, the selection of the most effective connection depends on the thickness of the timber member. Yet, the most effective connection could result in a brittle failure mechanism, whilst in some cases ductile behaviour is desired. The difference in ductile and brittle failure mecha-

nisms for connections will be discussed in more depth in section 2.4.5.

2.4.5. Ductile Behavior

In order to reduce the collapsing risk of a global structure as a consequence of failure in (a) structural element(s), a structural engineer may design a collapse-resistance structure that incorporates characteristics such as redundancy, robustness, or ductility in the structural design (Kirkegaard et al., 2011).

In this paragraph, ductility in the structural design will be focused on. In steel structures, the members are commonly designed to yield before the connections. The members generally provide sufficient structural ductility without generating a mechanism of collapse (Thelandersson & Larsen, 2003). The failure of wood members in timber structures is limited, since shear, tension, and bending for lower grade timber have brittle failure characteristics (Kirkegaard et al., 2011). To avoid possible brittle failures of the members, the joint can be designed as a ductile connection that fails before the members do, to ensure ductile failure mechanisms in the global system (Thelandersson & Larsen, 2003).

In order to design a connection that has ductile characteristics, the Eurocode 5 introduced minimal end and edge distances between the fasteners and the timber element and minimal spacing between the fasteners themselves perpendicular and parallel to the grain direction of the timber element. (NEN-EN-1995-1-1, 2004). Moreover, Jockwer et al. (2021) examined the parameters that influence the load-deformation behavior of connections with laterally loaded dowel-type fasteners. In terms of ductility, the test showed that the spacing of the fasteners has a positive impact on the level of ductility. Additionally, the test showed that the ductility decreases with an increasing number of fasteners in a row. This is in line with the reduction factor N_{ef} that the Eurocode 5 introduced for fasteners parallel to the grain direction (NEN-EN-1995-1-1, 2004).

The minimal distances are illustrated in figure 2.25 and have been given in order to ensure ductile behaviour and avoid brittle failure due to premature splitting (Blass et al., 1995a). The distances depend on the fastener type, the angle between the load and the grain of the timber element, and the diameter of the fastener (NEN-EN-1995-1-1, 2004). The minimal distances of bolts and lag screws, and dowels are illustrated in figure D.2 and figure D.3, which can be found in Appendix D.

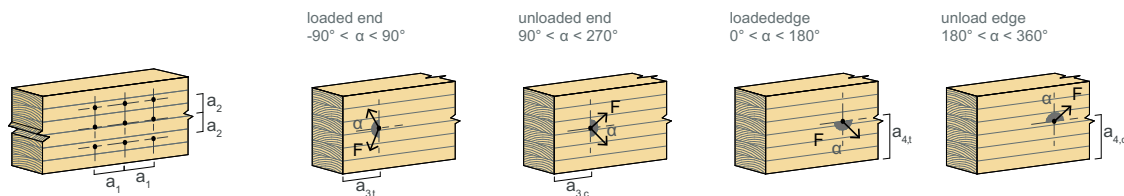


Figure 2.25: Minimal spacing, end and edge distance fasteners

2.5. Conclusions

Engineered Wood Product

The shapes and sizes of timber elements that can be achieved with sawn timber are limited, as this chapter has highlighted. In order to achieve more shapes and sizes, a wide range of engineered wood products (EWPs) has been invented. Not only do EWPs allow for more shapes and sizes to be achieved, EWPs also have higher mechanical properties than sawn timber due to the eliminations of defects. In this chapter, the existing literature on the engineered wood products glued laminated timber, laminated veneer lumber, and I-joist were examined for the members in the timber frame. Based on the existing literature, I-joist proves to be a suitable alternative for sawn timber in terms of saving material. However, the use of this product is limited for structures with large spans. As this research project involves structures with large spans, I-joist was not selected as the product used for the members. The timber engineered products glued laminated timber and laminated veneer lumber are produced in a different way, as discussed in this chapter. Still, the mechanical properties of both EWPs are generally similar in case the veneers are placed in longitudinal direction. Ultimately, glued laminated timber is selected in this research project to apply to the members. The selection of glued laminated timber is primarily based on the higher availability of wider standard widths and the many projects that have been built with this product in the past.

Mechanical Connections

In this chapter, the mechanical connection is separated into two types based on their force transfer. The first connection type transfers its forces by direct bearing contact, such as the supported plate of joist hangers and steel brackets. The second connection type transfers its force by lateral loading of the fasteners. (A) slotted-in steel plate(s) or (a) steel plate(s) on the outer side of the beam in combination with fasteners are an example of this type of connection. When calculating the loading capacity of a connection, one generally looks at the compressive strength of timber for connection type 1. For connection type 2, one generally looks at the embedment strength of timber. In this chapter, both strengths are compared for loading parallel and perpendicular to the grain. This comparison² shows that the embedment strength is approximately 10 % higher than the compressive strength parallel to the grain. Perpendicular to the grain, the compressive strength reduces with 91% and the embedment strength with 35% compared to the strength parallel to the grain. The difference in strength is the effect of membrane action that occurs by loading round dowels.

Connection type 2 shows great potential in generating high load capacity for joints that are loaded specifically perpendicular to the grain, which is the case for joints between primary and secondary beams. Moreover, the number of parameters that is involved in computing the capacity of connection type 2 is significantly higher than the number of parameters that determines the capacity of connection type 1. Therefore, connection type 2 matches with the parametric and computational approach of this research project, in which a wide range of possible configurations can be analyzed. According to these observations, the laterally loaded dowel-type connection is selected as the connection type to be examined further in this research project. By applying laterally loaded dowel-type connections to members, an additional moment occurs due to the eccentricity between the members. In this chapter two design approaches were discussed in order to resist the eccentricity moment. Ultimately, the approach whereby the fastener group of the slotted-in steel plate take up the eccentricity moment was selected to apply on further calculations in this research project. The related components of laterally loaded dowel-type connections are analysed further in this chapter and forms the basis of the tool that will be developed further in this research project.

²This comparison is based on an example of glued laminated timber with the strength of GL28h and a dowel diameter of 12 mm

3

Parametric Model

In order to perform a study wherein a high number of parameters are involved, a study that includes a parametric model is an efficient methodology for collecting data. In this research project, a parametric model is constructed that includes relevant parameters for the frame structure (global level) and parameters that construct the different configurations of the laterally loaded dowel-type connection (joint level). The coherence between these two levels is essential to perform an efficient analysis. The output of the system is generated by the implementations of design constraints that guarantee the design regulation in Ultimate Limit State (ULS) and Service Limit State (SLS) for both levels. With the aim of analysing the dimensional interaction between the joints and the members in different frame structures, a number of constructed cases are defined in this chapter. In order to reduce the computational complexity and costs of the study, various design assumptions are made, and the number of sub-parameters that construct the connection are reduced based on their influences on the loading capacity. The main goal of this chapter is to explain the design parameters, constraints, and loads which are implemented into the parametric model to collect the required data for the parametric study. Moreover, the selected sub-parameters, additional design assumptions, and constructed cases are outlined. This chapter will focus on answering the following research question:

- *"Which parameters and constraints will define the parametric model of the frame structure and the joints"*

3.1. Design Parameters

3.1.1. Frame structure

In timber structures, a commonly used frame structure consists of slabs, secondary beams, primary beams, and columns. In general, the secondary beam is directly connected to the primary beam and transfers the load from the slab. The primary beam is commonly connected directly to the column and shapes a column-beam joint. Secondary beams are generally used to reduce the deflection of primary beams and slabs by decreasing the span of the slabs. The design parameters of the frame structure used in this research project are shown in figure 3.1. The first parameter in the frame structure is the distance between the columns (grid sizes) in two directions.

All primary beams connect one column to another, as discussed in section 2.3.1. In this design approach, the length of the primary beams and secondary beams determines the grid sizes of the columns. The maximum length of the timber elements is in general determined by the following aspects. First the length is determined by the maximum available length offered by the glulam timber suppliers. Suppliers like Withagen and Nordlam managed to produce maximum lengths of approximately 18-24 m with their standard procedure. Second, in terms of transport, the maximum element size for standard¹ transport is 13.6 m ("Wettelijke Afmetingen Ontheffingen", n.d.). Third, the maximum height of the total floor construction² are limited to absolute heights to satisfy the required minimal free heights of the indoor space. Especially in buildings with multiple floors, the maximum required height of the total floor

¹Transport that does not need licences and assistance during transport

²primarily includes suspended ceilings, beams, slabs and, finishing layers

construction plays an important role to limit the total height of the building. The maximum total floor construction height have influences on the maximum allowable height of the beams, which limit the maximum span of the beams. Another parameter that is included in the frame structure is the spacing between the secondary beams (SB), as illustrated in figure 3.1.

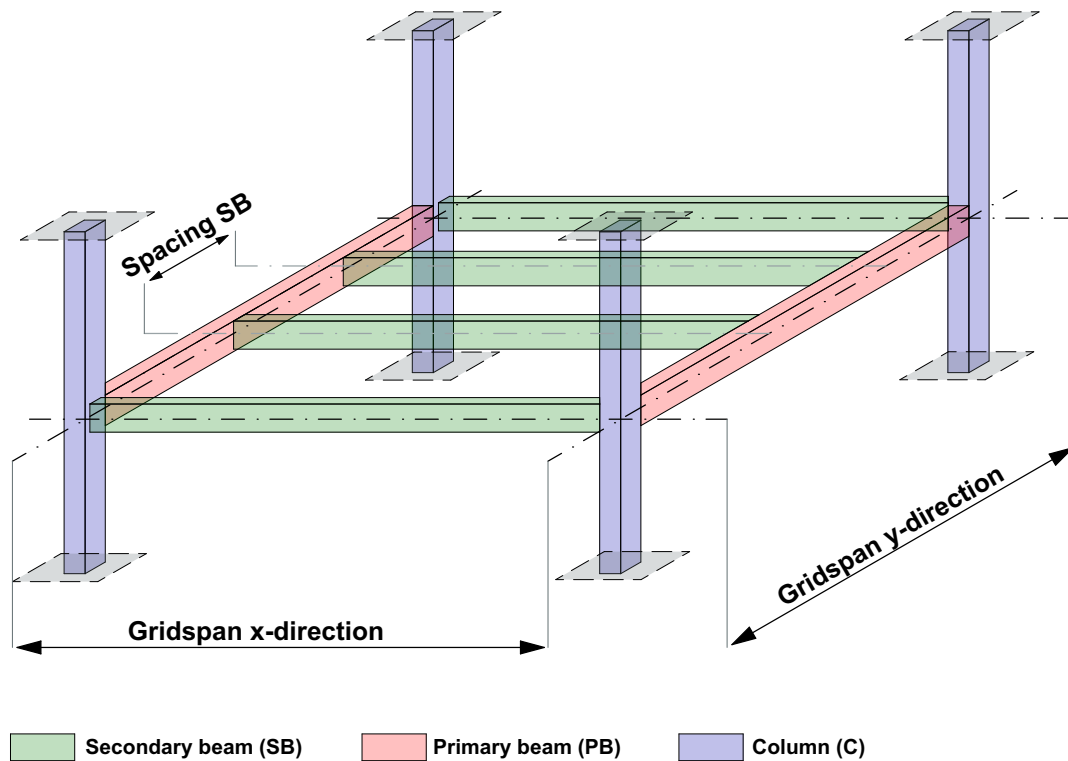


Figure 3.1: Global frame structure

In general, a building consists of multiple grid cells with equal or non equal sizes. In this research project, the grid cell is extended in two directions with the same dimensions, as illustrated in figure 3.2. In commercial construction and residential construction, standard grid sizes are generally adjusted to the standard interior finishing systems such as ceilings and wall systems (Kolb, 2008). In general, this standard module size is a multiple of 0.625 m. In this research project, the constructed cases as discussed in chapter 3.4 are based on this standard grid size.

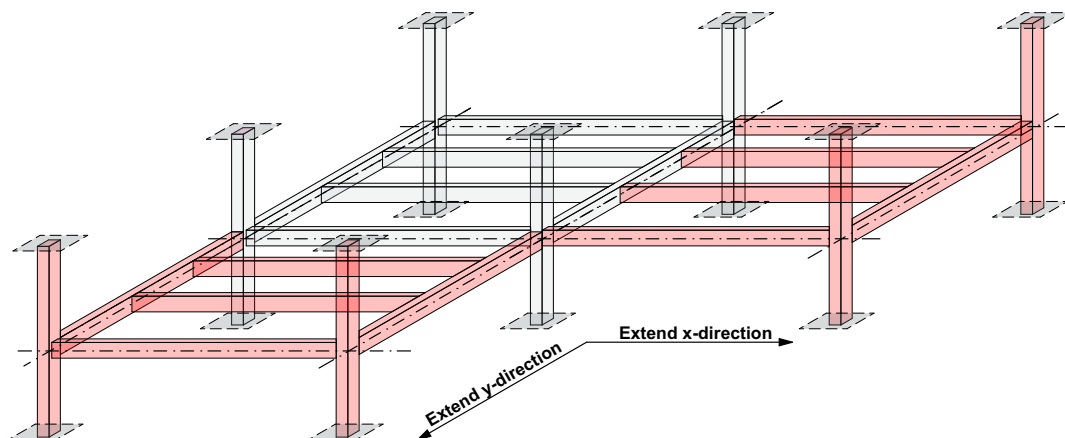


Figure 3.2: Extension grid cells

3.1.2. Joints

In chapter 2.3 'Mechanical Joints', different connections that are used in practice are examined. From this study, the joint types that transfer their forces by lateral loading of the fastener are selected as the mechanical joint type to analyse further in this research project. This joint type has a large number of parameters that are involved in determining the loading capacity, such as fastener type, fastener quality, diameter of the fastener, fastener layout, position of the steel plate(s), and thickness of the steel plate(s). In this paragraph, the sub-parameters used in this study are discussed. The number of sub-parameters was reduced in order to reduce the complexity of the model. The sub-parameters were selected based on whether they have a significant influence on the loading capacity of the connection. The joint is separated into two parts to have a clear overview of the parameters and sub-parameters as illustrated in figure 3.3. As the figure shows, the connection that included steel part A and B is applicable for joints between secondary beams and primary beams and between primary beams and columns. In this paragraph, steel part A is also known as a single or double steel-to-timber connection (depending on the configuration of the joint) and steel part B as slotted-in steel plate(s) connection.

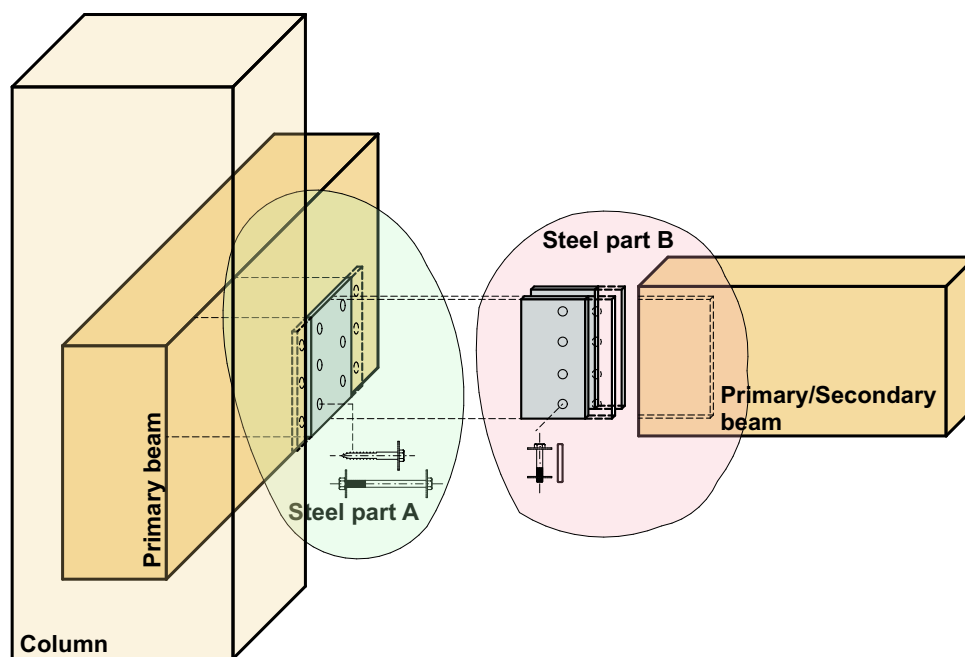


Figure 3.3: Steel elements in the joint

Fastener Type

In this research project, the fastener types bolts, dowels, and lag screws (also known as hexagon head wood screws) are examined, as discussed in section 2.3.3. The selected fastener type depends on the the steel part and the joint configuration. In this research project, steel part B consist of dowels and bolts and steel part A consist of lag screws and bolts.

Fastener Quality

In the construction industry, commonly used steel qualities for fasteners are 4.6, 6.8, 8.8, and 10.9. These steel qualities are examined in this study. Table 3.1 illustrates the corresponding ultimate steel strength for each steel quality. Moreover, generally, the steel quality of lag screws is limited to 4.6. This study therefore uses a steel quality of 4.6.

| Steel quality | f_u [N/mm ²] |
|---------------|----------------------------|
| 4.6 | 400 |
| 6.8 | 600 |
| 8.8 | 800 |
| 10.9 | 1000 |

Table 3.1: Ultimate steel strength of different steel qualities

Diameter Fastener

A wide range of diameters is chosen to examine the influence of the diameter on the loading capacity of the connection properly. The diameters 8, 12, 16, 20, and 24 mm are the selected sizes for the fastener types bolts and dowels. In comparison to bolts and dowels, the options in terms of the diameter of lag screws are limited. The diameters that are generally offered for lag screws are 8, 12, and 16 mm.

Layout Fastener Group

The layout of the fastener group illustrates the number of fasteners positioned vertically (rows) and horizontally (columns). The number of rows in a fastener group primarily depends on the minimal distance discussed in section 2.4.5 and the height of the member. The number of columns in the fastener group impacts the eccentricity moment caused by eccentricity between the center lines of two different members. Section 2.3.1 illustrates the eccentricity that occurs between the centroid of the fastener group in the secondary beam and the centre line of the primary beam. By increasing the number of column fasteners, the centroid of the fastener group shifts further away from the centre line of the primary beam/column. The increase in eccentricity generates a higher eccentricity moment, which results in higher force components due to the eccentricity moment in the individual fasteners. To limit the moment caused by eccentricity, the number of columns is set to a maximum of 2 columns.

Position Steel Plate(s)

Different possible positions of steel plate(s) and their corresponding failure mechanisms are discussed in section 2.4.4. The position of the steel plate is already determined for a single shear steel-to-timber connection, as illustrated in figure 3.3. However, for the connection part B, the position of the steel plates can be outside the member or integrated (slotted-in) in the member. Connections with thin steel plates on the outer side of the member are primarily efficient in terms of shear capacity for beam thicknesses between 60 and 100 mm, as observed in graph 2.24. Moreover, for beams that are wider than 100 mm, single slotted-in steel plates become more efficient in terms of steel quantity, since the shear capacity of the single slotted-in steel plate is equal to the connection with steel plates at the outer side of the member. This study therefore uses slotted-in steel plate(s) for the connection type B. In terms of the number of slotted-in steel plates the maximum steel plates is limited to 2 plates, discussed in section 2.4.4.

Thickness Steel Plate(s)

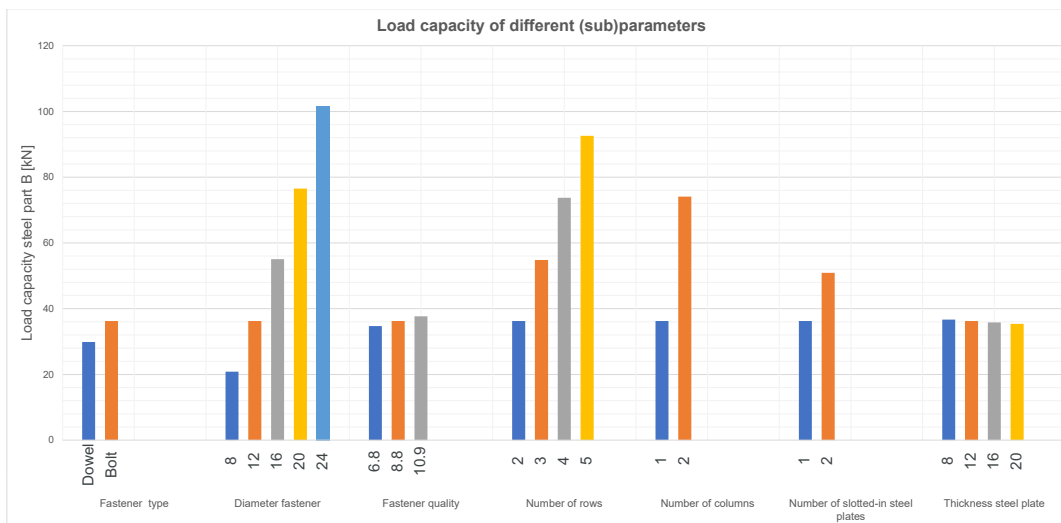
The selecting of steel plate thicknesses is different for steel part A and B by reason of the different failure mechanisms that are involved. The type of failure mechanisms for steel part A depends on the thickness of the steel plate as discussed in section 2.4.4. This study therefore uses a wide range of steel plate thicknesses to examine the effect of thick steel plates and thin steel plates on the shear capacity. The selected thicknesses are 8, 12, 16, and 20 mm

For steel part B (e.g. single or double slotted-in steel plate(s)), the thickness of the steel plate has/have no direct influence on the failure mechanisms. The failure mechanisms related to steel part B, are not categorized into 'thin' and 'thick' steel plate(s) compared to steel part A. Although the steel plate(s) thickness(es) has/have influence on the t_1 and/or t_2 of the timber member. These parameters determine the shear capacity of the related failure mechanisms, which means that the steel plate(s) thickness(es) has indirect influence on the governing failure mechanism. This study therefore uses the steel thicknesses 6,8,10, and 12 mm.

3.1.3. Reduction Parameters

In order to decrease the amount of iterations of the analysis, the number of (sub)-parameters are reduced for steel part A and B. The reduction of parameters is based on the contribution of the (sub)-parameters to the total load capacity of the steel part.

Steel part B consist of all parameters discussed above. In order to find the effect of the sub-parameters on the loading capacity of steel part B, graph 3.4 displays the load capacity of the different (sub)-parameters, while 'locking' the other parameters. At the bottom of the graph the basis 'locked' values are illustrates. The number of fasteners in the row were limited to 5, since the height of the member was 400 mm and the fastener diameter locked to 12 mm. The graph illustrates that the differences in diameter of the fasteners, the number of fastener rows (vertically), and the number of fastener columns (horizontally) have high influence on the total load capacity of steel part B. Moreover, the differences in fastener type and number of slotted-in steel plates have medium effect on the total load capacity of steel part B. Finally, the differences in steel quality of the fasteners and the thickness of the steel plates have low influence on the loading capacity of steel part B. Based on these observations the fastener quality is reduced to solely 8.8 and the steel plate thickness to solely 12 mm.



Basic 'locked' values:

Fastener type: Bolt ; Diameter fastener: 12 ; Fastener quality: 8.8 ; Number of rows: 2 ; Number of columns: 1 ; Number of slotted-in steel plates: 1 ; Thickness steel plate: 12

Figure 3.4: Load capacity different (sub)-parameters

The observations found from the analysis in loading capacity of steel part B is applied on the (sub)-parameters of steel part A. That means that the fastener quality of bolts are reduced to solely 8.8 and the thickness of the steel plate to solely 12 mm.

The failure mechanisms related to steel part A is separated into mechanisms for 'thin' and 'thick' steel plates as discussed in section 2.4.4. The influences of different steel plate thicknesses on the loading capacity of steel part A would be expected higher than steel part B. Especially the combination of a large fastener diameter and a thick steel plate generates a higher loading capacity. A large diameter causes a high yield moment in the fastener, as illustrated in equation 2.2. In general that means that the failure mechanisms, as formulated in equation E.2 becomes the governing mechanism (e.g. the failure mechanisms wherein the embedment strength of the timber is reached). Commonly this mechanism has a brittle failure characteristic. In this research project brittle failure mechanisms are excluded from the analysis's output as discussed in section 3.5. Based on that this research project do not consider different steel plate thicknesses for steel part A in case of single and double steel-to-timber configurations.

Final (Sub)-Parameters

Figure 3.5 shows the final parameters that are analysed further in this research project.

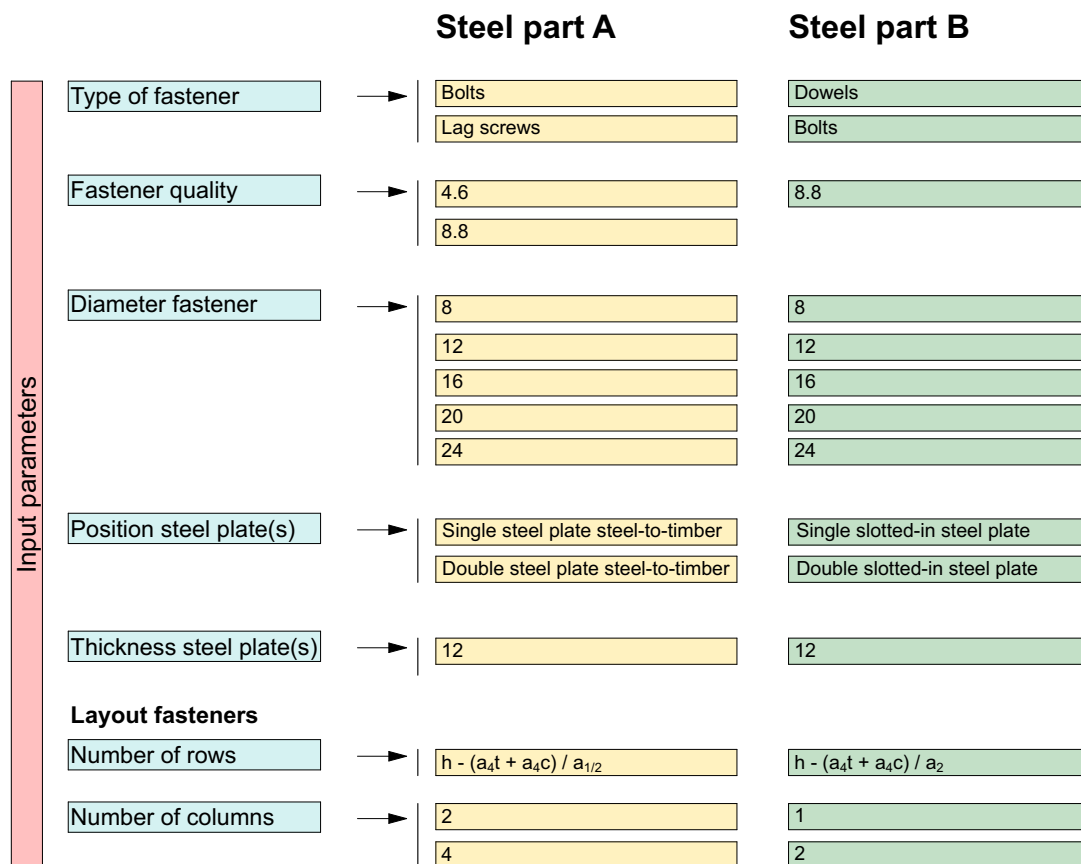


Figure 3.5: Final (sub)-parameters

3.1.4. Members

In section 2.2 different types of engineered wood product are examined. In this analysis glued laminated timber is selected as the wood product to apply on all members in the parametric model. As discussed different strength class are available in glued laminated timber. Although the strength class is defined as a parameter into the tool, for the further analysis one strength class is selected to apply on all constructed cases.

The cross-sectional sizes of the members are parameters in the parametric study. This study therefore uses standard sizes offered by timber suppliers. As discussed in section 2.2 glued laminated timber is construed of multiple lamellas. The standard height of a individual lamella and the number of applied lamellas determined the total height of the member. In this study a distinction is made between the cross-sectional sizes of the beams and columns. According to the sizes of the beams, in this study the lamella with a height of 40 mm and a minimum total height of 120 mm is determined, as illustrated in figure 3.6. Depending on the selected width of the member, the tool determines a corresponding height that fulfills the shear, compression, and bending requirements in ULS and deflection requirements in SLS. The width of the beams has a range between the 140 mm and 240 mm in steps of 20 mm. The cross-sectional sizes of the column has initially the same width as the selected primary beam with the largest width to guarantee that the connection fits at the column. In case these cross-sections does not satisfy the verification, larger dimensions will be applied.

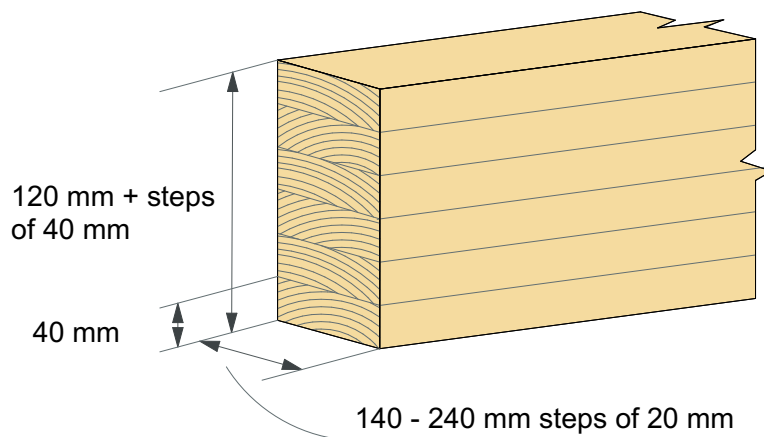


Figure 3.6: Size requirements members

3.2. System Loads

In terms of loads, this study focused solely on the vertical loads applied on the structural frame, as discussed in chapter 1. The vertical loads are explained in this section and determined under the assumption that the structure will be utilized as a office building.

3.2.1. Vertical Loads

The vertical load of the structure is separated into permanent and imposed loads. The permanent load consist of self-weight of the structure, which is variable and depends on the geometry of the frame structure. The CLT floor panels are limited to one dimensional size (height) as discussed in section 1.6. The verification of the panel is computed in section 3.3.1. Moreover, additional loads that represent the finishing of floors and installations, such as electricity and ventilation that is commonly integrated in a suspended ceiling are part of the permanent load.

A frame structure is characterized by their extensive design freedom in the interior, as discussed in section 1.1. This freedom in interior, can lead to changes in the layout of the non-structural interior walls over time. Considering the possibility of changing the layout of the non-structural interior walls, the self-weight of interior walls is categorized as imposed load. Moreover, according to NEN-EN-1991-1-1 (2004), the standard imposed load for office building is applied. A complete overview off all the loads are illustrated in table 3.2.

| Load type | Load pressure [kN/m ²] |
|------------------------|------------------------------------|
| Permanent loads | |
| CLT 5S 140 DL mm | 0.80 |
| Screed floor 60 mm | 1.20 |
| Installation + ceiling | 0.40 |
| Finishing floor | 0.10 |
| Total | 2.50 |
| Imposed loads | |
| Category B - offices | 2.50 |
| Interior walls | 1.00 |
| Total | 3.50 |

Table 3.2: Overview applied loads

3.2.2. Load Combination

NEN-EN-1990 (2004) provides load combinations based on the consequence class (CC) of the structure. The consequence class is introduced to ensure the level of quality required for a structure. In this research project the consequence class is determined as CC2, which leads to the following load combinations for the ULS as shown in equation 3.1 and 3.2.

$$1.35G'' + \sum_{i>1} 1.5\psi_{0,1}Q_{k,i} \quad (3.1)$$

$$1.2G'' + 1.5Q_{k,1}'' + \sum_{i>1} 1.5\psi_{0,1}Q_{k,i} \quad (3.2)$$

In case of SLS-load combination, safety factors are equal to 1.0. According to NEN-EN-1990 (2004) the formula as shown in equation 3.3 need to be applied.

$$G'' + Q_{k,1}'' + \sum_{i>1} \psi_{0,1}Q_{k,i} \quad (3.3)$$

3.2.3. Additional Load Columns

The investigated frame structure in this research project represent a part of the total frame structure of a office building. The columns in the parametric model are designed with additional loads that represent the mass of the upper floor levels of the building. In this study a building of 4 floor levels is assumed. The additional load applied on the columns is a multiplication of the normal force due to mass of one floor. In this calculation, a imposed load of 1 kN/m² is assumed, which represents maintenance activities on the roof. Moreover, the factor for combination value of a variable action (ψ_0) is considered for 2 of the 4 floors.

3.3. Design Constraints

The design verification of all members is performed by applying the Eurocode 5 and NEN-EN 14080 (NEN-EN-14080, 2013; NEN-EN-1995-1-1, 2004). The structural strength of the glued laminated timber depends on the structural class as discussed in section 2.2. NEN-EN-14080 (2013) provides the characteristics strength (R_k) of glued laminated timber. In order to obtain their design strength (R_d), equation 3.4 must be applied, which considered the load-duration, service class and design factor.

$$R_d = \frac{K_{mod}R_k}{\gamma_M} \quad (3.4)$$

The safety factor (γ_M) for glued laminated timber is determined as 1.25 and the selection of the modification number (K_{mod}) is determined by using table 3.3 This table is integrated into the tool, as discussed in more detail in section 4.1.

| Service class | Permanent | Long term | Medium term | Short term | Instantaneous |
|---------------|-----------|-----------|-------------|------------|---------------|
| 1 | 0.60 | 0.70 | 0.80 | 0.90 | 1.10 |
| 2 | 0.60 | 0.70 | 0.80 | 0.90 | 1.10 |
| 3 | 0.50 | 0.55 | 0.65 | 0.70 | 0.90 |

Table 3.3: Modification factor (K_{mod}) based on service class, load-duration according to EC5 and NEN-EN 14080

In this research project the the service class is determined as 1, since the structural frame is assumed to be inside of the building envelop. Service class 1 is characterised by a moisture constant in the materials corresponding to a temperature of 20°C and the relative humidity of the surrounding air only exceeding 65% for a few weeks per year (NEN-EN-1995-1-1, 2004). Moreover, the load-duration is dictated by the predominated imposed load. In this study the imposed load is related to the user-load in offices. According to table 2.2 illustrated in NEN-EN-1991-1-1 (2004), this load corresponds to a load-duration of medium-term. Based on the selection of the service class and the load-duration the K_{mod} factor is determined as 0.80.

3.3.1. Verification Members

Beams and Columns

The design stresses on the members caused by the different load cases in ULS must be verified with the resistance capacity of the members. The resistance capacity is determined by the mechanical properties of the glued laminated timber and the cross-sectional dimensions of the members. The shear and bending, and axial stresses must be verified individually, as well combined. The calculations developed into the tool follows the validation methodology proposed by NEN-EN-1995-1-1 (2004). This methodology can be found in Appendix A.

The global deflection verification of the frame structure need to be verified in the SLS and the resistance of the members is determined by the stiffness capacity of the glued laminated timber and the cross-sectional dimensions of the members. Moreover, the effect of creep as discussed in section 2.1, need to be considered. The calculations developed into the tool follows the validation methodology proposed by NEN-EN-1995-1-1 (2004). This methodology can be found in Appendix A. The criteria related to the maximum deflection of the members are proposed by the Dutch National Annex for NEN-EN 1990+A1+A1/C2 (NEN-EN-1990, 2004). The maximum deflection depends on the function of the floor structure (e.g. intermediate floor or roof) and the appearance of the structure. The latter requirement is related with the crack sensitivity of the walls resting on the floor structure. The deflection criteria is separated into two categories. The first category is the deflection caused by the long-term part of the deflection under permanent loads including quasi-permanent loads (w_2) plus the instantaneous deflection due to the variable actions excluding the quasi-permanent loads (w_3). The second category verified the total deflection which is the summation of w_1 (initial part of the deflection under permanent loads and variable load), w_2 , and w_3 . All the requirements related to the deformation in SLS are illustrated in table 3.4

| | $w_2 + w_3$ | $w_1 + w_2 + w_3$ |
|-----------------------------------|----------------|-------------------|
| Floors | $\leq 0.003 L$ | $\leq 0.004 L$ |
| Floors with crack sensitive walls | $\leq 0.002 L$ | $\leq 0.004 L$ |
| Roof | $\leq 0.004 L$ | $\leq 0.004 L$ |

L = effective span of the member

Table 3.4: Deflection criteria for beams and slabs according to the NEN-EN-1990

CLT Floor Panels

The calculation of the CLT-panel is illustrated in Appendix C. The calculation contains the verification of bending, shear, bearing pressure, deflection, and vibration.

3.3.2. Verification Connections

The design verification of all connections is performed similar to the verification of the members by applying the Eurocode 5 and NEN-EN 14080 (NEN-EN-14080, 2013; NEN-EN-1995-1-1, 2004). All the relevance formulas that determine the load bearing capacity of the connection are discussed in section 2.4. Moreover, the calculation developed into the tool follows the validation methodology proposed by the NEN-EN-1995-1-1 (2004). This methodology can be found in Appendix B. In contrast to the safety factor of members, the safety factor (γ_M) for connections is determined as 1.30.

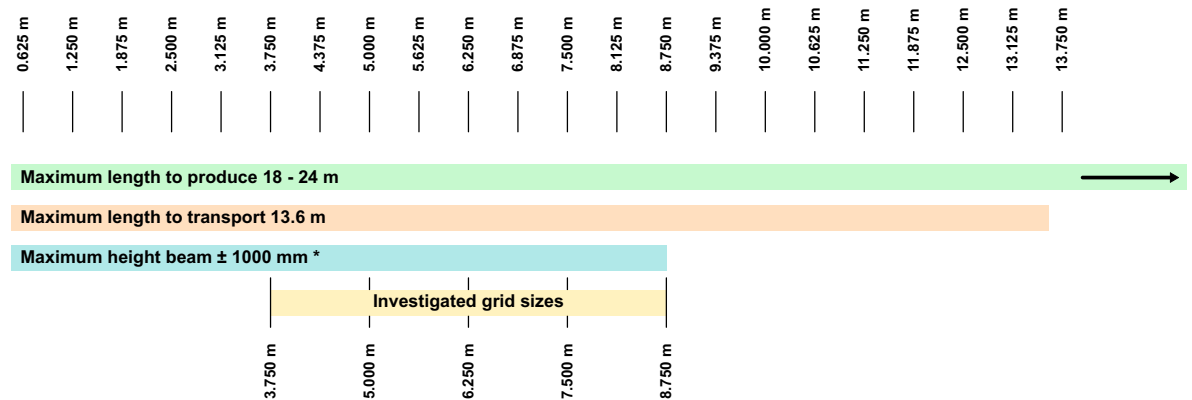
3.4. Constructed Cases

In this section different cases are constructed, which represent the different geometrical configurations of the timber frame structure and defines a number of parameters that are defined for all constructed cases. These cases are analysed by using the self-developed tool, which is explained in more detail in chapter 4. The data that is generated from the tool supports the analysis in examining the influences on the configuration of a laterally loaded dowel-type connection by different geometrical designs of a timber frame structure.

3.4.1. Grid Dimensions Columns

Based on the design approach of the joints made in section 3.1.1, the primary beams and secondary beams are attached to the continuous columns. With this approach the two beams determines the grid sizes of the columns in two directions, as illustrated in figure 3.1. The maximum length of the beams are in general determined by the maximum production length, transport length or maximum allowable height of the beam in order to fulfill the maximum required total height of the floor construction, as discussed in section 3.1.1. Moreover, grid sizes are generally adjusted to the standard module size, which is a multiple of 0.625 m. Based on these observations the following grid size range is determined as illustrated in figure 3.7.

Grid sizes based on standard module 0.625 m



* Based CC2; $G_k = 2.5 \text{ kN/m}^2$; $Q_k = 3.5 \text{ kN/m}^2$

Figure 3.7: Investigated grid dimensions

The graph demonstrates that the maximum height of the beam has the most influence on the maximum grid dimension. Moreover, Kolb (2008) states that proven grid dimension in timber frame structure are 2.50, 5.00, 6.25, and 7.50 m. According to these observations in this research project the following grid dimensions of the columns are set-up for the frame structure.

- 3.75 m
- 5.00 m
- 6.25 m
- 7.50 m
- 8.75 m

Design Constraints for all Cases

In order to analyse solely the geometrical effect of the frame structure, the following parameters as discussed are defined for all cases. These parameters are discussed in more detail in chapter 3.

Input Loads

- Permanent load: 2.5 kN/m^2
- Imposed load: 3.5 kN/m^2

User Related

- Type of floor system: (intermediate) floor
- Appearance non-loading bearing interior wall system: Important
- Load category: Medium-term
- Service class: I

Cross-section Related

- Timber type: Glued laminated timber
- Strength class: Beams = GL28h and columns = GL24h

3.4.2. Analysis 1: Variable Distance Between Secondary Beams

In analysis 1 the distances between the secondary beams vary in sizes 1.25, 2.50, and 3.75 m as illustrated in figure 3.8. The grid sizes of the columns are equal to 7.5 m for all three cases.

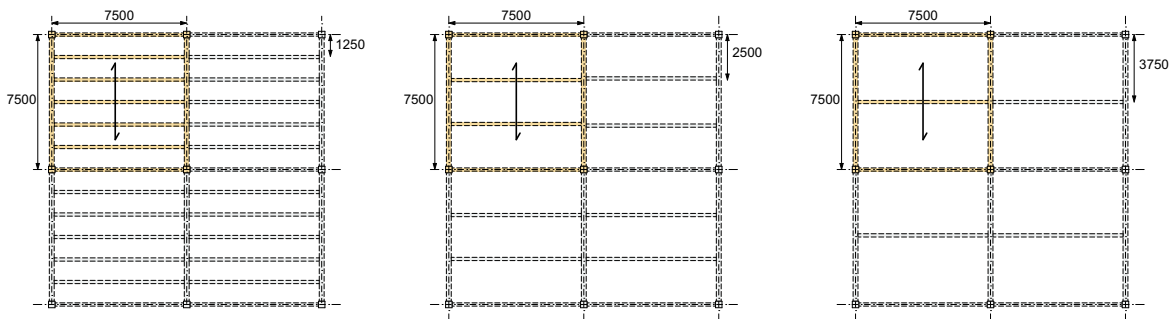


Figure 3.8: Different distances secondary beams

3.4.3. Analysis 2: Different Grid Sizes Columns

In analysis 2 the distances between the secondary beams are all set to 1.25 m and the column grid sizes vary in sizes, 3.75, 5.00, 6.25, 7.50, and 8.75 m.

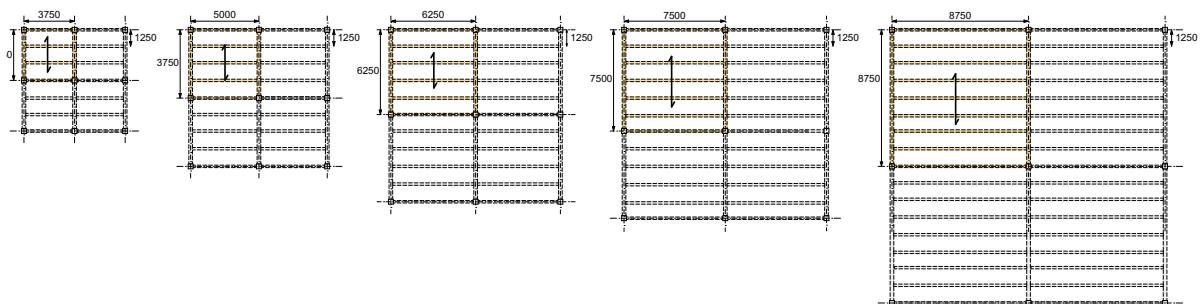


Figure 3.9: Different column grid sizes

3.5. Design Assumptions

In order to develop an efficient parametric model design assumptions need to be made. The following assumptions are made which have an effect on the results.

Brittle Failure Mechanisms

As mentioned in section 2.4.5, structural engineers prefer ductile failure mechanisms over brittle failure mechanisms in connections to guarantee a ductile behaviour of the global system. The failure mechanisms discussed in section 2.4.4 consist of the brittle failure mechanisms that are shown in figure 3.5. The output of the computational study includes the related mechanisms of each configuration. This allows one to extract the brittle failure mechanisms from the data.

| Steel-to-timber connections | Mechanism | Equation |
|--------------------------------------|-----------|----------|
| Single shear with $t_{steel} < 0,5d$ | C | E.3 |
| Double shear with $t_{steel} < 0,5d$ | J | E.9 |
| Double shear with $t_{steel} > d$ | L | E.11 |
| Slotted-in steel plate | F | E.6 |
| Double slotted-in steel plate | I | E.13 |

Table 3.5: Brittle failure mechanisms of different steel-to-timber connections

Criteria Cross-sectional Size Members

In this research project the cross-sectional size of the members are parameters in the parametric study. The member widths has an range between 140 mm and 240 mm in steps of 20 mm, which represent the standard widths offered by timber suppliers. For each constructed case the tool calculates a set of cross-sectional sizes for each member that satisfy the requirements, as discussed in section 3.1.4. For each member two cross-sectional sizes are selected based on the following criteria.

1. Lowest cross-sectional area (LCA)
2. Lowest height beam (LHB)

The first criteria is relevant for projects wherein the total amount of material an important aspect is within the design. The second criteria is important for projects wherein the total height of the floor construction ³ is limited as discussed in section 3.1.1. In general the member selected based on the lowest cross-sectional area is relatively large in height and small in width and the member selected based on the lowest height is relatively wide in width and small in height. The introduction of these criteria generates in general the two extremes of the design spectrum, which enlarge the research scope for the design of the connection.

The ratio between height and width of the selected members based on the the lowest cross-sectional area criteria will become relatively high for the larger constructed cases such as 7.50 and 8.75 m. In order to avoid large h/w ratio, the following maximum heights are determined for each constructed case.

| Grid sizes column | Maximum height [mm] |
|-------------------|---------------------|
| 3.75x3.75-1.25 | 400 |
| 5.00x5.00-1.25 | 600 |
| 6.25x6.25-1.25 | 800 |
| 7.50x7.50-1.25 | 1000 |
| 8.75x8.75-1.25 | 1200 |

Table 3.6: Maximum height members for each constructed case

³primarily includes suspended ceilings, beams, slabs and, finishing layers

Selected Joints and Member in the Frame Structure

Specific joints and members are selected into the tool, to limit the calculation time of designing and verifying the different configurations of the connections. In both analyses the two joints and corresponding members are analysed as shown in figure 3.10. Joint 1 represent a joint between a primary beam, two secondary beams and a column. In order to simplify the analysis the connection between the column and the primary beam is solely examined. Joint 2 represent a joint between two secondary beams and a primary beam. The dimensional size of the column is determined by column 1, which is the column that carries the highest load in this frame structure.

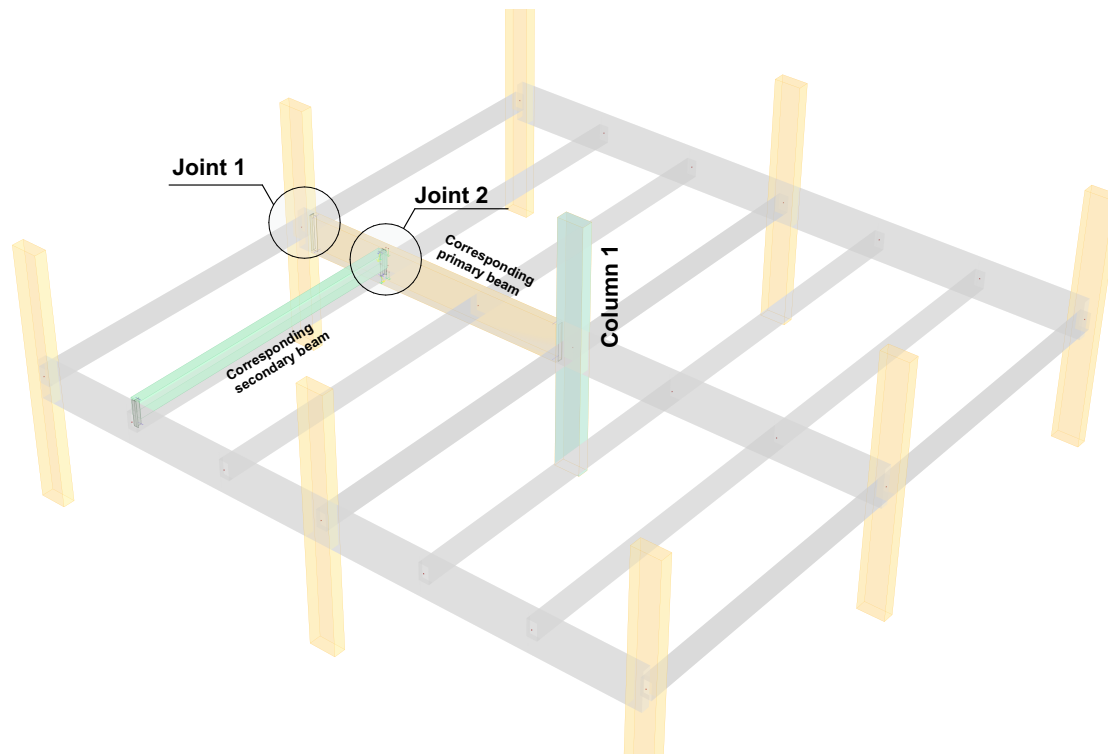


Figure 3.10: The investigated joints in the frame structure

3.6. Conclusions

When performing a parametric study, a common first step is to construct a parametric model. A parametric model includes relevant parameters whose magnitude can be easily changed. When such changes are made, the model automatically adjusts itself. In this research project, the parametric model consists of two parts, which represent the frame structure and the local joints. These two parts have their own parameters. The parameters that are involved for the frame structure are the grid-sizes of the columns in two directions and the distance between the secondary beams. At joint level, the parameters that are involved construct the configuration of the laterally loaded dowel-type connection. This connection is separated into steel part A and steel part B, since these steel parts have different parameters and failure mechanisms, which are related to the load capacity of the connection. For both steel parts, the amount of (sub-)parameters is limited in order to reduce the computational complexity of the model. The selection of the (sub-)parameters is based on the contribution of the (sub-)parameters to the total load capacity of the steel part. This study shows that the parameters diameter of the fastener, fastener type, number of slotted-in steel plate(s), the layout of the fastener group⁴ have a significant effect on the total load capacity of steel part B. Therefore, these parameters were selected.

For steel part B, the influence of different steel plate thicknesses on the load capacity was limited. Based on the related failure mechanism, the influence of different steel plate thicknesses on the load capacity is larger for steel part A than for steel part B. Especially the combination of a large fastener

⁴Consists of the number of fasteners in row(s) and column(s)

diameter and a thick steel plate generates a higher loading capacity. The corresponding failure mechanism shows characteristics of brittle failure behaviour, leading to the parameter thickness of the steel plate to be excluded from this research project for steel part A. The final (sub-)parameters for steel part A and B can be found in figure 3.5.

As explained in section 3.3, the validation of each design variable was done by implementing design constraints related to the members and the connections in the frame structure. Moreover, different constructed cases were determined, which represent the different geometrical configurations of the timber structure. Two categories were introduced that contain constructed cases and provide the input for the parametric study. The first category consists of the frame structure with the variable distances of 1.25, 2.50, and 3.75 m between the secondary beams and a fixed column grid of 7.50x7.50 m. The second category consists of constructed cases that contain column grid sizes of 3.75, 5.00, 6.25, and 8.75 m.

In order to develop a representative and efficient parametric model, several design assumptions were made, as illustrated in section 3.5. Finally, figure 3.11 shows an overview of all the parameters and constraints that were incorporated in the parametric model.

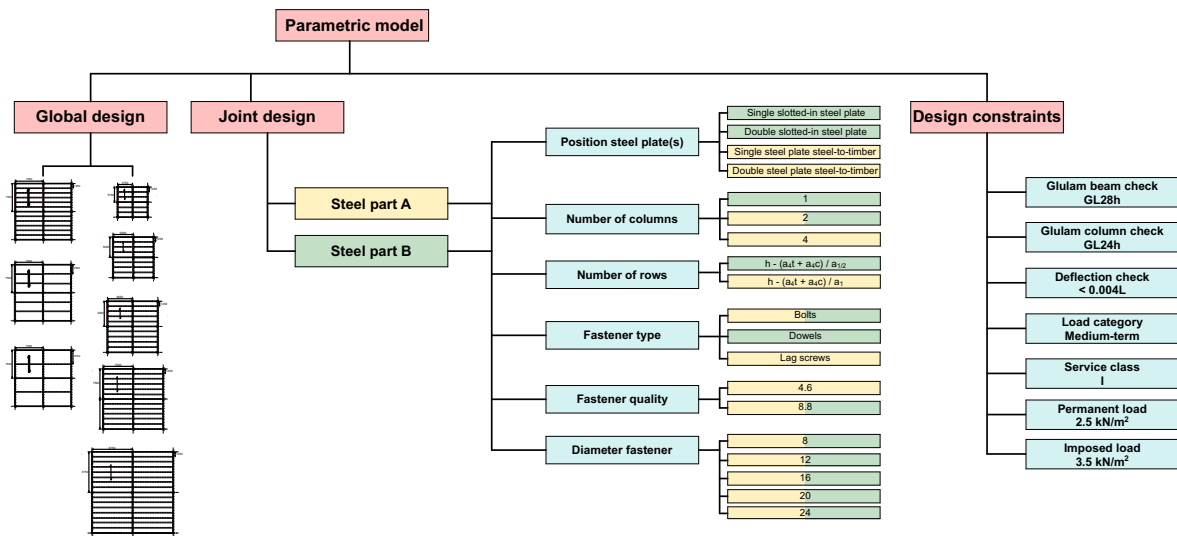
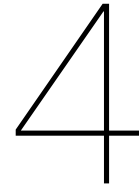


Figure 3.11: Parametric model overview



Development Tool

In this research project, a tool is developed that supports the parametric analysis in examining the influences of laterally loaded dowel-type connections on the cross-section of the members in timber frame structures. The tool provides an output in terms of cross-sectional sizes of the different members in the frame structure and different configurations of the applied connection, including the total mass. Considering the aim of this research project, the tool consists of two parts. The first is the design part, which consists of a parametric model of the frame structure and a parametric model of the connection within the joint. The second part is the calculation part of the tool. This part calculates and verifies different cross-sections that can be applied to the members in the frame structure. Moreover, based on the selected member's cross-section, this part calculates and verifies different configurations according to the relevant parameters found in chapter 3. All of the verifications that are performed in this tool are based on the ULS and SLS regulations. The main challenge within the tool was to create one environment for the analysis of the frame structure and the local joints. The main goals of this chapter are to explain how the tool was constructed and provide insight into the workflow between the different parts described above. Moreover, this chapter outlines the definition of a few key components within the tool. This chapter focuses on answering the following research question:

- *"How can the calculation of structural members and connections be developed and integrated into the tool?"*

4.1. Set-up Tool

As briefly discussed, the tool consist of fundamental elements, such as the parametric model, calculation part, and visualisation part that need to be integrated into a tool. For each element various software packages have been analysed to create a successful workflow. For this research project the following software programs are applied to the individual elements.

Grasshopper

Grasshopper is a visual programming language that is suitable as a plug-in for Rhinoceros. The program Rhinoceros is a 3D computer aided design application software that in combination with Grasshopper parametric geometry can create. In this project, the Grasshopper environment serves as the central 'boardroom' of the tool. In this environment the following processes are generated.

- Generating the geometry of the frame structure.
- Calculating, verifying, and assigning cross-sections to the members.
- Generating the geometry of the connection.
- Calculating, verifying, and assigning different configurations of the connection.
- Determining the total mass of each configuration.

Many processes are generated in the Grasshopper environment, however the two software programs finite element software Dlubal RFEM and Excel applied in the tool runs outside the Grasshopper environment. For these two programs plug-ins are applied to generates a successfully dynamical interaction between Grasshopper and the programs.

RFEM

After the geometry of the frame structure is generated by Grasshopper and the corrected loads and supports are defined, the forces in the structure is analysed by applying the finite element software RFEM. As discussed, this program is not compatible directly with the grasshopper environment. The plug-in parametric FEM toolbox allows an interoperability between the RFEM and Grasshopper through implementing an Application Programming Interface (API) (Apellániz, 2022). This plug-in allows the tool to analyse the forces of the frame structure by applying a certified Finite Element Analysis (FEA) program.

Excel

The components that are programmed in grasshopper to calculate and verify cross-sectional resistance of the members and the load bearing capacity of the connections are partly supported by written formulas in Excel. The introduction of the plug-in Spreax (Spreax, n.d.) allows a dynamic interaction between Grasshopper and Excel. This interaction can be seen as an calculator (in this case Excel) that is working on the background of the Grasshopper environment to calculate the output based on the given input and the predefined formulas in Excel. The advantage of applying this approach, is that the overview of the formulas is clearer and it is more easier to verify the formulas by another person. Moreover, an Excel database is constructed in which the following information is stored. The complete database is shown in appendix F.

- Mechanical properties of the different glued laminated timber classes, such as tension parallel to the grain ($f_{t,0,k}$), compression perpendicular to the grain ($f_{c,90,k}$), mean modulus of elasticity parallel ($E_{m,0,mean}$), and 5 percent density (ρ_k).
- k_{mod} values
- k_{def} values
- Load category
- Load-duration classes
- Permissible additional and final deformation requirements

With the input values load category, service class, appearance of the structure, and configuration of the floor or roof, the corresponding values from the database is automatically selected and applied to the calculation components.

4.2. Workflow

The workflow of the tool, as shown as a flowchart in figure 4.1, demonstrates the interaction between the individual components constructed into the tool. Moreover, it illustrates the process (e.g. the steps that are made) from the input parameters until the generated output. The flowchart consist of the following segments.

First, the constructed cases (green), which defines the input of each constructed case. The constructed case consist of geometrical parameters, which are case depending and parameters that are defined for all cases, such as loads, load category, service class, strength class, and cross-sectional sizes of the members

Second, the global structure (orange), which consists of the analysis and verification of the members in the global structure. After the global geometry of the structure is defined, the structure is analysed by RFEM and the internal forces in the members and nodes are returned to grasshopper environment. Component I applies all the forces to the primary beams, secondary, beams, columns, and nodes of the grasshopper global geometry. The following step is selecting a member in the frame structure in which the tool assigned a cross-section to that specific member. After the member is selected, component

I generates different cross-section that satisfy the shear, compression, and bending requirements in ULS and deflection requirements in SLS. Depending on the selected criteria, which is the smallest cross-sectional area or smallest height member, a cross-sectional size is assigned to the member.

Third, the joint (blue), which consist of the developing of different configurations of the laterally loaded doweled type connection. As discussed in section 3.1.2 the connection consists of steel parts A and B. Each steel part has its own workflow, since the parameters and the resultant forces on the fasteners are different. Component III generates the design space of the group fasteners, which is explained in more detail in section 4.3.1. Depending on the forces in the joint and the layout of the fastener group, component IV and component V calculate the resultant forces for each individual fastener. In section 4.3.2 the distribution of the forces on the individual fasteners are explained in more detail. Parallel to the calculation of the resultant forces of each individual fastener, the load capacity of each individual fastener is computed by component VI for steel part A and component VII for steel part B. The load capacity depends on the configuration of the steel parts which is generated by the predefined parameters (purple). Each configuration of steel part A and B is verified by calculating the unity check between the applied forces on the fasteners and their resistance. Beside the unity check, the total mass and the D_{ratio} of each configuration is computed. The D_{ratio} is introduced to ensure the minimum required distances between the fasteners perpendicular to the grain and parallel to the grain. Finally, a selection has been made for the configurations that has all the same parameters, except from the number of fasteners in the row. For these configurations the configuration with the lowest number or fastener in rows is selected. For the configurations that fulfill all the discussed requirements the total mass of each configuration is part of the output of the tool. In case there is no available configuration, the tool resized the member and the iteration process starts again.

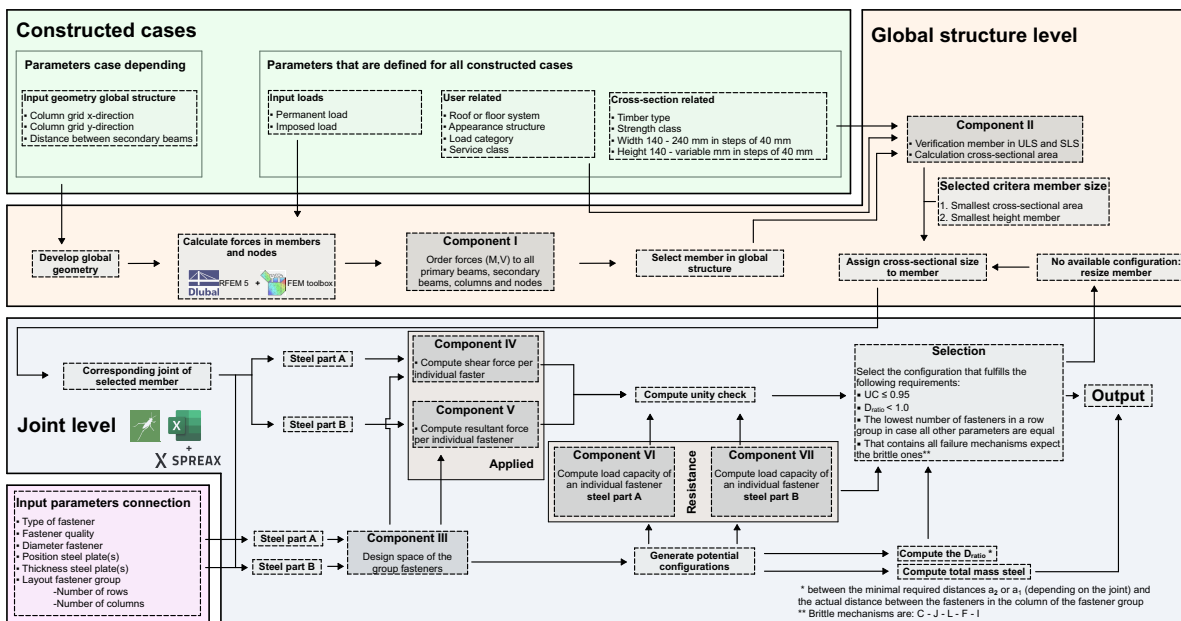


Figure 4.1: General workflow tool

4.3. Development Components

Different components are constructed within the tool to perform processes such as calculating the member sizes and the configurations of the connections, generating design spaces for the fastener group, computing the forces on the individual fasteners and visualizing the connections. In this section some components of the tool are outlined in detail in terms of definition and how they set-up within the tool.

4.3.1. Component III - Layout Fastener Group

The design space of the fastener group, shown in figure 4.2, is created by applying the minimal edge- and end distance according to NEN-EN-1995-1-1 (2004). The angle between the force and the grain, the diameter and the type of fastener determine the minimal distance between the fastener group and the edge and end of the member. In case of the minimum distance between the fasteners itself parallel to the grain, the same variables are involved. The minimal spacing between the fasteners itself perpendicular to the grain is determined solely by the diameter and the type of fastener. These distances are automatically generated in this component of the tool. The boundary of the created design space is the starting point of the first row, last row, and the first column of the fastener group, shown in figure 4.2.

Subsequently, the fasteners placed in the rows are increased until the minimum spacing of the rows perpendicular to the grain (a_2) is reached for the fastener with the smallest diameter. Taking this approach, the spacing between the fasteners perpendicular to the grain with larger diameters is smaller than the required minimal spacing a_2 . In order to avoid this, the component verifies the spacing between the fasteners in the rows for each diameter and removes the configurations that do not fulfill the a_2 spacing requirement. Moreover, the distance between the columns is related to the minimal spacing parallel to the grain (a_1). The position of the fasteners in the rows is defined in such a way that the spacing of each row is always the same, by increasing the number of fasteners.

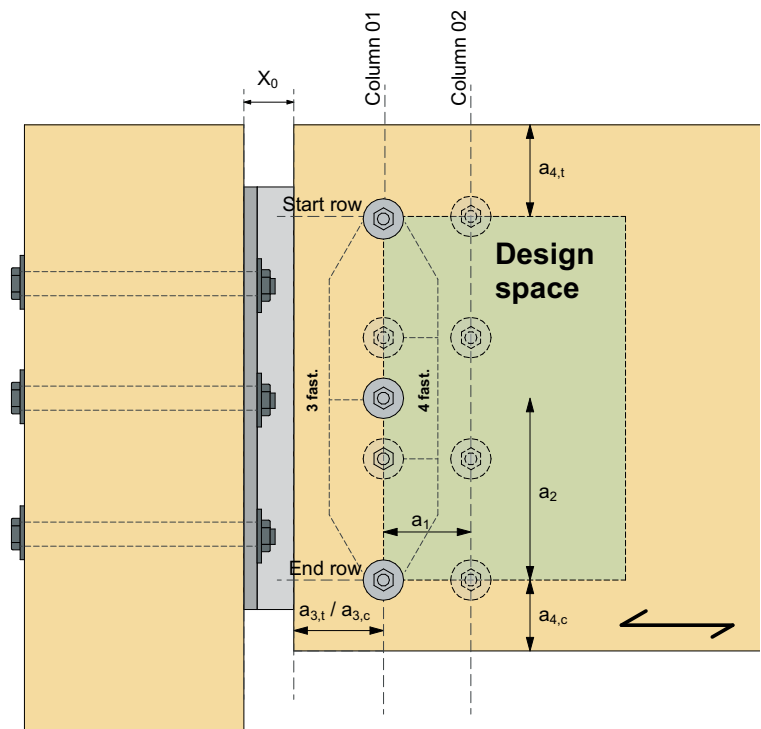


Figure 4.2: Design space of the group fasteners

The size of the slotted-in steel plate(s) is determined by the outer fasteners and has a offset of two times the diameter, as shown in figure 4.3. Moreover, the position(s) of the slotted-in steel plate(s) in the member is/are equally divided as illustrated in figure 4.3. Moreover, the distance between the two members (X_0) must be small to reduce the lever arm of the eccentricity moment. However, the sizes of tools such as wrench or spanner are important to consider in terms of demountability. In this research project a distance of 40 mm is assumed.

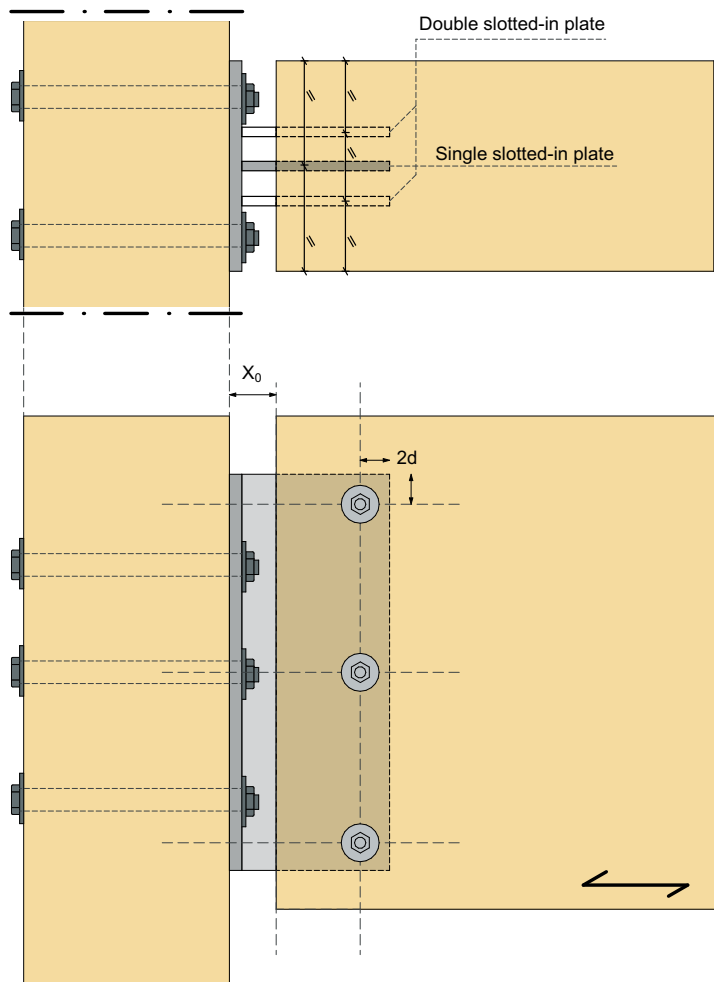


Figure 4.3: Size slotted-in steel plate

4.3.2. Component V - Forces Fasteners

Steel part B that contains slotted-in steel plates have an additional moment due to the eccentricity between the centroid of each member, as shown in figure 4.1. In this thesis, the approach discussed in section 2.3.1 has been chosen in order to determine the moment due to the eccentricity. The position of the total shear force from the member that contains the slotted-in steel plate is determined at the vertical axis of the centroid of the fastener group. Figure 4.4 illustrates the centroid of the fastener group for a double column fastener and a single column fastener. The horizontal distance between the vertical axis of the centroid and the edge of the other member causes the eccentricity (e), shown in figure 4.4. The eccentricity times the total shear force from the member with the slotted-in steel plate creates the eccentricity moment. This moment is taken by the fastener group. Depending on the configuration of the fastener group, each individual fastener is loaded by force components from the shear force and/or the eccentricity moment. The total shear force is assumed to be equally distributed across the total number of fasteners. Moreover, the force component of the eccentricity moment depends on the lever arm (r_i) between the centroid of the fastener group and each individual fastener, shown in figure 4.4.

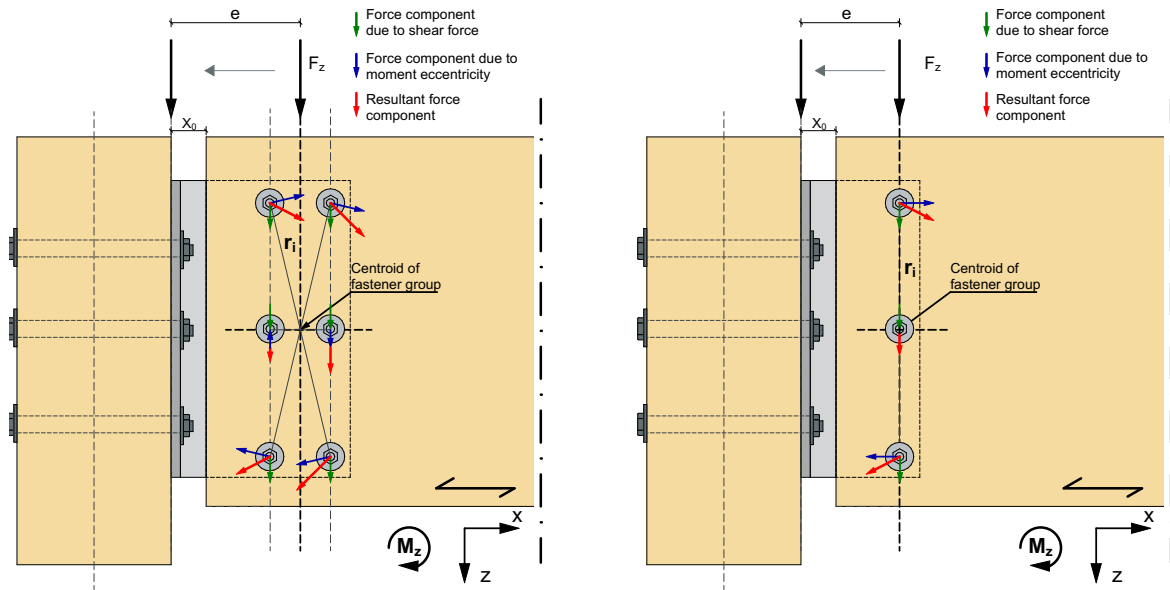


Figure 4.4: Force components fasteners

By applying the equation 4.1, the force component due to eccentricity for each individual fastener can be computed.

$$F_{v;exm,Rd,i} = \frac{r_i}{\sum r_i^2} M_d \quad (4.1)$$

The eccentricity moment is assumed as linearly distributed over the fastener group. The force component acting on the individual fastener is perpendicular to the lever arm, as shown in figure 4.4. The component calculates for each individual fastener the force components due to shear and moment eccentricity, for all possible configurations. These force components are expressed as vectors in the component, which generates the resultant force component of each individual fastener, as shown in figure 4.4. In addition, the angle between the resultant force of each fastener and the grain of the member is computed, as shown in figure 4.5. With these angles, the embedment strength of each individual fastener can be determined, which is the input for component VI and VII. A similar approach is taken for determining the individual forces on the fasteners of steel part A in component V. In this case only shear forces are acting on the fasteners.

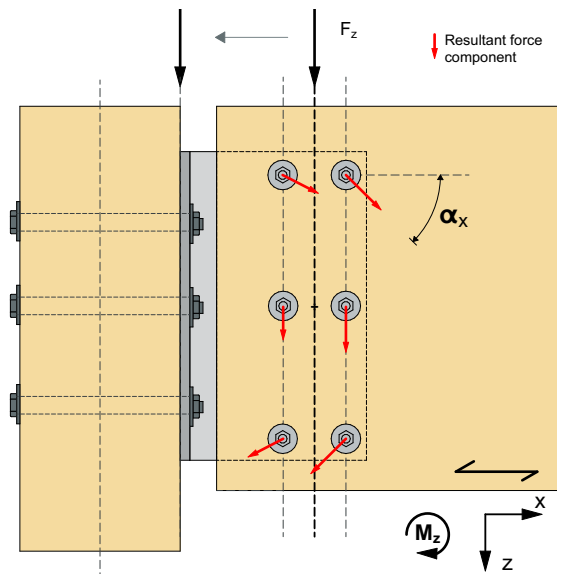


Figure 4.5: Angle between resultant force and grain direction

4.3.3. Component VI - Load Capacity Steel Part A

As illustrated in figure 4.1 component V computes the load capacity of the individual fasteners for steel part A. In this section the workflow of component V is demonstrated and shown in figure 4.6.

As discussed in section 2.4.4 different failure mechanisms are linked to different configurations between steel and timber. In case of steel part A, the configurations of single shear steel-to-timber and double shear steel-to-timber are feasible. The selection of these two types depends on the joint between the members, as shown in figure 2.8 and the fastener type. In case the joint that is selected in the tool consist of a single secondary beam and primary beam and is connected with bolts or lag screws, steel part A is determined as a single shear steel-to-timber connection. In case the selected joint consists of a primary beam with two secondary beams, which are in line with each other the following two situations are possible. First, if steel part A consist of bolts, the steel part is determined as a double shear steel-to-timber connection. Second, if steel part A consist of lag screws, the steel part is determined as a single shear steel-to-timber connections.

Another aspect that plays a role in determining the failure mechanism is the identification of the steel plate, as discussed in section 2.4.4. The component automatically determine the steel plate category based on the steel plate thickness and diameter of the fastener for each configurations. After the corresponding failure mechanisms are determined, the next step in the tool is computing the load capacity of the corresponding failure mechanism. One of the elements that determine the load capacity is the additional rope effect of the fastener. In case the configuration consists of lag screws, the tool select first the lengths that suits with the member width. Second, for each available length the axial withdrawal capacity of the fasteners is determined. Later in the process, the tool determines whether the total loading capacity of the available lag screw lengths fulfills the applied forces in the joint. In case the configurations consists of bolts, full penetrations is required to generate any withdrawal capacity of the bolt, which is computed by the tool. In combination with the computed embedment strength at the angle and the yield moment of the fasteners, the load capacity is determined and the governing mechanisms including the load capacity for each configuration is the output of component VI.

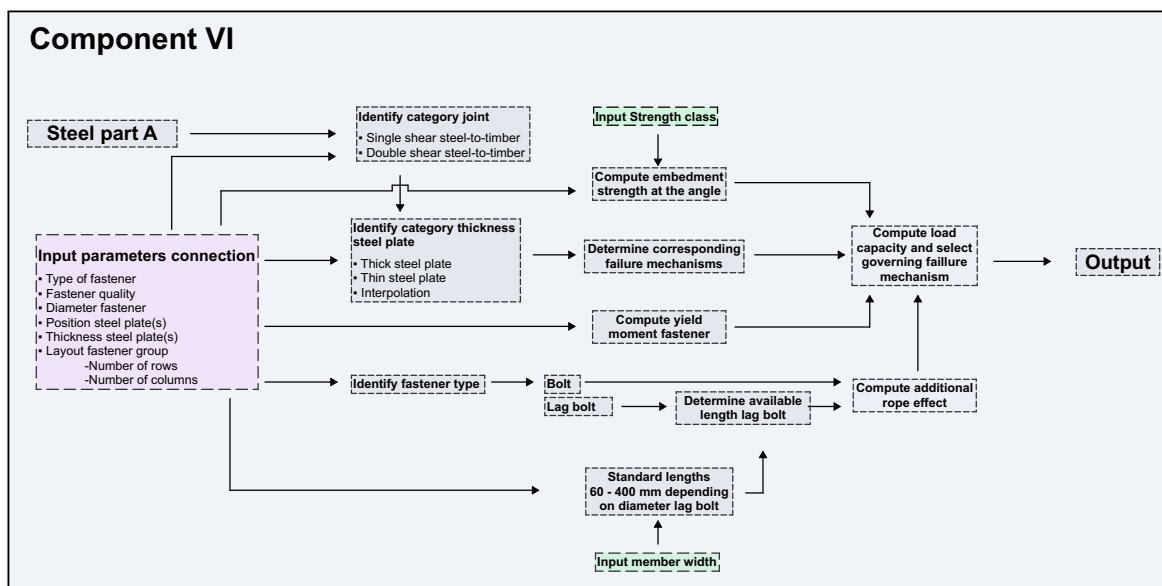


Figure 4.6: Workflow component VI

4.3.4. Component VII - Load Capacity Steel Part B

The workflow of component VII, which calculate the load capacity of steel part B is partly similar to the workflow of component VI as shown in figure 4.7. In this case the single or double slotted-in steel plate determine the corresponding failure mechanism. Moreover, the additional withdrawal capacity are generated only by the bolts.

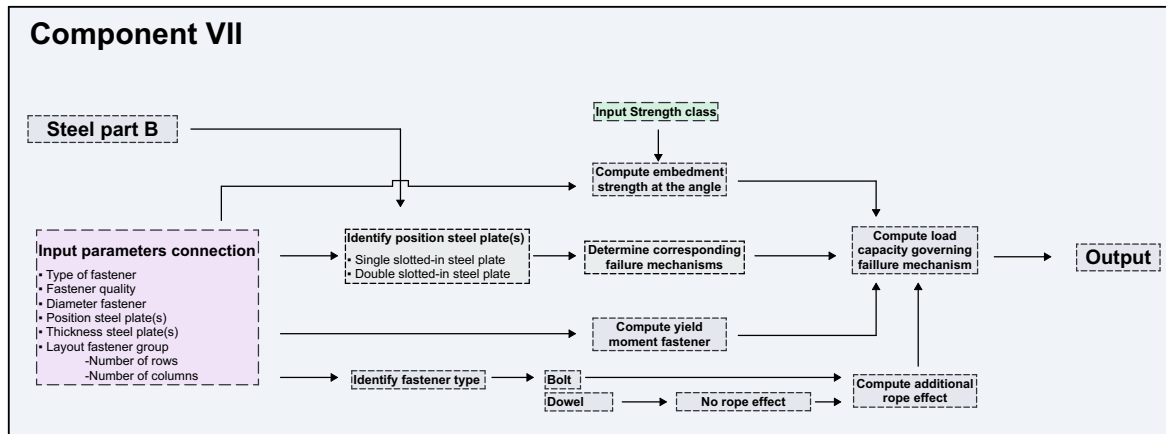


Figure 4.7: Workflow component VII

4.4. Brute Force Method

The aim of this research project is to collect data of different configurations rather than finding the 'optimal' configuration. According to this aim, the tool is constructed based on the brute-force algorithm. This allows the tool to collect the data for all possible combinations, within a constrained search space. Since this method generates all possible combinations, a number of combinations will not satisfy certain requirements. In the tool a component is constructed that exclude these combinations based the requirements which are discussed in section 4.5.

4.5. Output Tool

The complete output of steel part A and B are separately stored in Excel as shown in figure 4.8. The output contains a list of unique configurations that satisfy the prescribed requirements defined in the selection component as illustrated in figure 4.1. The prescribed requirements are the following.

- The load capacity unity check (UC) of the configuration ≤ 0.95
- $D_{ratio} < 1.00$
- Exclude the brittle failure mechanisms (C, J, L, F, I)
- The lowest possible number of fastener in a column of a fastener group of each configuration

Each unique configuration includes the following data.

- Fastener type
- Diameter fastener
- Steel strength fastener
- Thickness steel plate
- Number of fasteners in row
- Number of fasteners in column
- U.C. configuration
- Governing failure mechanism
- Length of lag screw (steel part A)
- Total mass configuration
- D_{ratio}

Steel part A

| Fastener type | Diameter fastener | Steel strength fastener | Thickness steel plate | Number of fasteners in row | Number of column fasteners | UC connection configuration | Governing failure mechanism | Length of lag bolt [mm] | Total mass connection [kg] | Verification fastener distance perpendicular/parallel to the grain [C] |
|---------------|-------------------|-------------------------|-----------------------|----------------------------|----------------------------|-----------------------------|-----------------------------|-------------------------|----------------------------|--|
| Lag | 8 | 4.6 | 12 | 4 | 2 | 0,914927 | Mechanism d | 70 | 3,38185 | 0,190476 |
| Bolt | 8 | 8,8 | 12 | 3 | 2 | 0,888705 | Mechanism m | Full penetration | 3,49993 | 0,126984 |
| Lag | 12 | 4,6 | 12 | 3 | 2 | 0,914927 | Mechanism d | 70 | 5,00352 | 0,190476 |
| Lag | 8 | 4,6 | 12 | 2 | 4 | 0,914927 | Mechanism d | 70 | 5,155008 | 0,063492 |
| Bolt | 8 | 8,8 | 12 | 2 | 4 | 0,866529 | Mechanism m | Full penetration | 5,177728 | 0,063492 |
| Bolt | 12 | 8,8 | 12 | 2 | 2 | 0,949039 | Mechanism m | Full penetration | 5,182074 | 0,095238 |
| Lag | 16 | 4,6 | 12 | 3 | 2 | 0,662207 | Interpolation | 70 | 6,794054 | 0,233968 |
| Bolt | 16 | 8,8 | 12 | 2 | 2 | 0,484626 | Interpolation | 70 | 7,104637 | 0,126984 |
| Lag | 12 | 4,6 | 12 | 2 | 4 | 0,49059 | Mechanism d | 70 | 7,76169 | 0,095238 |
| Bolt | 12 | 8,8 | 12 | 2 | 4 | 0,324519 | Mechanism m | Full penetration | 7,842411 | 0,095238 |
| Bolt | 20 | 8,8 | 12 | 3 | 2 | 0,297506 | Interpolation | Full penetration | 8,133688 | 0,15873 |
| Lag | 16 | 4,6 | 12 | 2 | 4 | 0,496655 | Interpolation | 70 | 10,536371 | 0,126984 |
| Bolt | 16 | 8,8 | 12 | 2 | 4 | 0,247413 | Interpolation | Full penetration | 10,650754 | 0,126984 |
| Bolt | 20 | 8,8 | 12 | 2 | 4 | 0,198753 | Interpolation | Full penetration | 13,563984 | 0,15873 |

Steel part B

| Fastener type | Diameter fastener | Steel strength fastener | Number of row fasteners | Number of column fasteners | Number of slotted-in plate(s) | Thickness of the slotted-in steel plate(s) | UC connection configuration | Governing failure mechanism | Total mass connection [kg] | Verification fastener distance perpendicular to the grain [C] |
|---------------|-------------------|-------------------------|-------------------------|----------------------------|-------------------------------|--|-----------------------------|-----------------------------|----------------------------|---|
| Dowel | 8 | 8,8 | 7 | 1 | 1 | 12 | 0,948611 | Mechanism g | 1,819727 | 0,545455 |
| Bolt | 8 | 8,8 | 6 | 1 | 1 | 12 | 0,936218 | Mechanism g | 3,905894 | 0,606061 |
| Dowel | 12 | 8,8 | 3 | 1 | 1 | 12 | 0,826381 | Mechanism g | 4,232724 | 0,610819 |
| Bolt | 12 | 8,8 | 3 | 1 | 1 | 12 | 0,937615 | Mechanism g | 4,239976 | 0,40678 |
| Dowel | 8 | 8,8 | 4 | 2 | 1 | 12 | 0,891218 | Mechanism g | 4,539552 | 0,272727 |
| Bolt | 8 | 8,8 | 3 | 2 | 1 | 12 | 0,864608 | Mechanism g | 4,795474 | 0,141414 |
| Dowel | 12 | 8,8 | 2 | 2 | 1 | 12 | 0,820668 | Mechanism g | 5,066187 | 0,152542 |
| Bolt | 16 | 8,8 | 2 | 1 | 1 | 12 | 0,894911 | Mechanism g | 5,173852 | 0,307692 |
| Dowel | 16 | 8,8 | 4 | 1 | 1 | 12 | 0,8324 | Mechanism g | 5,257228 | 0,692686 |
| Bolt | 12 | 8,8 | 2 | 2 | 1 | 12 | 0,692637 | Mechanism g | 5,724188 | 0,203139 |
| Dowel | 20 | 8,8 | 3 | 1 | 1 | 12 | 0,895379 | Mechanism g | 6,091084 | 0,686667 |
| Dowel | 16 | 8,8 | 2 | 2 | 1 | 12 | 0,488565 | Mechanism g | 6,473711 | 0,230192 |
| Bolt | 20 | 8,8 | 2 | 1 | 1 | 12 | 0,786657 | Mechanism g | 6,488427 | 0,444444 |
| Dowel | 24 | 8,8 | 2 | 1 | 1 | 12 | 0,943593 | Mechanism g | 6,651051 | 0,473684 |
| Dowel | 8 | 8,8 | 5 | 1 | 2 | 12 | 0,924498 | Mechanism Iia | 7,145441 | 0,363636 |
| Bolt | 8 | 8,8 | 4 | 1 | 2 | 12 | 0,889288 | Mechanism Iia | 7,184589 | 0,363636 |

Figure 4.8: Data output for steel part A and B

Besides the numerical data that the tool generates, it visualize the different configurations as well. Figure 4.9 shows some configuration examples of the connections applied to the joint between a primary beam and a secondary beam and a joint between a primary beam and a column.

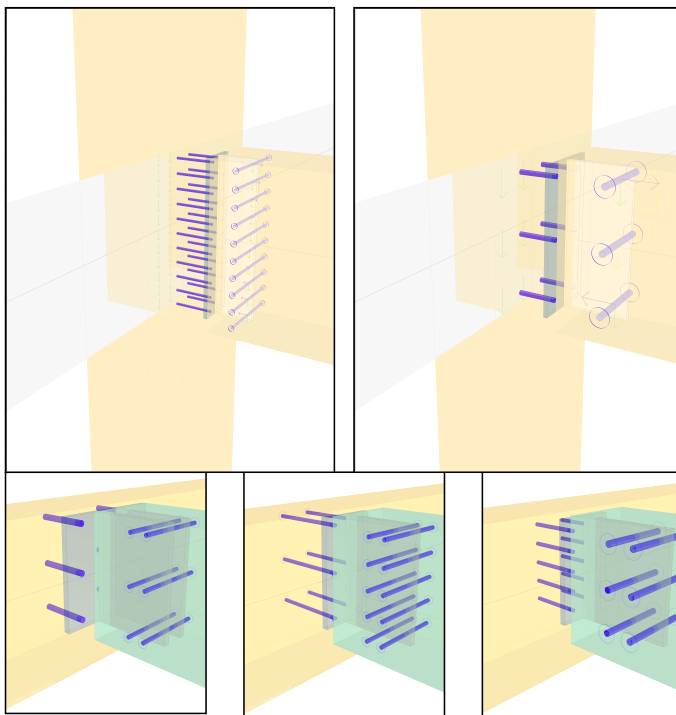


Figure 4.9: Example of different configurations of the joint between primary beam and secondary beam and a primary beam and column

4.6. Design Implications

The tool constructed in this research project was built to study the dimensional interaction between laterally loaded dowel-type connections and structural members in different timber frame structures. The tool generates different possible configurations of a specific connection based on a selected member in the frame structure. These configurations offer a large amount of data, such as the fastener type, the diameter of the fastener, the number of slotted-in steel plates, and the total mass. In this section, the collected data of analysis 2 is visualized by Design Explorer developed by CORE studio (COREStudio, n.d.). This visualization interface allows the engineer to search through all the individual characteristics or a specific range to examine different possible configurations in an efficient manner. Moreover, this section outlines different scenarios in order to demonstrate how the tool can support the engineer in selecting configurations of steel part A and B in joint 1 and 2, based on the predefined criteria.

4.6.1. Visualization Output Tool

In order to display the data from the tool in an accessible manner, the output of the tool, which is discussed in section 4.5, is connected to the visualization interface program Design Explorer. Figure 4.10 shows the interface of grid size 6.25x6.25-1.25 m. By selecting a specific parameter or a range of parameters in the interface, a set of possible configurations appears.

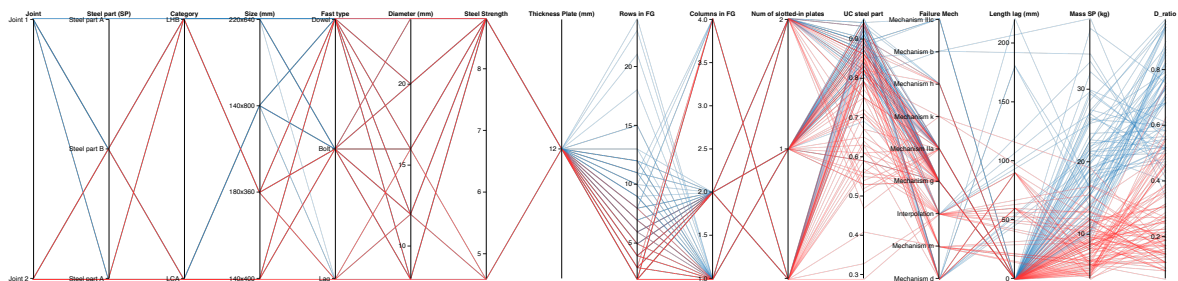


Figure 4.10: Design explorer interface for grid size 6.25x6.25-1.25 (analysis 2)

All grid sizes studied in analysis 2 are visualized by using Design Explorer. Figure 4.11 consists of a QR code and a hyperlink that can be used to access the results of each individual grid size.



(a) Grid size 3.75x3.75-1.25 m (analysis 2)
http://tt-acm.github.io/DesignExplorer/?ID=BL_3VVSbvR



(b) Grid size 5.00x5.00-1.25 m (analysis 2)
http://tt-acm.github.io/DesignExplorer/?ID=BL_3FolQZ1



(c) Grid size 6.25x6.25-1.25 m (analysis 2)
http://tt-acm.github.io/DesignExplorer/?ID=BL_3P0X5VQ



(d) Grid size 7.50x7.50-1.25 m (analysis 2)
http://tt-acm.github.io/DesignExplorer/?ID=BL_3Y1Kaay



(e) Grid size 8.75x8.75-1.25 m (analysis 2)
http://tt-acm.github.io/DesignExplorer/?ID=BL_3h0DWqA

Figure 4.11: QR code and hyperlink of the output of analysis 2 presented in Design Explorer Interface

4.6.2. Different Scenarios in Joint Design Phase

In order to demonstrate how the tool can support the engineer in selecting configurations of steel part A and B, a number of scenarios are outlined.

Lowest Material Quantity

Reduction in material quantity can be an important criterion during the design phase in order to reduce the costs and the environmental footprint of the structure. For instance, for a project, the engineer decides that the amount of timber needs to be minimal. The amount of steel in joint 1 must be limited to 7.5 kg, and the amount of steel in joint 2 must be limited to 20 kg for both steel parts. Applying these criteria to grid size 6.25x6.25-1.25 results in a certain set of possible configurations for joint 1. These are illustrated in figure 4.12. The possible configurations for joint 2 are illustrated in figure 4.13.

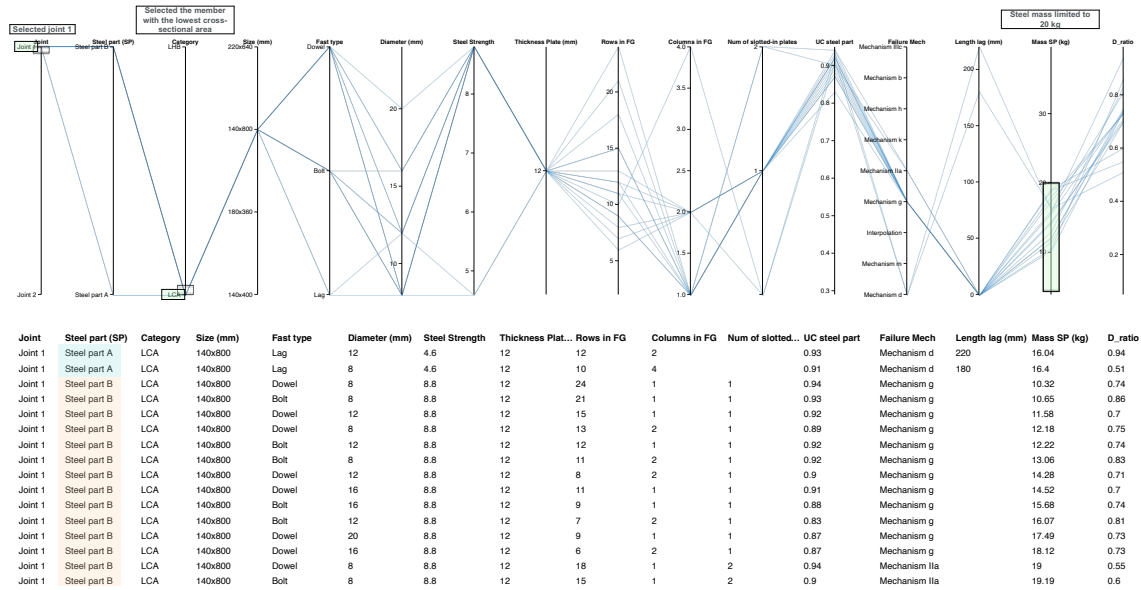


Figure 4.12: Design explorer interface for grid size 6.25x6.25-1.25 - Material quantity criteria for joint 1

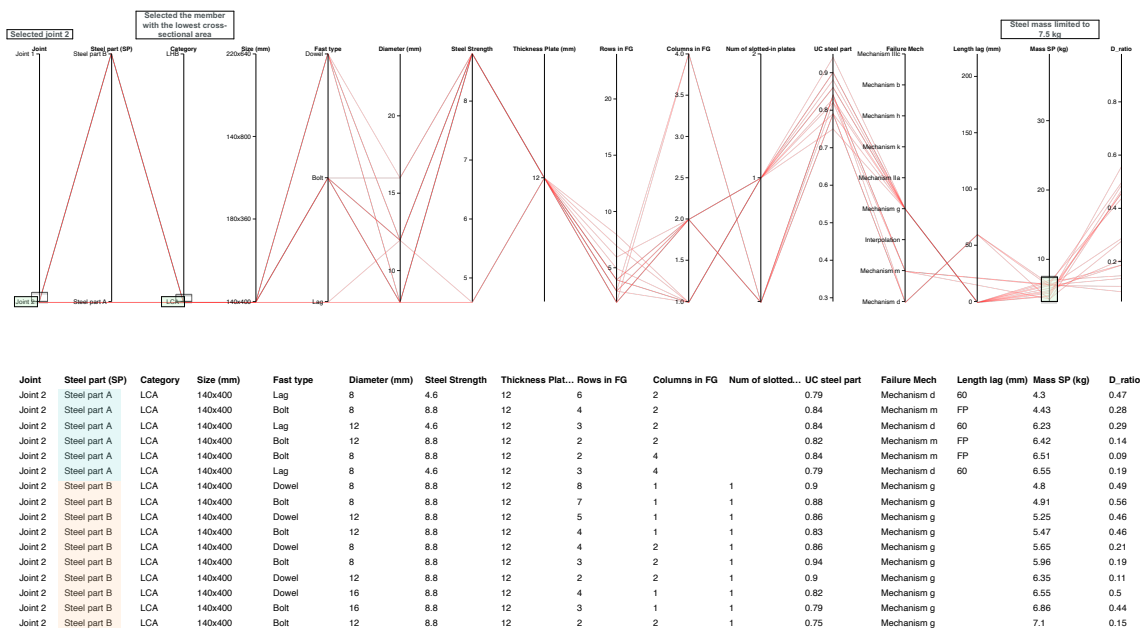


Figure 4.13: Design explorer interface for grid size 6.25x6.25-1.25 - Material quantity criteria for joint 2

Production Speed

Another aspect that could play a role in the building process is the request for fast delivery of the connections by the supplier in order to reduce the construction time. In this case, a 'simple' connection is assumed in the joint design phase. In this research project, the 'simple' connection for steel part B is defined as follows. The connection consists of less than 10 fasteners for joint 1 and less than 4 fasteners for joint 2 in order to reduce the time needed to drill holes in the steel plate. Moreover, for both joints, steel part B consists of solely 1 column in the fastener group and a single slotted-in steel plate in order to reduce the welding time. Applying these criteria to grid size 6.25x6.25-1.25 results in a set of possible configurations for joint 1. These are illustrated in figure 4.14. The possible configurations for joint 2 are illustrated in figure 4.15.

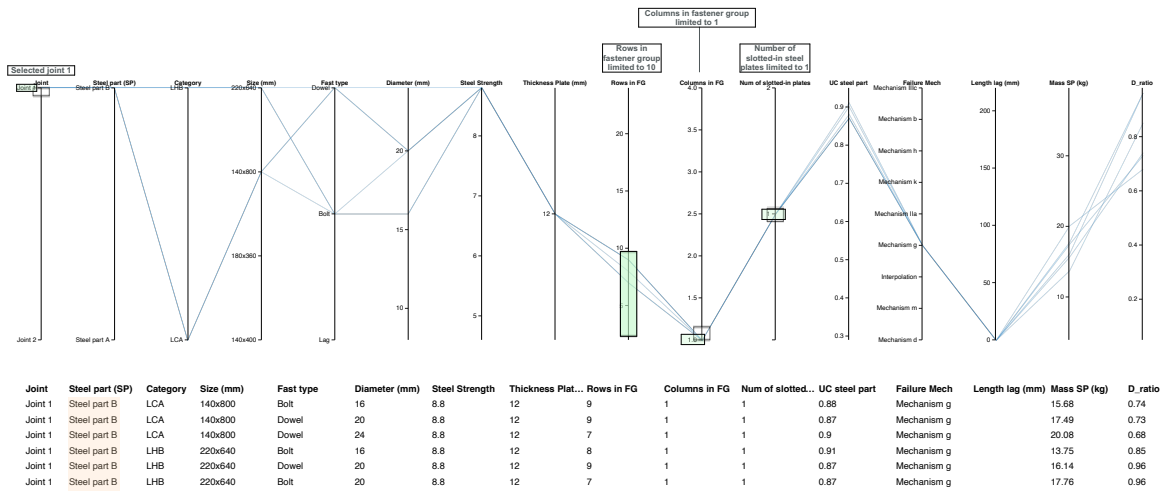


Figure 4.14: Design explorer interface for grid size 6.25x6.25-1.25 - Material quantity criteria for joint 1

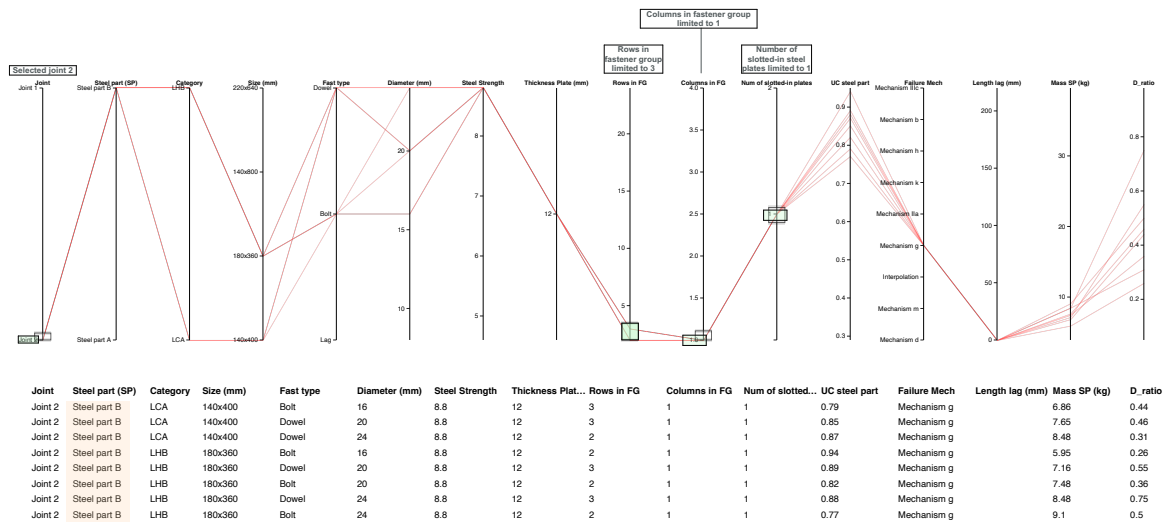


Figure 4.15: Design explorer interface for grid size 6.25x6.25-1.25 - Material quantity criteria for joint 2

Over-capacity Joint

An over-capacity in the joints can be required in order to allow for larger permanent and/or imposed loads to be applied in the future. In the example that is illustrated in figure 4.16, the Unity Check (U.C.) of the joint is limited to 0.60, which means that approximately 40% of the load capacity of the joint is not activated. Yet, in this example taken from analysis 2, the members do not include an over-capacity. The U.C. requirement related to the members should be changed in the tool.

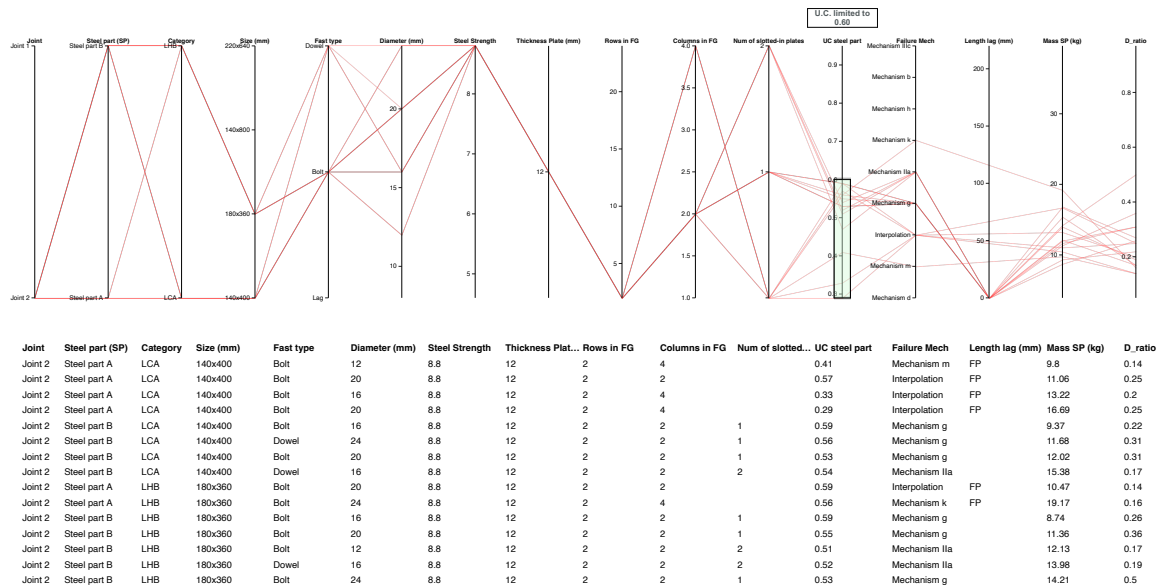


Figure 4.16: Design explorer interface for grid size 6.25x6.25-1.25 - over-capacity 2

Other scenarios

In this section, a number of scenarios was sketched to demonstrate that the tool can assist the engineer in selecting different configurations of steel part A and B based on the predefined criteria. Other scenarios such as the preference of the building contractor in certain connection components or a specific fastener type or diameter being out of stock can easily be incorporated as criteria into the design space.

4.7. Conclusions

This chapter has demonstrated how the developed tool in this research project is constructed and how the workflow between different components is defined. In general, the tool consists of two levels, which is the global structure level and the joint level. Each level is represented in a parametric model. The parametric model is dynamically linked to the finite element software RFEM by using the plug-in FEM toolbox. This allows the tool to calculate the forces in the members and nodes for different geometrical configurations of the global frame structure. With the use of self-developed components constructed in Grasshopper and dynamically linked to Excel-calculations, the cross-sectional sizes of the selected member in the frame structure was calculated. Based on the predefined criteria 'lowest cross-sectional area' and 'lowest height beam', the final cross-sectional sizes are selected. These cross-sectional sizes then move to the part of the tool that focuses on the joint level.

This part of the tool generates different configurations for steel part A and B based on the corresponding parameters. Different processes, such as generating the design space for the fastener group, computing the individual forces on the fasteners, identifying the correct failure mechanisms, and computing the load capacity of each configuration, are constructed within self-developed components. A list of configurations that consist of the different parameters is verified by the prescribed requirements that are discussed in section 4.5. With this selection, a data set of unique configurations is generated for the two specified cross-sections of the selected member. Figure 4.17 provides a schematic overview of the input and output of the tool.

The constructed tool in this project demonstrates how different components within one environment and outside the environment successfully interact with each other. The implementation of the brute force method, which studies all possible solutions in a constrained search space, allowed for the following step in this research project to be made, which is analysing the influences of different geometrical frame structures on the configurations of a laterally loaded dowel-type connection.

The tool constructed in this research project was built to study the dimensional interaction between laterally loaded dowel-type connections and structural members in different timber frame structures. However, the different scenarios outlined in this chapter have shown that the tool is also valuable on its own. The large amount of data that is generated by the tool allows the engineer to explore the different possible configurations when designing joints. By connecting the output of the tool to the Design Explorer interface, the engineer has the opportunity to search through all the individual characteristics or a specific range and examine different possible connections in an efficient manner. Important to note is that the data visualized in Design Explorer is based on the geometries of the timber frame structures studied in analysis 2. In practice, the tool is widely applicable on geometries with different column grid sizes and different distances between the secondary beams.

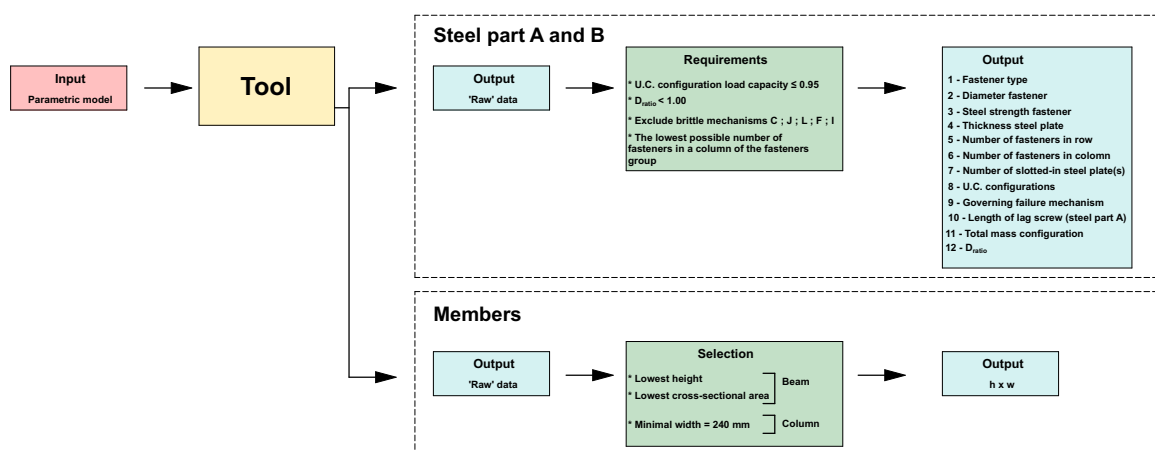


Figure 4.17: Schematic overview input - output tool

5

Results and Discussion

In order to analyse the influences of different geometrical configurations of the timber structure on the configuration of laterally loaded dowel-type connections, two analyses were performed, as discussed in section 3.4. Analysis 1 examined the different distances between the secondary beams, and analysis 2 studied the different grid sizes of the columns. Both analyses were performed by using the brute-force algorithm. The output contains the number of unique configurations including the corresponding parameters, as discussed in section 4.5. The main goal of this chapter is to summarize the findings collected from the two analyses and to discuss relevant observations from the collected data. This chapter focuses on answering the following research question:

- *"How do the different geometrical designs of a timber frame structure influence the configuration of a laterally loaded dowel-type connection?"*

5.1. Results and Observations

This section presents the data collected in analysis 1 and 2. The configurations of steel parts A and B were determined by the parameters that are outlined in section 4.5. Graphs 1a present the ratio between the sub-parameters of the parameters that are listed below. The ratio is expressed as the number of unique configurations for the specified steel part, selected member, and frame design.

- Fastener type
- Diameter fastener
- Number of columns in fastener group steel part B
- Number of columns in fastener group steel part A
- Number of slotted-in steel plates in steel part B

Moreover, graphs 1b present an overview of the total number of possible configurations for each constructed case. Finally, graphs 1c illustrate the steel mass ratio between the unique configurations of steel part A and B. Although this is not one of the aims of this research project, the difference between the amount of material used in the different configurations has an effect not only on the costs, but also on the environmental footprint of the structure, caused by the large amount of CO₂ released during the production of steel (van der Lugt, P., 2020). This makes the steel mass ratio an interesting factor to consider. Therefore, the steel mass ratio between the unique configurations of steel part A and B is shown in graphs 1c.

5.1.1. Graph Interpretation Corresponding Parameters

In order to allow the reader to interpret the graphs properly, the layout of the graphs is explained. The horizontal axis represents the different geometrical constructed cases from analysis 1 and 2. The vertical axis illustrates the joint between the primary beam and secondary beam (joint 2) and the joint

between the primary beam and column (joint 1), as discussed in section 3.5. The two joints are separated into two member size categories. The first category is the member size that contains the lowest cross-sectional area (LCA), and the second category represents the members with the lowest height beam (LHB), as discussed in section 3.5. The corresponding cross-sectional size of each member is displayed in the graph. Finally, the connection within the joint is separated into steel part A and B, as discussed in section 3.1.2.

5.2. Analysis 1: Variable Distances Between Secondary Beams

The observations that are linked to the following graphs represent the outcome of analysis 1. This analysis focuses on the variable distances between the secondary beams with a fixed column grid size.

5.2.1. Graphs 1a: Corresponding Parameters

The following graphs represent the ratio between the sub-parameters that construct the different laterally loaded dowel-type configurations.

Ratio Fastener Type - Steel Part B

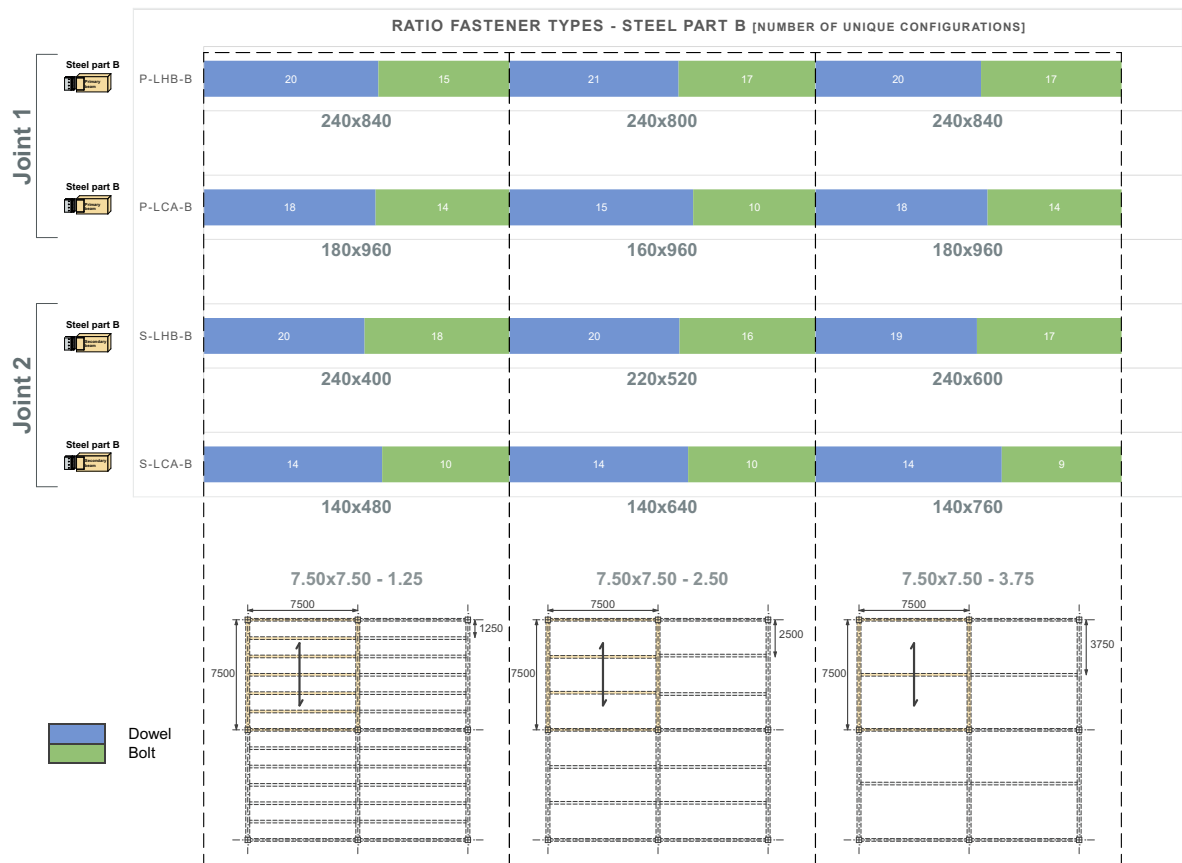


Figure 5.1: Ratio fastener type - steel part B

The following observations can be made from the graph that is shown in figure 5.1.

Joint 1

1. The contribution of dowels is higher compared to bolts for both member categories and all constructed cases.

- There is no significant difference between the contribution of dowels and bolts for the different constructed cases. In general, the difference is approximately four for both member categories.

Joint 2

- A similar pattern is observed between the contribution of dowels and bolts compared to joint 1.
- In case of the LHB-member (220x520), the differences in contribution between dowels and bolts is twice as large compared to the remaining constructed cases.

Ratio Fastener Type - Steel Part A

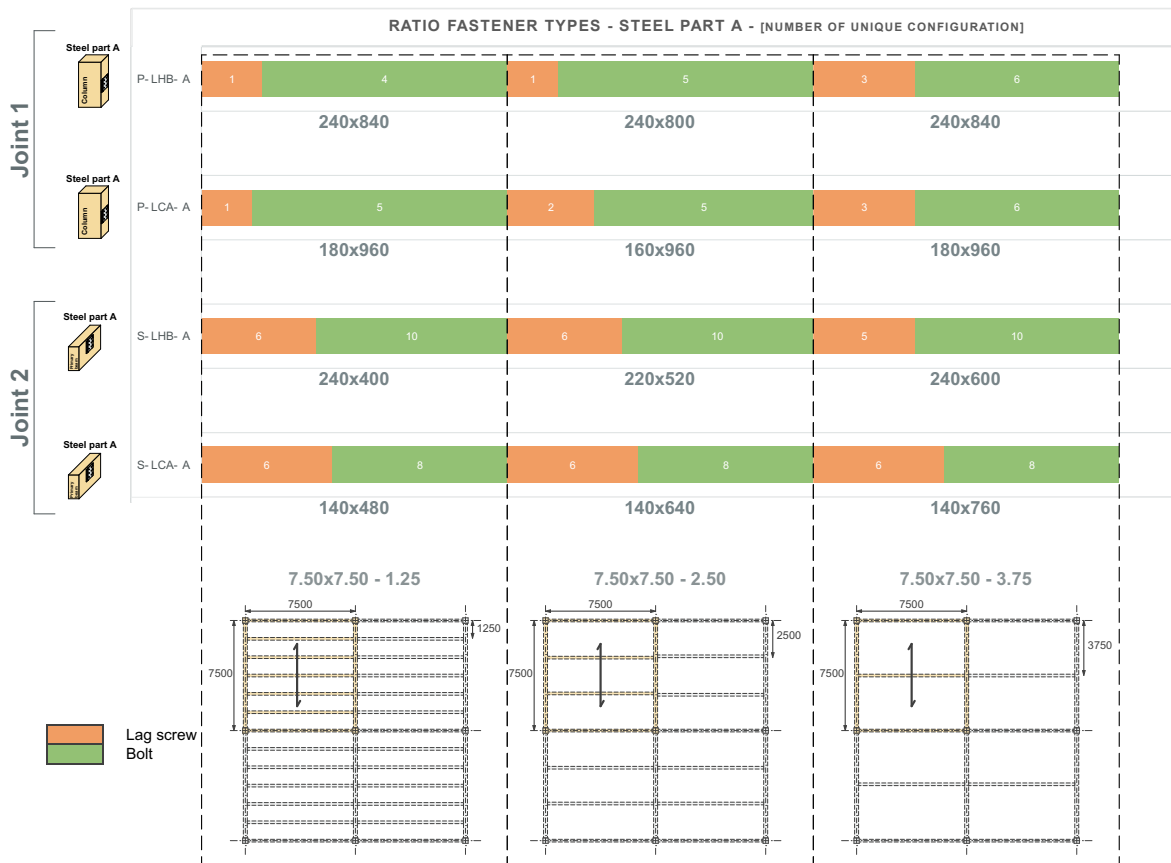


Figure 5.2: Ratio fastener type - steel part A

The following observations can be made from the graph that is shown in figure 5.2.

Joint 1

- Bolts strongly dominate lag screws for both member categories and all constructed cases.
- The number of unique configurations that consist of lag screws slightly increases with the enlargement of the secondary beam spans.

Joint 2

- The number of configurations that contain lag screws is significantly higher compared to joint 1 for both member categories and all constructed cases.
- The ratio between lag screws and bolts is constantly distributed over all constructed cases for both beams, except for the LHB-member (240x600).

Ratio Diameter Fastener - Steel Part B

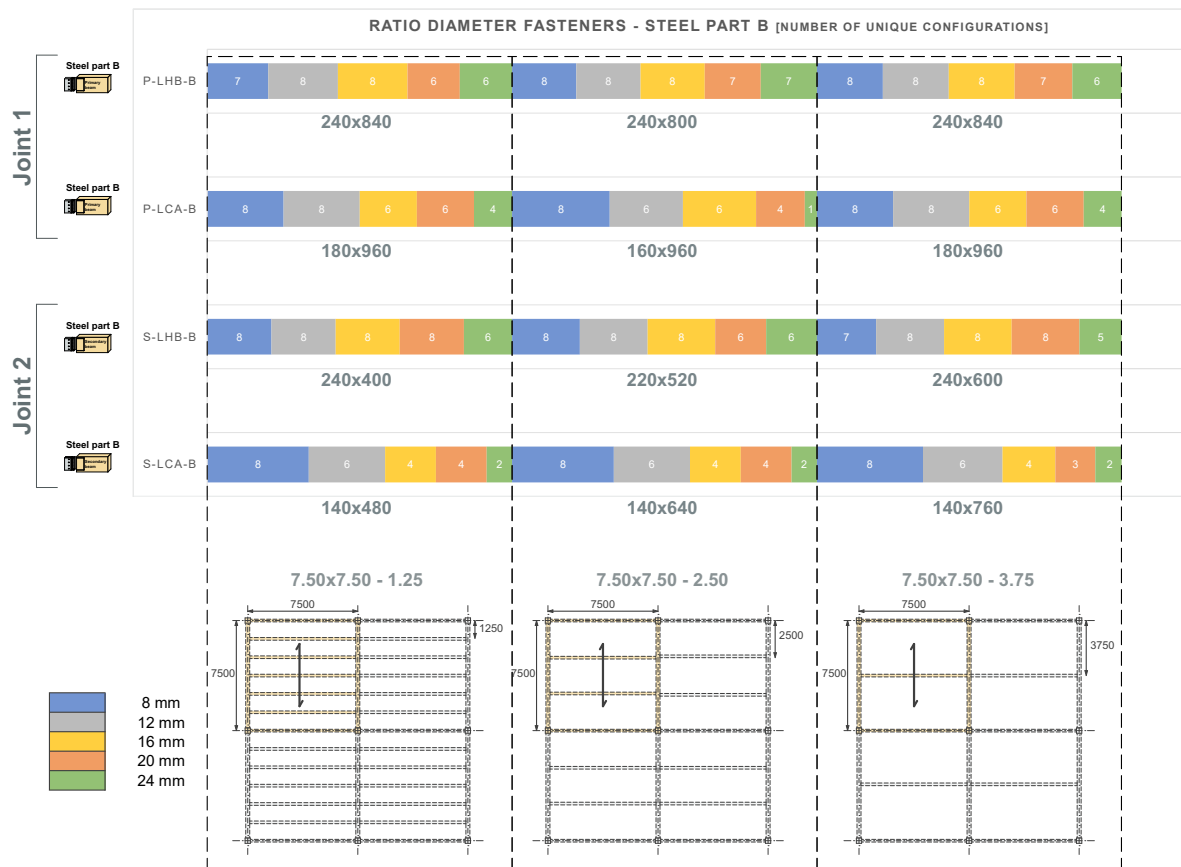


Figure 5.3: Ratio diameter fastener - steel part B

The following observations can be made from the graph that is shown in figure 5.3.

Joint 1

1. In general, the diameters 8, 12, and 16 mm slightly dominate the larger diameters (20, 24) for both member categories in all constructed cases.
2. Span 2.5 m shows a reduction in the number of unique configurations that consist of diameters 20 and 24 mm for the LCA-member.

Joint 2

1. The larger diameters 16, 20, 24 mm at the LHB-members are significantly more present compared to the LCA-members for all constructed cases.
2. The fastener diameters in the LCA-members are all constantly distributed over all constructed cases.

Ratio Diameter Fastener - Steel Part A

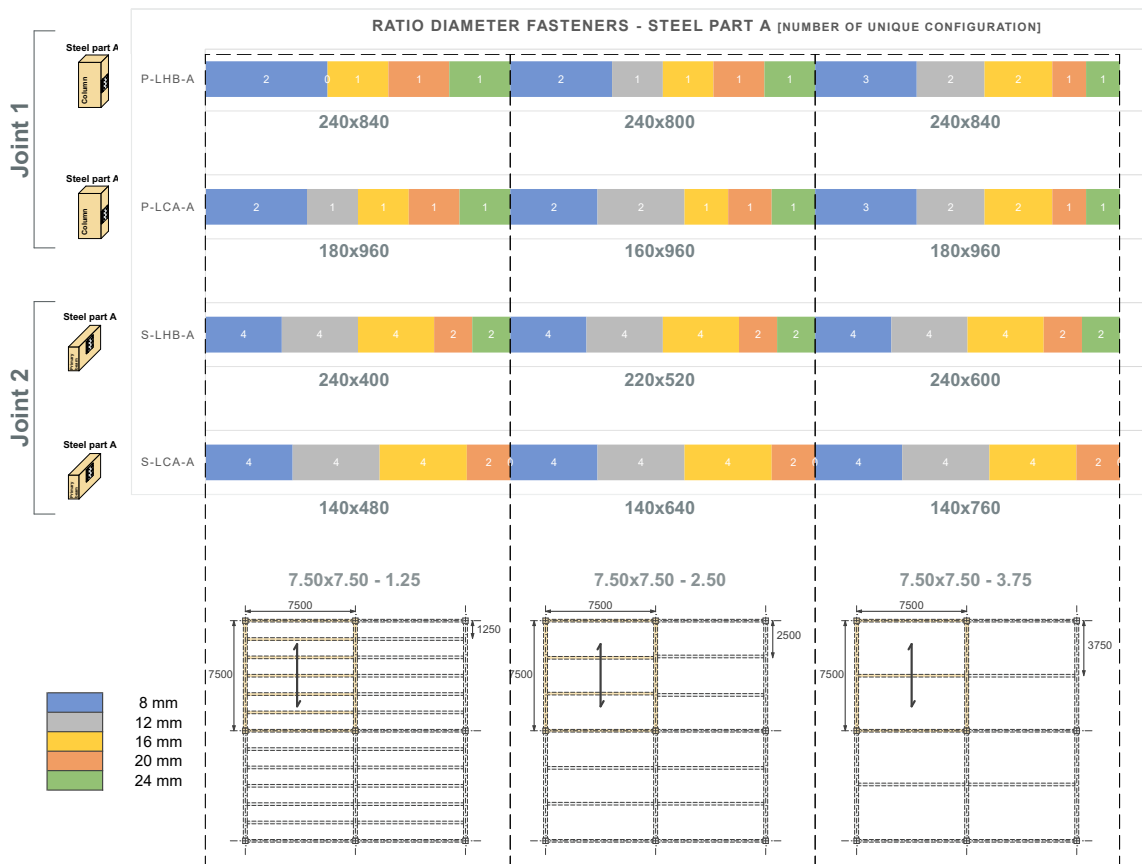


Figure 5.4: Ratio diameter fastener - steel part A

The following observations can be made from the graph that is shown in figure 5.4.

Joint 1

1. In both member categories and all constructed cases, the number of configurations that contain diameter 20 and 24 is limited to one.
2. There are no configurations available that contain diameter 12 mm for the LHB-member (240x840).

Joint 2

1. The ratio between all examined diameters of all constructed cases is equally distributed for each member category.
2. The number of configurations that contain diameter 24 is zero for the LCA-members.

Ratio Number of Columns in Fastener Group - Steel Part A

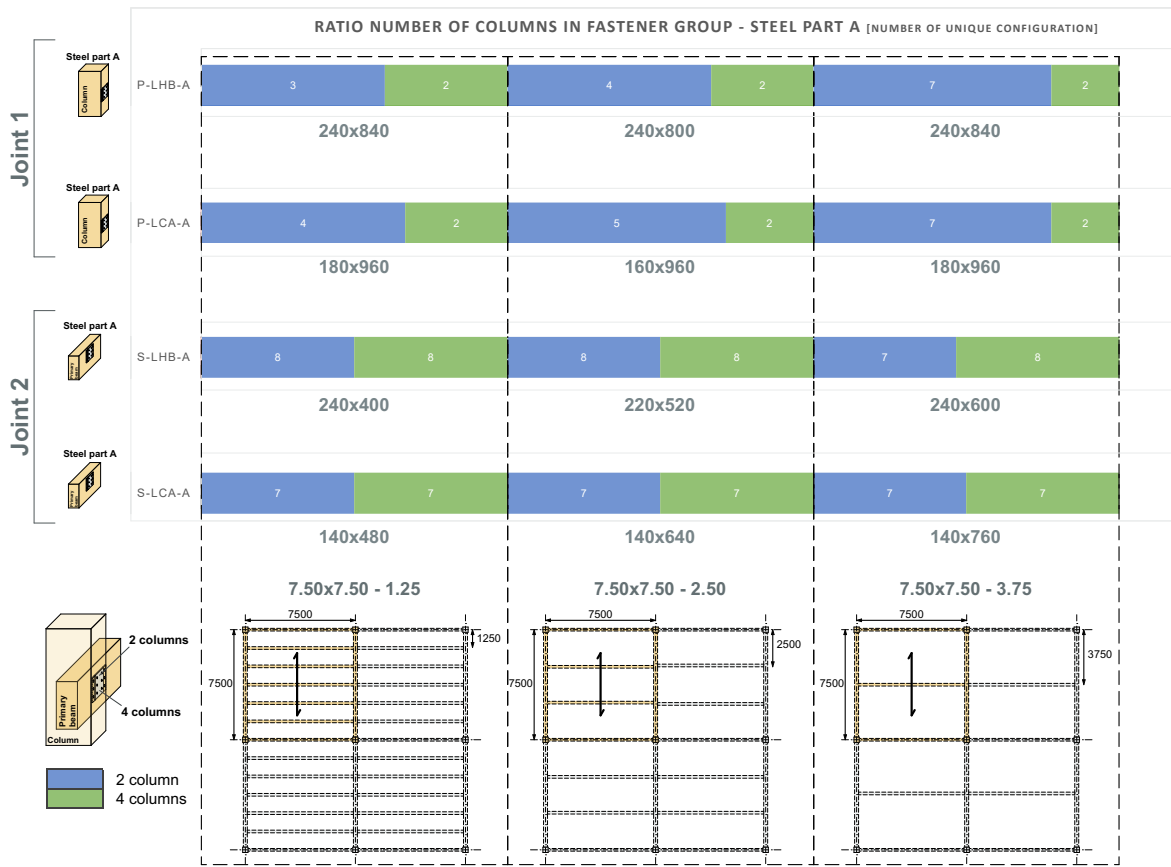


Figure 5.6: Ratio number of columns in fastener group - steel part A

The following observations can be made from the graph that is shown in figure 5.6.

Joint 1

1. Both member categories in all three constructed cases illustrate that the number of unique configurations that contain four columns in the fastener group is constantly equal to two.
2. The number of unique configurations that contain 2 columns in the fastener group decreases when the distance between the secondary beams decreases.

Joint 2

1. The ratio between two columns and four columns in the fastener group is equally distributed for the LCA-members except for the constructed case with a distance between the secondary beams of 3.75 m.
2. The ratio between two columns and four columns in the fastener group is equally distributed for the members selected on their lowest cross-sectional area.

Ratio Number of Slotted-in Steel Plates - Steel Part B

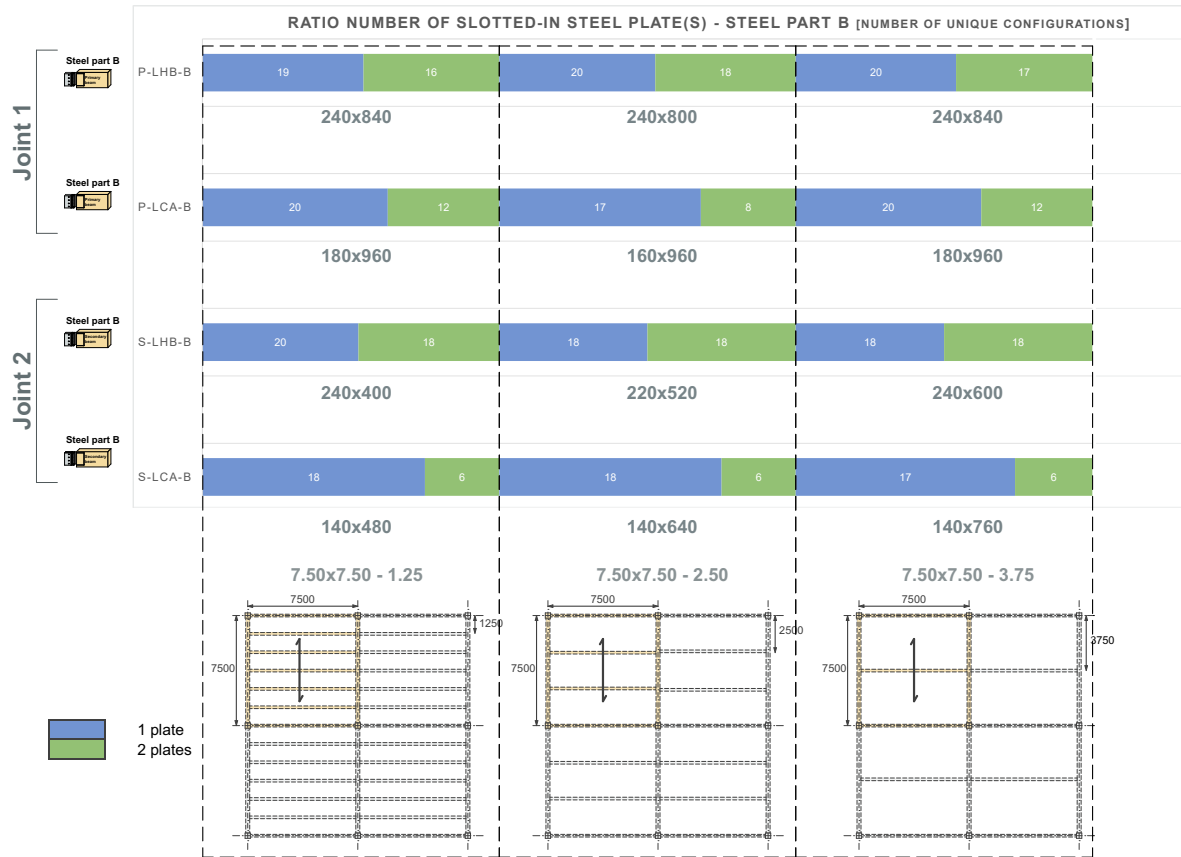


Figure 5.7: Ratio number of slotted-in steel plate(s) - steel part B

The following observations can be made from the graph that is shown in figure 5.7.

Joint 1

1. The single slotted-in steel plate slightly dominates the double slotted-in steel plate in the LHB-members for all constructed cases.
2. Compared to the LHB-members, the single slotted-in steel plate strongly dominates the double slotted-in steel plate in the LCA-members for all constructed cases.

Joint 2

1. The number of slotted-in steel plates is equally distributed for all constructed cases of the LHB-members except for the 1.25 m distances.
2. The single slotted-in steel plate strongly dominates the double slotted-in steel plate in the LCA-members for all constructed cases.
3. The slotted-in steel plates are constantly distributed in the LCA-member except for the 3.75 distances.

5.2.2. Graph 1b: Number of Unique Configurations

Graph 5.8 provides an overview of the total number of unique configurations for each constructed case including the corresponding members.

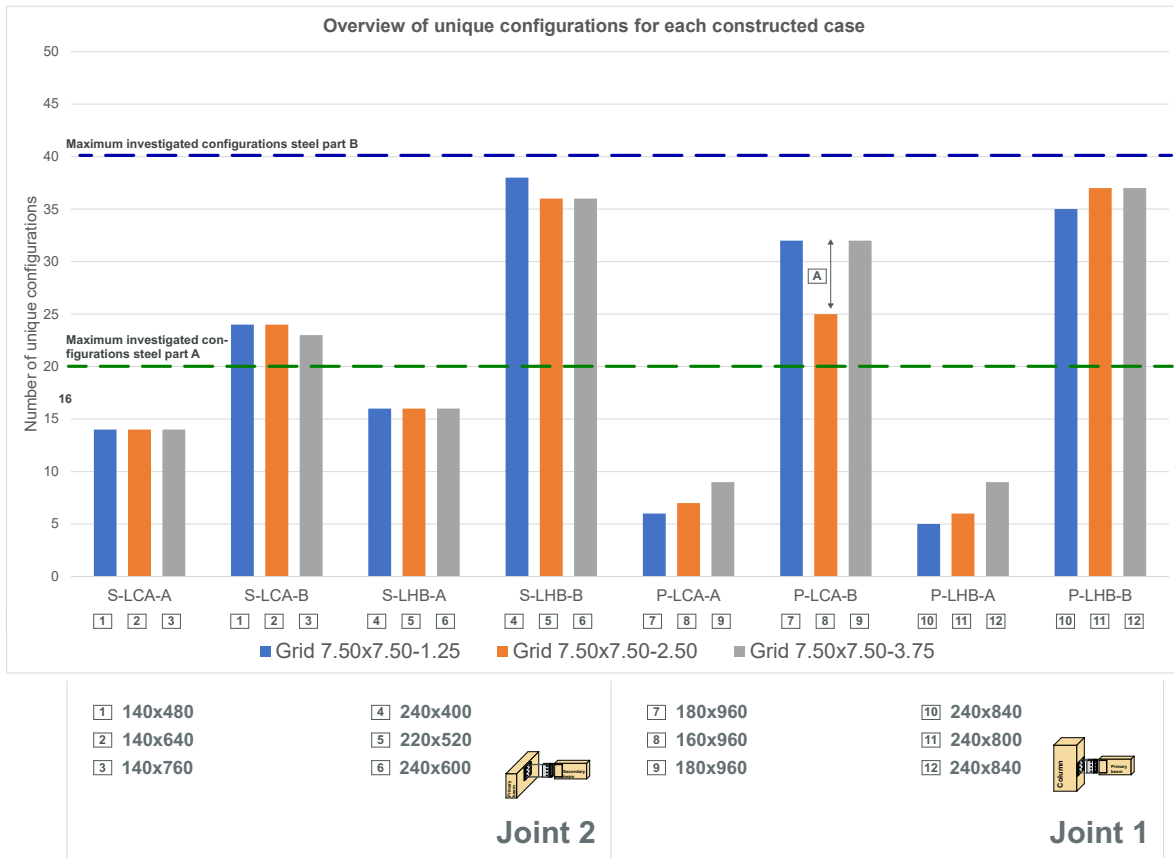


Figure 5.8: Overview number of unique configurations for each constructed case - analysis 1

The following observations can be made from the graph that is shown in figure 5.8.

1. The different distances between the secondary beams have no influence on the number of unique configurations for steel part A for both member categories in joint 2.
2. The LHB-members generate slightly more unique configurations for steel part A than the LCA-members in joint 2.
3. The different distances between the secondary beams have less effect on the number of configurations for steel part B in joint 2. A small drop is visible for the LCA-member at the 3.75 m distance. Moreover, for the LHB-member, a drop starts from 2.50 m and is followed by an equal number of unique configurations at 3.75 m.
4. The number of unique configurations for steel part B is significantly higher for the LHB-member compared to the LCA-member in joint 2.
5. The number of unique configurations for steel part B in the LHB-member in joint 2 almost reaches the maximum number of investigated configurations.
6. The number of unique configurations for steel part A for both member categories in joint 1 slowly increases with the expansion of the distances between the secondary beams.
7. A significant drop (A) is visible in the number of configurations for steel part A in joint 1 at the distance 2.50 m.

8. The number of unique configurations for steel part B in the LHB-member is higher compared to the LCA-member in joint 1.
9. The number of configurations for steel part B in joint 1 is significantly higher than the number of configurations generated by steel part A.

5.2.3. Graphs 1c: Steel Mass Ratio Unique Configurations

Graphs 5.9 and 5.10 provide an overview of the steel mass ratio between all unique configurations of steel part A and B applied to the two member categories for each constructed case. These graphs present the steel mass of the lowest and highest configurations. Moreover, they show the average steel mass of all unique configurations. Finally, the graphs illustrate the trend of the average steel mass applied to the primary and secondary beams over all constructed cases.

Mass Ratio Steel Part A

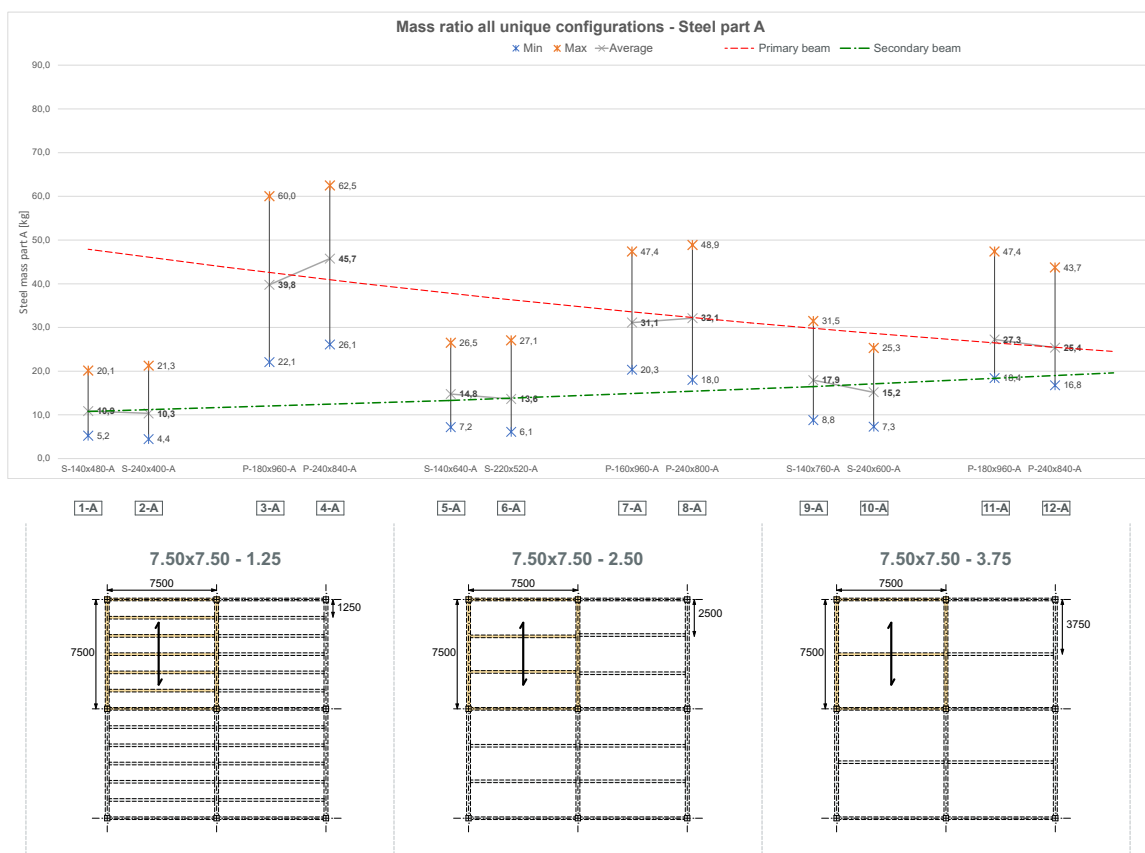


Figure 5.9: Mass ratio steel part A of each constructed case - analysis 1

The following observations can be made from the graph, that is shown in figure 5.9.

1. In general, the difference between the minimum and maximum steel mass is significant. For instance, for the constructed case with a distance between the secondary beams of 1.25 m, the difference between the configurations with the highest mass and lowest mass for steel plate A at the primary beam is approximately 38 kg.
2. The average steel mass in the primary beam reduces linearly as the distance between the secondary beams increases.

3. In terms of average mass in the primary beam, the LHB-member dominates in the constructed case with a distance of 1.25 m. This dominance reduces as the distance between the secondary beams increases. A tilting point is visible for the constructed case with a distance of 3.75 m.
4. The average steel mass in the secondary beam increases linearly as the distance between the secondary beams increases.
5. The average steel mass in the secondary beam is approximately equal for both member categories in the constructed case with a distance of 1.25 m. When the distance between the secondary beams increases further, the LCA-member becomes dominant and the difference in average steel mass between the two members starts to grow.
6. The average steel mass of the primary and secondary beam starts to converge when the distance between the secondary beams increases.

As discussed in section 5.1, the amount of steel applied in the connection has an effect on the costs and environmental footprint of the structure. In order to add more value to graph 5.9, table 5.1 offers an overview of the configurations that contain the lowest steel mass.

| Configuration | Fastener type | Diameter | Rows in FG | Columns in FG | Length screw [mm] |
|---------------|---------------|----------|------------|---------------|-------------------|
| 1-A | Lag screw | 8 | 6 | 2 | 80 |
| 2-A | Lag screw | 8 | 6 | 2 | 100 |
| 3-A | Lag screw | 8 | 17 | 4 | 240 |
| 4-A | Lag screw | 8 | 19 | 4 | 220 |
| 5-A | Lag screw | 8 | 12 | 2 | 70 |
| 6-A | Lag screw | 8 | 11 | 2 | 110 |
| 7-A | Lag screw | 8 | 12 | 4 | 220 |
| 8-A | Lag screw | 8 | 13 | 4 | 240 |
| 9-A | Lag screw | 8 | 17 | 2 | 80 |
| 10-A | Lag screw | 8 | 16 | 2 | 110 |
| 11-A | Lag screw | 12 | 9 | 2 | 280 |
| 12-A | Lag screw | 12 | 9 | 2 | 300 |

Table 5.1: Overview of the configurations of steel part A with the lowest steel mass in kg // FG = fastener group

Table 5.1 illustrates that the lag screws in combination with the smaller diameters 8 and 12 mm generate the lowest configurations of steel part A. This applies to both to the secondary beam as well as the primary beam.

Mass Ratio Steel Part B

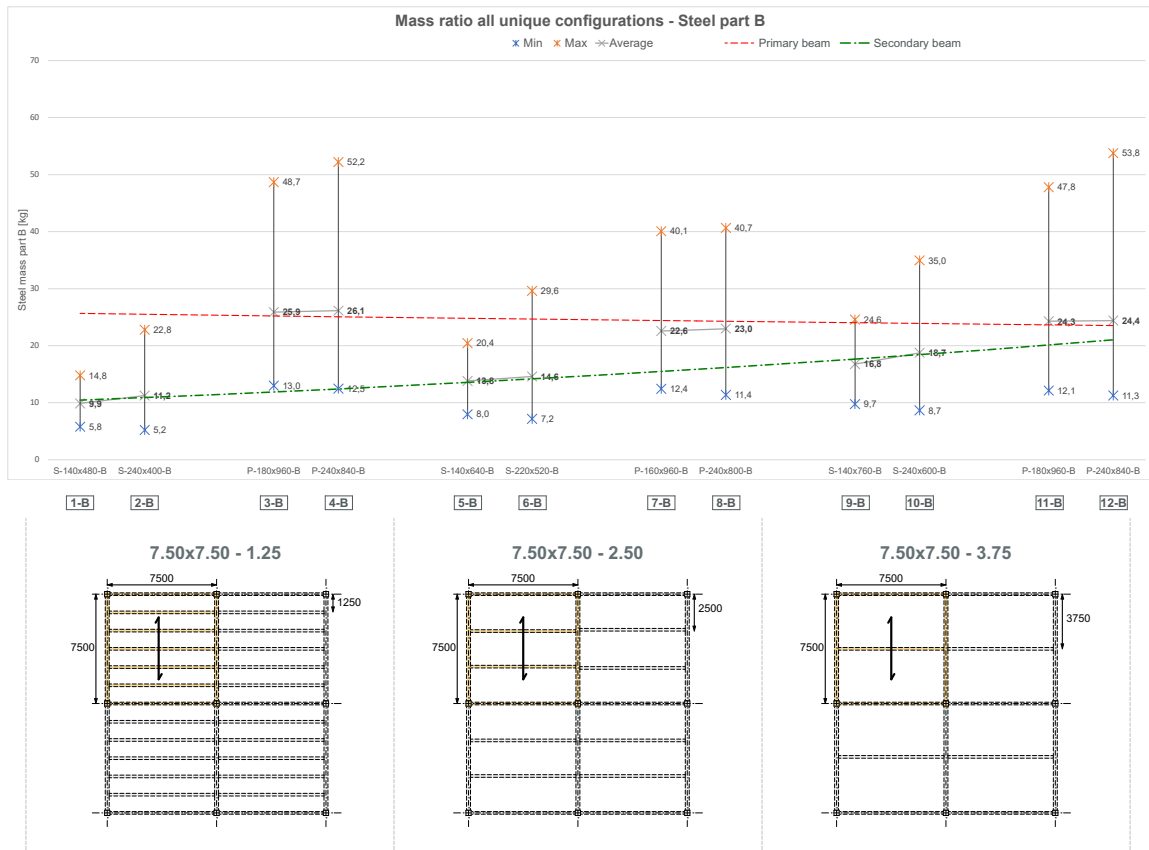


Figure 5.10: Mass ratio steel part B of each constructed case - analysis 1

The following observations can be made from the graph that is shown in figure 5.10.

1. Similar to steel part A, the difference between the minimum and maximum steel mass is significant.
2. The average steel mass in the primary beam reduces linearly as the distance between the secondary beams increases.
3. In all constructed cases, the average steel mass of the primary beam is approximately equal for steel part B for both member categories.
4. The average steel mass in the secondary beam increases linearly as the distance between the secondary beams increases.
5. The LHB-members of the secondary beam dominate the LCA-members in terms of average steel mass.
6. The average steel mass of the primary and secondary beam starts to converge when the distance between the secondary beams increases.

Table 5.2 illustrates an overview of the configurations that contain the lowest steel mass.

| Configuration | Fastener type | Diameter | Rows in FG | Columns in FG | Slotted-in steel plate(s) |
|---------------|---------------|----------|------------|---------------|---------------------------|
| 1-B | Dowel | 8 | 9 | 1 | 1 |
| 2-B | Dowel | 8 | 9 | 1 | 1 |
| 3-B | Dowel | 8 | 30 | 1 | 1 |
| 4-B | Dowel | 8 | 32 | 1 | 1 |
| 5-B | Dowel | 8 | 15 | 1 | 1 |
| 6-B | Dowel | 8 | 15 | 1 | 1 |
| 7-B | Dowel | 8 | 25 | 1 | 1 |
| 8-B | Dowel | 8 | 25 | 1 | 1 |
| 9-B | Dowel | 8 | 22 | 1 | 1 |
| 10-B | Dowel | 8 | 21 | 1 | 1 |
| 11-B | Dowel | 8 | 18 | 1 | 1 |
| 12-B | Dowel | 8 | 19 | 1 | 1 |

Table 5.2: Overview of the configurations of steel part B with the lowest steel mass in kg // FG = fastener group

Table 5.2 illustrates that the dowel with a diameter of 8 mm in combination with a single slotted-in steel plate generates the lowest configurations for steel part B. This applies to the secondary beam as well as the primary beam.

5.3. Analysis 2: Different Grid Sizes Columns

The observations that are linked to the following graphs represent the outcome of analysis 2. This analysis focuses on the different grid sizes of the columns.

5.3.1. Graphs 2a: Corresponding Parameters

The following graphs present the ratio between the sub-parameters that construct the different laterally loaded dowel-type configurations.

Ratio Fastener Type - Steel Part B

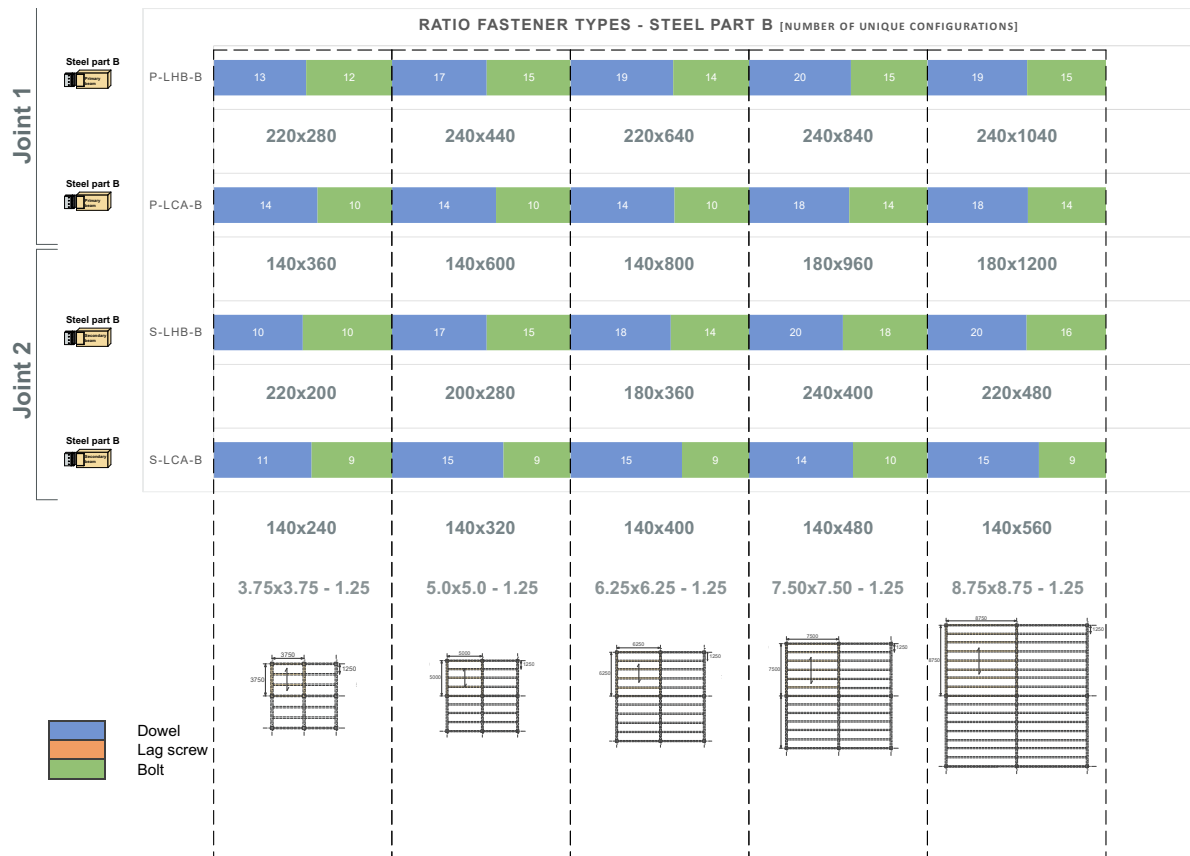


Figure 5.11: Ratio fastener type - steel part B

The following observations can be made from the graph that is shown in figure 5.11.

Joint 1

1. In general, the dowels dominate the bolts for both member categories in all constructed cases.
2. The difference in the distribution between bolts and dowels slightly increases for the LHB-members with the enlargement of the grid sizes.
3. A constant distribution between bolts and dowels is visible for the LCA-members for constructed cases 3.75, 5.00, and 6.25. For constructed cases 7.50 and 8.75, the distribution between bolts and dowels changes.

Joint 2

1. The dowels become dominant in the LHB-members after grid 3.75 m.
2. The dowels dominate the bolts in the LCA-members for all constructed cases.

Ratio Fastener Type - Steel Part A

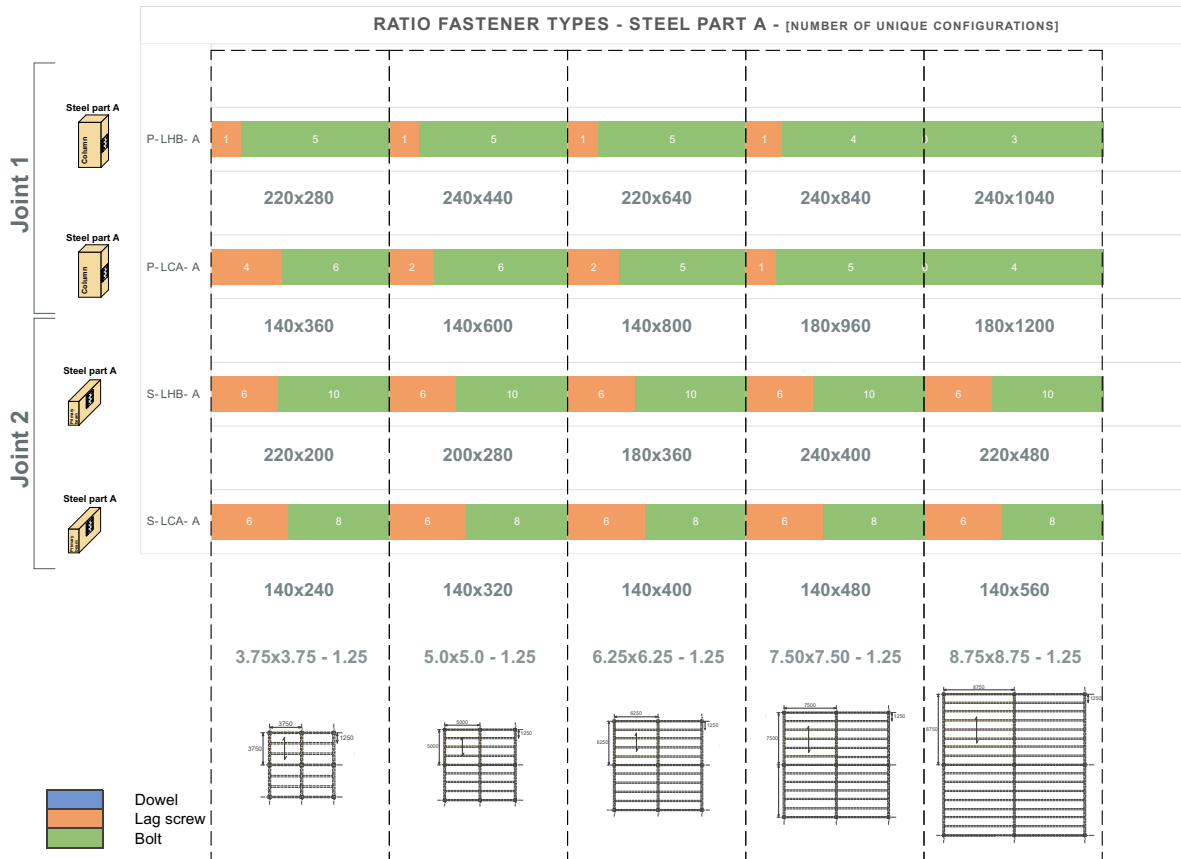


Figure 5.12: Ratio fastener type - steel part A

The following observations can be made from the graph that is shown in figure 5.12.

Joint 1

1. The bolts dominate the lag screws when increasing the grid sizes. Especially for the LHB-beam, the lag screws are already limited at the smaller grid sizes.
2. No configuration that contains lag screws is available in both member categories for grid size 8.75 m.

Joint 2

1. The bolts dominate the lag screws in both member categories for all constructed cases.
2. The number of configurations that consist of lag screws and bolts is constant for both member categories for all grid sizes.

Ratio Diameter Fastener - Steel Part B

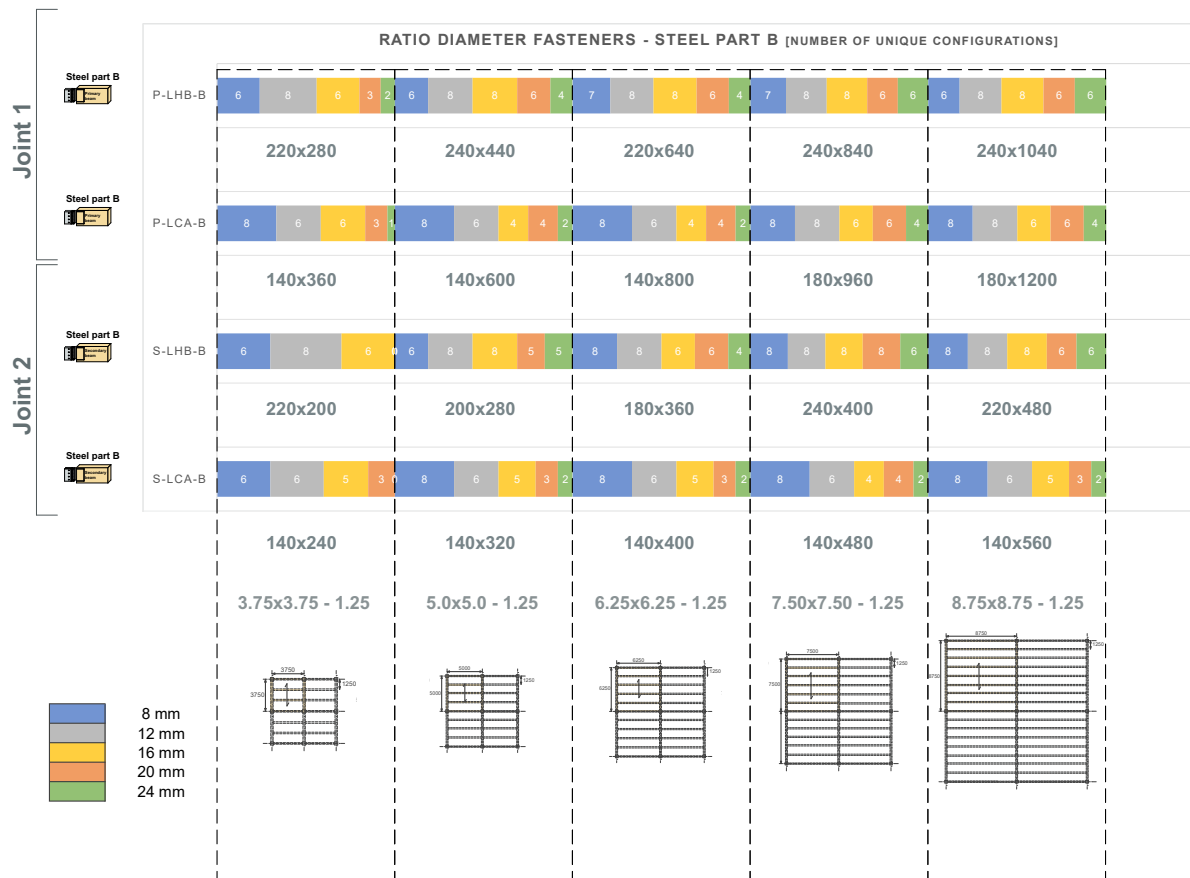


Figure 5.13: Ratio Diameter Fastener - Steel part B

The following observations can be made from the graph that is shown in figure 5.13.

Joint 1

1. The diameters 20 and 24 mm are limited at grid size 3.75 m compared to the larger grid sizes for the LHB-members.
2. The contributions of the diameters 12, 16, and 20 mm become larger for the grid sizes 7.50 and 8.75 m.

Joint 2

1. Grid size 3.75 m illustrates configurations that do not include the diameter 20 and 24 mm for the LHB-member (220x200). Moreover, the LCA-member does not contain the diameter 24 mm.
2. The contribution of the diameters 16, 20, and 24 mm in the LHB-members is significantly larger compared to the LCA-members.

Ratio Diameter Fastener - Steel Part A

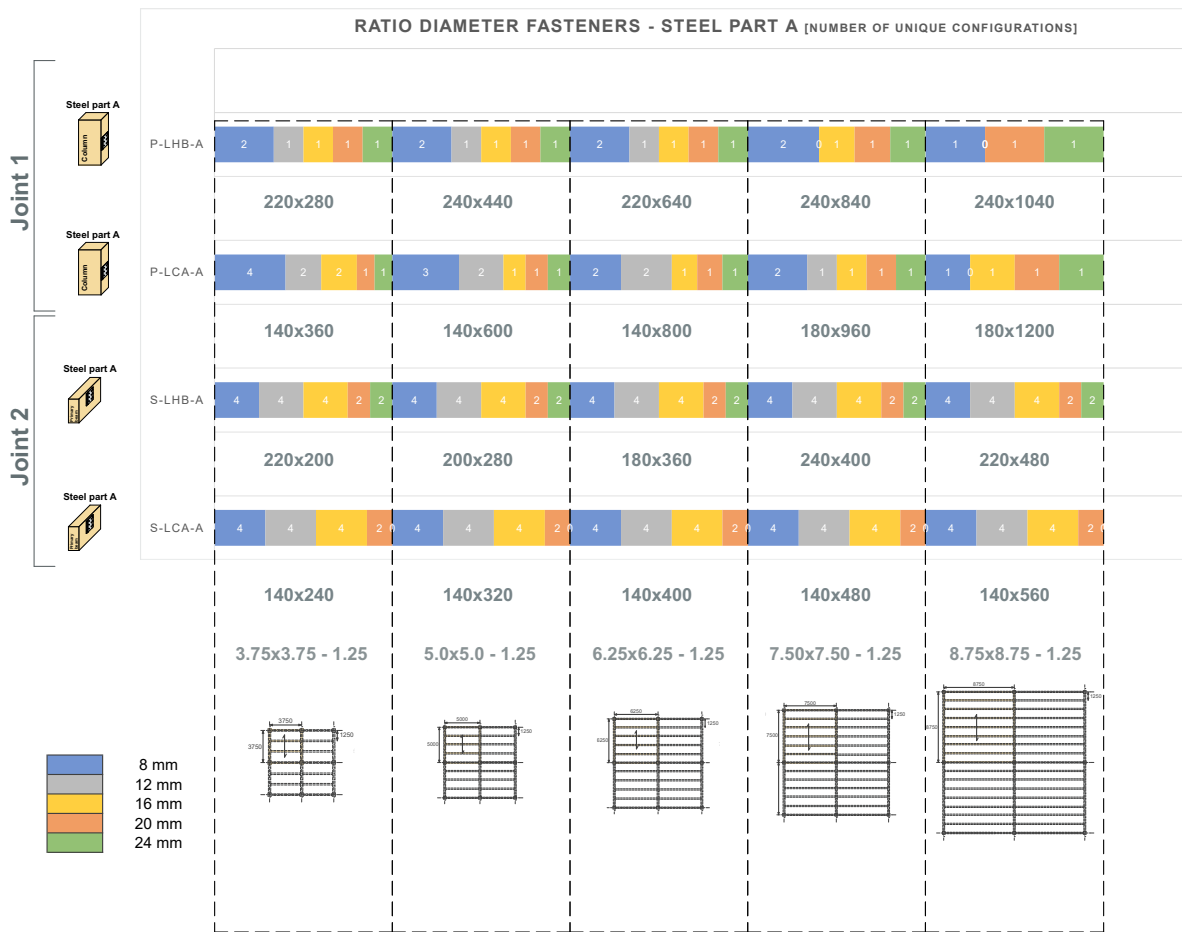


Figure 5.14: Ratio Diameter Fastener - Steel part A

The following observations can be made from the graph that is shown in figure 5.14.

Joint 1

1. The contribution of 8 mm in the LHB-members is two times larger than the remaining diameters for all constructed cases except for grid size 8.75 m.
2. The configurations of grid size 7.50 m and 8.75 m do not contain the diameter 12 mm in the LHB-members.
3. The diameters 24, 20, and 16 slightly reduce in the LCA-members with the enlargement of the grid sizes.
4. The configurations of grid size 8.75 m do not contain the diameter 12 mm in the LHB-members.

Joint 2

1. The diameters are constantly distributed for both member categories for all constructed cases. No configuration is available that contains the diameter of 24 mm in the LCA-members.

Ratio Number of Columns in Fastener Group - Steel Part B

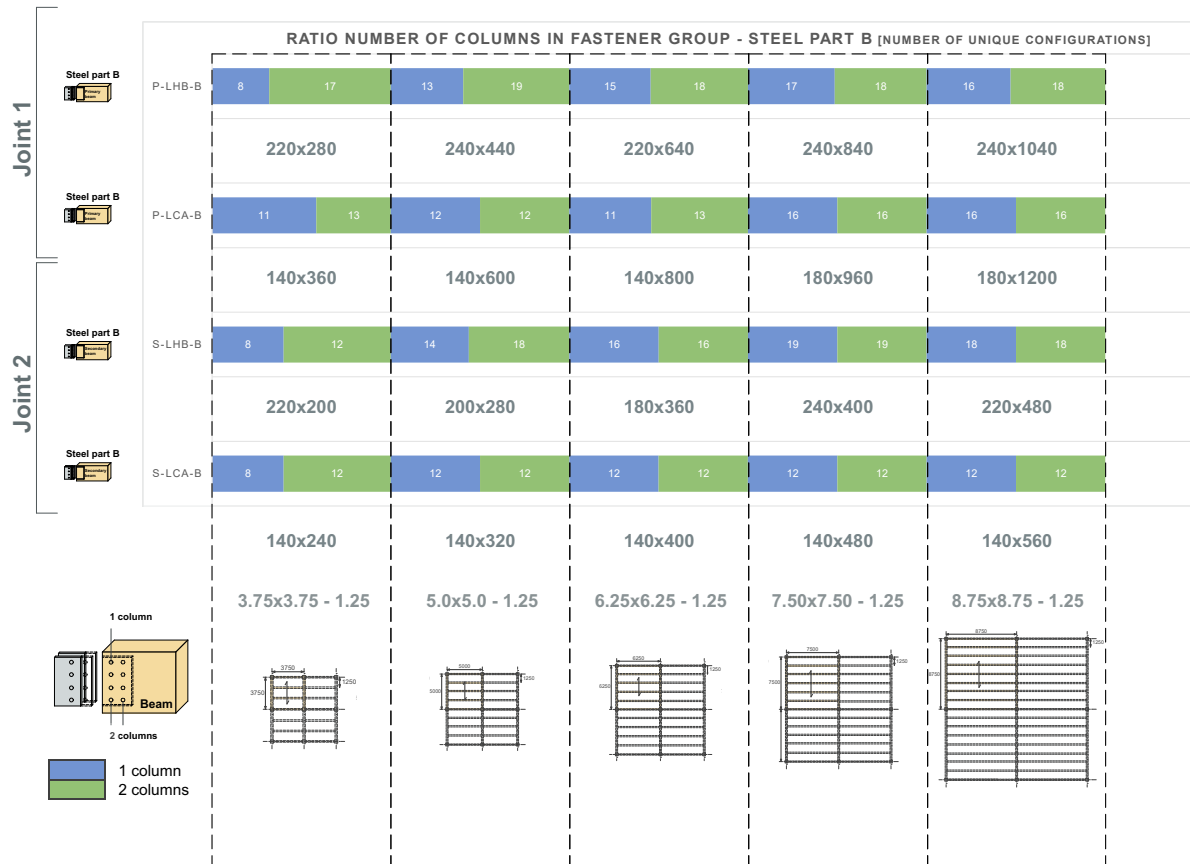


Figure 5.15: Ratio Number of columns in fastener group - steel part B

The following observations can be made from the graph that is shown in figure 5.15

Joint 1

1. The two columns strongly dominate the one column in the fastener group of the LHB-member for grid size 3.75 m. This dominance reduces with the enlargement of the grid sizes.
2. In general, the distribution between one column and two columns is equal in the LCA-member for all constructed cases.

Joint 2

1. In general, the ratio between one column and two columns in the fastener group is equally distributed in the LHB-member for all constructed cases, except for grid sizes 3.75 m and 5.00 m. In these two cases, the two columns in the fastener group dictate.
2. The distribution of one column and two columns in the fastener group is equal in the LCA-members except for grid size 3.75 m. In this grid size, the two columns dominate.

Ratio Number of Columns in Fastener Group - Steel Part A

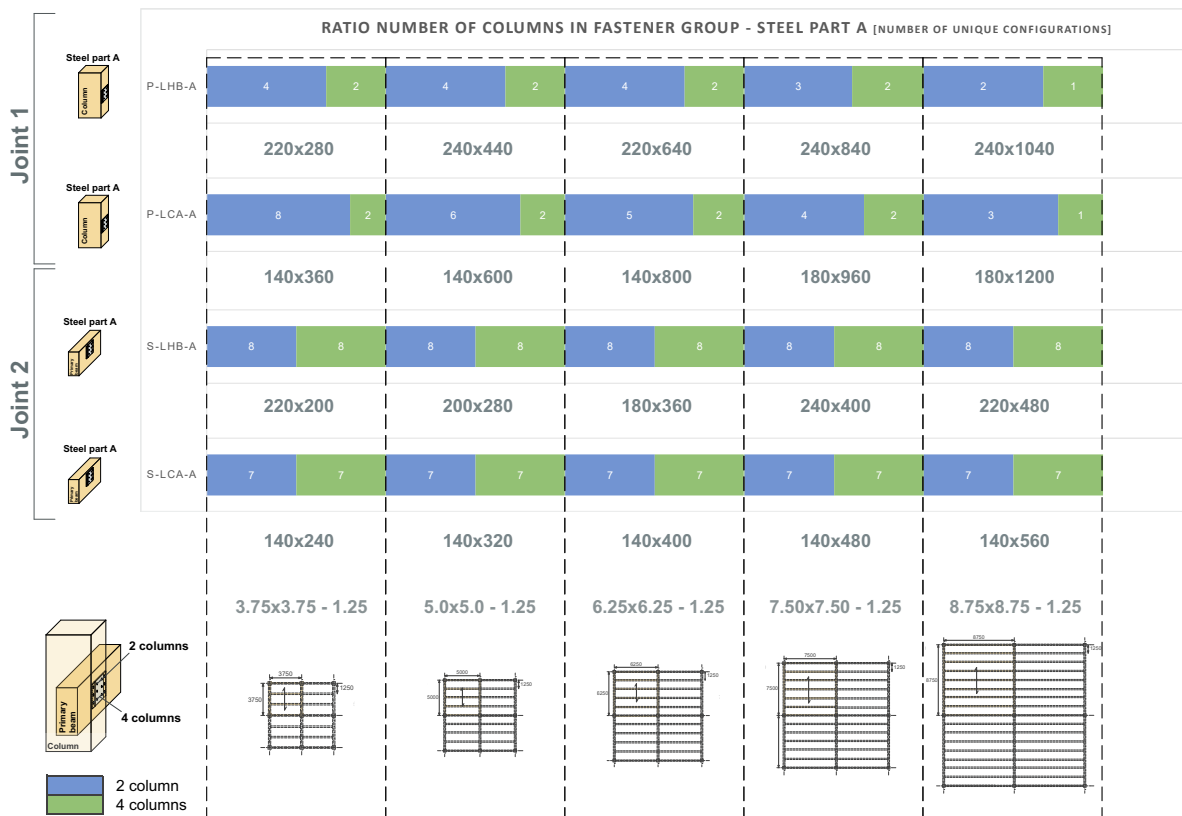


Figure 5.16: Ratio Number of columns in fastener group - steel part A

The following observations can be made from the graph that is shown in figure 5.16.

Joint 1

1. The two columns dominate the four columns in the fastener group for the LHB-members. This dominance slightly reduces with the enlargement of the grid sizes.
2. The pattern observed for the LCA-members is similar to the LHB-members, although the dominance of the four columns in the fastener group is higher.

Joint 2

1. In general, the ratio between one column and two columns in the fastener group is equally distributed in the LHB-member for all constructed cases.
2. A similar pattern is observed for the LCA-members in all constructed cases.

Ratio Number of Slotted-in Steel Plate - Steel Part B

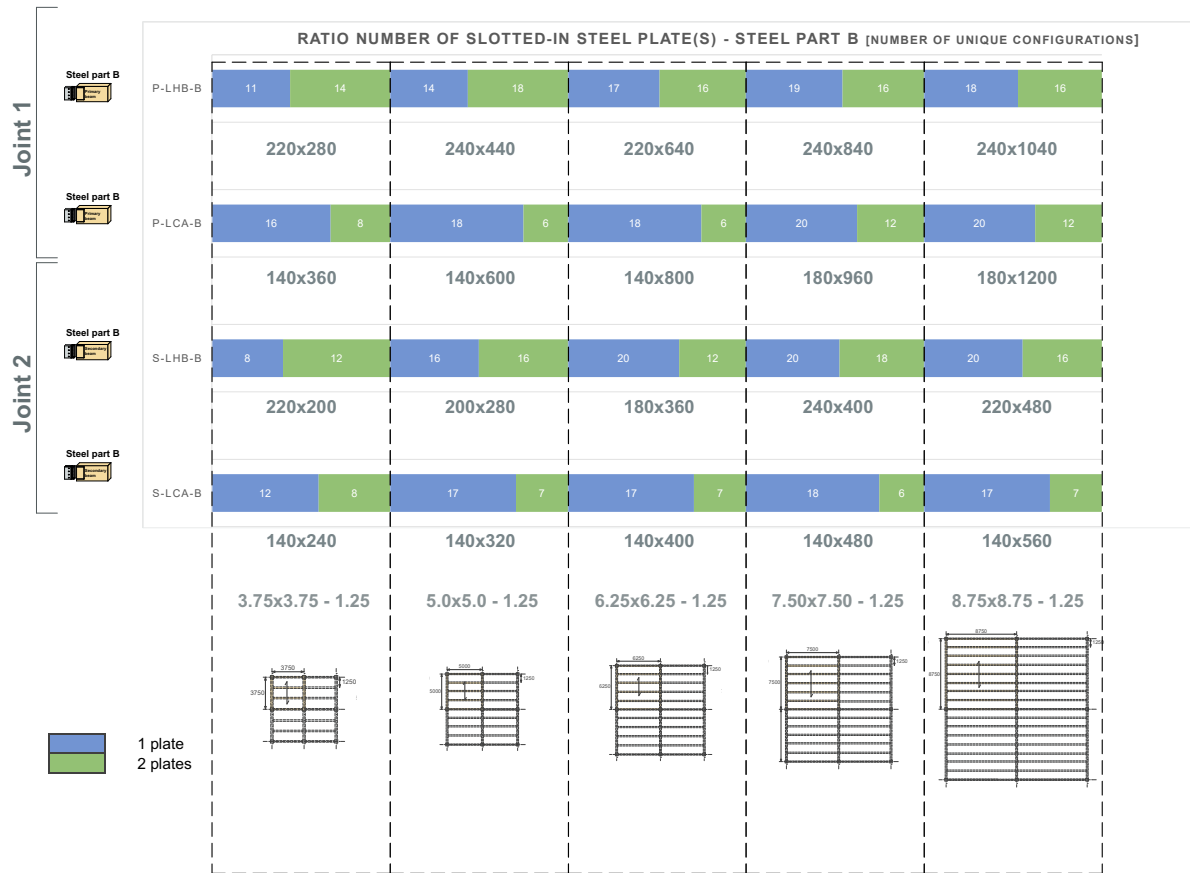


Figure 5.17: Ratio Number of slotted-in steel plate(s) - steel part B

The following observations can be made from the graph that is shown in 5.17.

Joint 1

1. In general, the single slotted-in steel plate slightly dominates the double-slotted-in steel plate for the grid sizes 3.75 m and 5.00 m. The opposite occurs for the grid sizes 6.35 m until 7.50 m for the LHB-members.
2. The single slotted-in steel plate strongly dominates the double slotted-in steel plate in the LCA-member for all constructed cases.

Joint 2

1. A similar pattern as the pattern observed for joint 1 is seen for the LHB-members, although the distribution between the single and double slotted-in steel plate is equal.
2. A similar pattern as the pattern observed for joint 1 is seen in the LCA-members, although the dominance of the single slotted-in steel plate is larger for the grid sizes 7.5 m and 8.75 m compared to joint 1.

5.3.2. Graph 2b: Number of Unique Configurations

Graph 5.18 illustrates an overview of the total number of unique configurations for each constructed case.

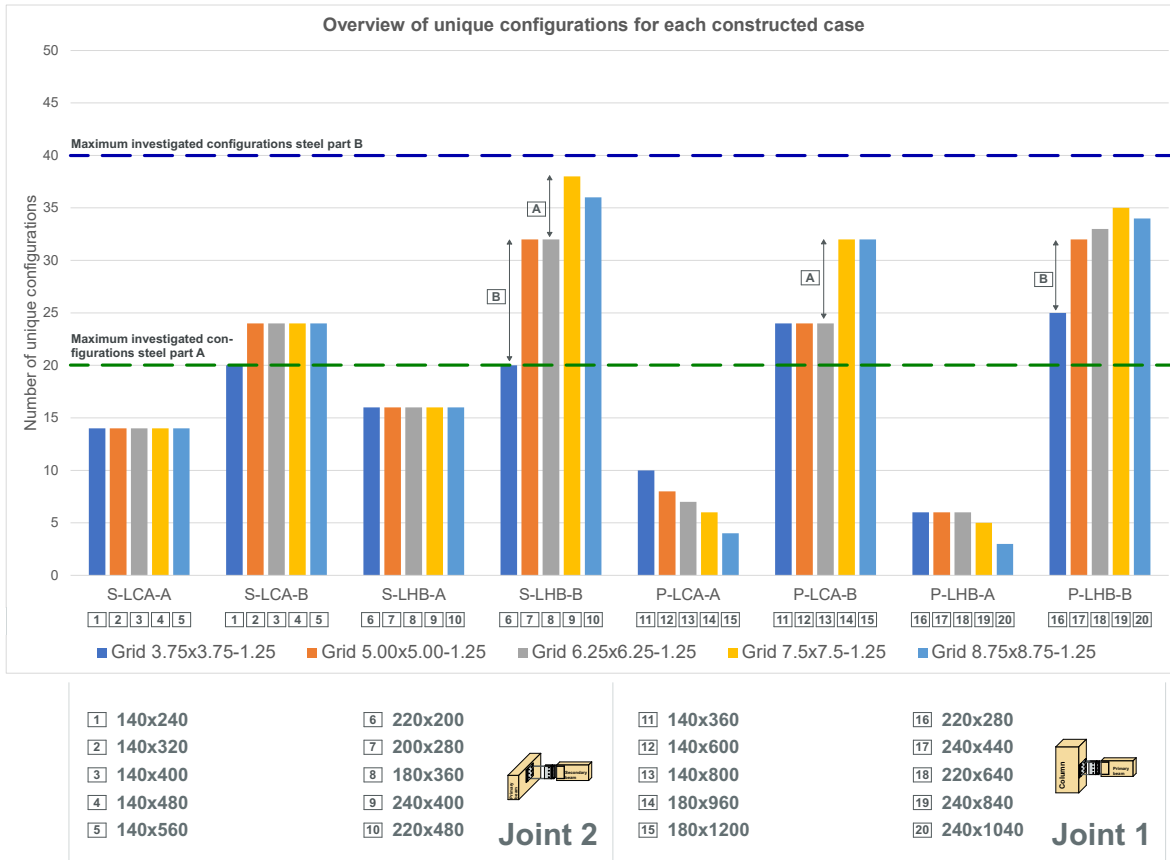


Figure 5.18: Overview number of unique configurations for each constructed case - analysis 2

The following observations can be made from the graph that is shown in figure 5.8.

1. The different grid sizes have no influence on the number of unique configurations for steel part A for both member categories in joint 2.
2. The number of unique configurations for steel part B in the LCA-member is lower for the grid size 3.75 m compared to the remaining grid sizes.
3. In general, the number of unique configurations for steel part B in the LHB-member in joint 2 increases as the grid sizes increase. This growth shows two big steps, indicated with B and A. Moreover, a small drop is visible at grid size 8.75 m.
4. The number of unique configurations for steel part B is significantly higher for the LHB-member compared to the LCA-member in joint 2.
5. The number of unique configurations for steel part B in the LHB-member in joint 2 at grid size 7.50 m almost reaches the maximum number of investigated configurations.
6. The number of unique configurations for steel part A in the LCA-member decreases linearly in joint 1 with the expansion of the grid sizes.
7. The first three grid sizes generate the same number of unique configurations for steel part A in the LHB-member in joint 1. Thereafter, the number of unique configurations slightly reduces.

8. In general, the number of unique configurations for steel part B in the LHB-member in joint 1 increases when the grid sizes increases as well. This growth shows one big step, indicated with B. Moreover, a small drop is visible at grid size 8.75 m.
9. The number of configurations for steel part B in joint 1 is significantly higher than the number of configurations generated by steel part A.

5.3.3. Graphs 2c: Mass Ratio Unique Configurations

Graphs 5.19 and 5.20 provide an overview of the steel mass ratio between all unique configurations for steel part A and B applied to the two member categories for each constructed case. These graphs present the steel mass ratio between the lowest and highest configuration. Moreover, they show the the average steel mass for all unique configurations. Finally, the graphs illustrate the trend of the average steel mass applied to the primary and secondary beam across all constructed cases.

Mass Ratio Steel Part A

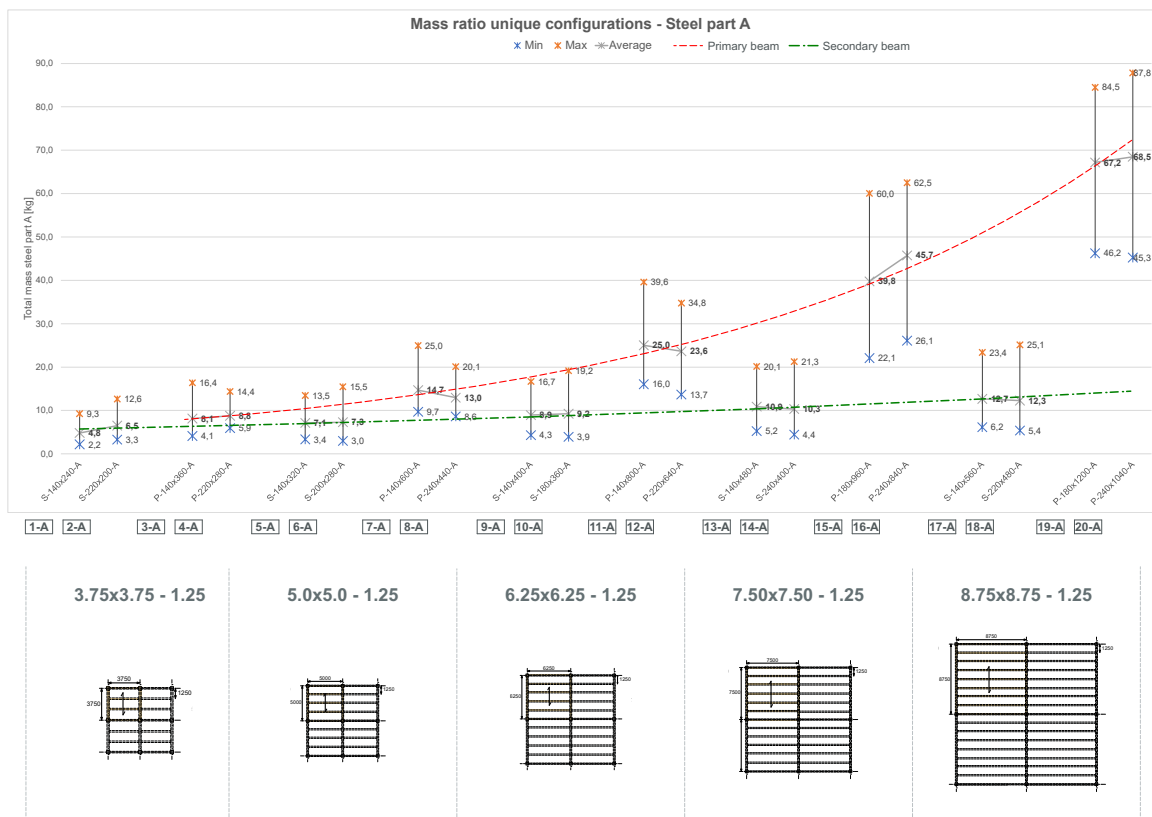


Figure 5.19: Mass ratio steel part A of each constructed case - analysis 2

The following observations can be made from the graph that is shown in figure 5.19.

1. In this analysis, the difference between the minimum and maximum steel mass is significant.
2. The average steel mass in the primary beam shows an exponential growth as the grid sizes increase.
3. The LHB-members of the primary beam have a higher average steel mass for grid sizes 3.75 m until 6.25 m. For the remaining grid sizes, the LCA-members have a higher average steel mass.
4. The average steel mass in the secondary beam increases linearly as the grid sizes increase.
5. In general, the average steel mass of both member categories of the secondary beam is equal.

As discussed in section 5.1, the amount of steel applied in the connection has an effect on the costs and environmental footprint of the structure. In order to add more value to graph 5.19, table 5.3 offers an overview of the configurations that contain the lowest steel mass.

| Configuration | Fastener type | Diameter | Rows in FG | Columns in FG | Length screw [mm] |
|---------------|---------------|----------|------------|---------------|-------------------|
| 1-A | Lag screw | 8 | 3 | 2 | 60 |
| 2-A | Lag screw | 8 | 3 | 2 | 90 |
| 3-A | Lag screw | 8 | 7 | 2 | 110 |
| 4-A | Lag screw | 8 | 3 | 4 | 110 |
| 5-A | Lag screw | 8 | 4 | 2 | 60 |
| 6-A | Lag screw | 8 | 4 | 2 | 90 |
| 7-A | Lag screw | 8 | 5 | 4 | 140 |
| 8-A | Lag screw | 8 | 6 | 4 | 140 |
| 9-A | Lag screw | 8 | 6 | 2 | 60 |
| 10-A | Lag screw | 8 | 5 | 2 | 90 |
| 11-A | Lag screw | 12 | 12 | 2 | 220 |
| 12-A | Lag screw | 8 | 11 | 4 | 180 |
| 13-A | Lag screw | 8 | 6 | 2 | 80 |
| 14-A | Lag screw | 8 | 6 | 2 | 100 |
| 15-A | Lag screw | 8 | 17 | 4 | 240 |
| 16-A | Lag screw | 8 | 19 | 4 | 220 |
| 17-A | Lag screw | 8 | 7 | 2 | 80 |
| 18-A | Lag screw | 8 | 7 | 2 | 100 |
| 19-A | Bolt | 8 | 20 | 4 | Full penetration |
| 20-A | Bolt | 8 | 21 | 4 | Full penetration |

Table 5.3: Overview of the configurations of steel part A with the lowest steel mass in kg // FG = fastener group

Table 5.3 illustrates that lag screws in combination with the smaller diameters 8 mm and 12 mm generate the configurations with the lowest steel mass, except for the configuration generated in grid size 8.75 m.

Mass Ratio Steel Part B

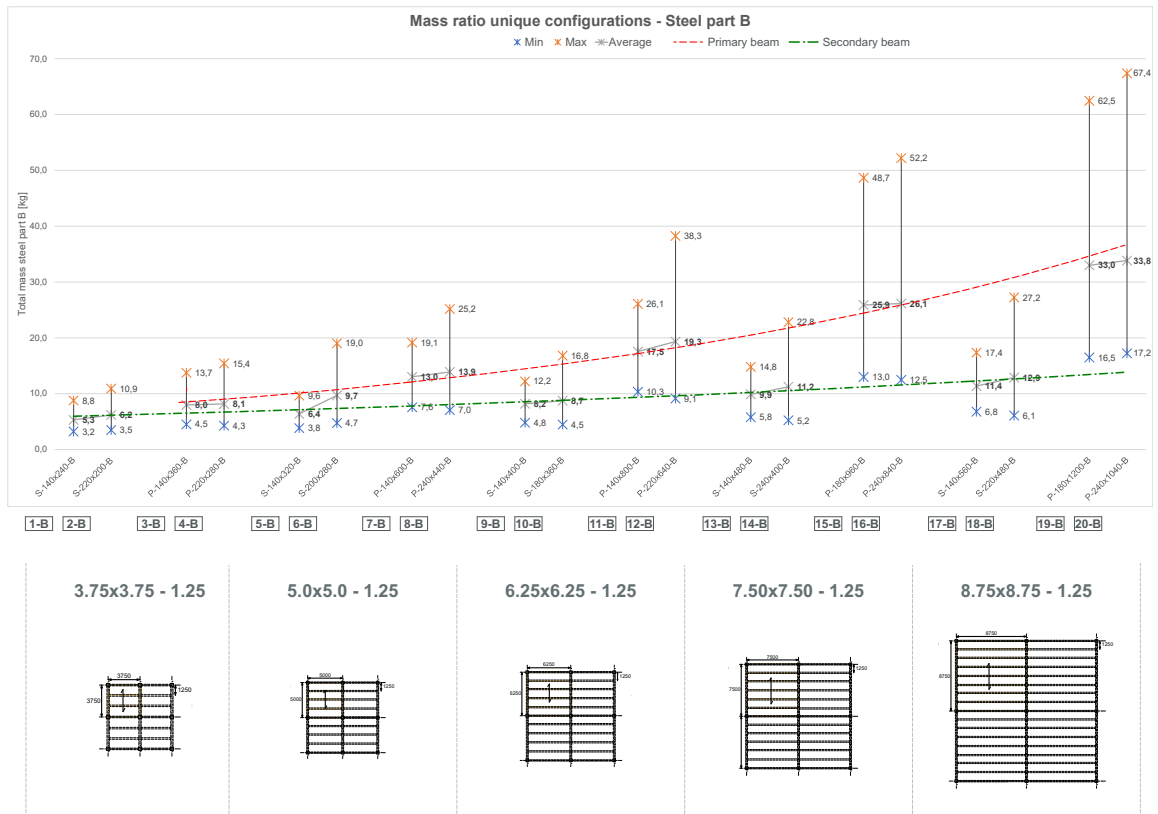


Figure 5.20: Mass ratio steel part B of each constructed case - analysis 2

The following observations can be made from the graph that is shown in figure 5.19.

1. Similar to steel part A, the difference between the minimum and maximum steel mass is significant.
2. The average steel mass in the primary beam shows a light exponential growth as the grid sizes increase.
3. In general, the LHB-members of the primary beam have a higher average steel mass as the grid sizes increase. The difference in mass gradually decreases for the larger grid sizes.
4. The average steel mass in the secondary beams increases linearly as the grid sizes increase.
5. In general, the LHB-members of the secondary beam have a larger average steel mass than the LCA-members.

Table 5.4 provides an overview of the configurations that contain the lowest steel mass.

| Configuration | Fastener type | Diameter | Rows in FG | Columns in FG | Slotted-in steel plate(s) |
|---------------|---------------|----------|------------|---------------|---------------------------|
| 1-B | Dowel | 12 | 5 | 1 | 1 |
| 2-B | Dowel | 12 | 4 | 1 | 1 |
| 3-B | Dowel | 8 | 11 | 1 | 1 |
| 4-B | Dowel | 12 | 6 | 1 | 1 |
| 5-B | Dowel | 8 | 7 | 1 | 1 |
| 6-B | Dowel | 12 | 4 | 1 | 1 |
| 7-B | Dowel | 8 | 16 | 1 | 1 |
| 8-B | Dowel | 12 | 9 | 1 | 1 |
| 9-B | Dowel | 8 | 8 | 1 | 1 |
| 10-B | Dowel | 8 | 8 | 1 | 1 |
| 11-B | Dowel | 8 | 24 | 1 | 1 |
| 12-B | Dowel | 8 | 23 | 1 | 1 |
| 13-B | Dowel | 8 | 9 | 1 | 1 |
| 14-B | Dowel | 8 | 9 | 1 | 1 |
| 15-B | Dowel | 8 | 30 | 1 | 1 |
| 16-B | Dowel | 8 | 32 | 1 | 1 |
| 17-B | Dowel | 8 | 10 | 1 | 1 |
| 18-B | Dowel | 8 | 9 | 1 | 1 |
| 19-B | Dowel | 8 | 40 | 1 | 1 |
| 20-A | Dowel | 12 | 21 | 1 | 1 |

Table 5.4: Overview of the configurations of steel part B with the lowest steel mass in kg // FG = fastener group

Table 5.4 illustrates that dowels in combination with the smaller diameters 8 mm and 12 mm and a single slotted-in steel plate generates the configurations with the lowest steel mass. This applies to the secondary beam as well as the primary beam.

5.4. Discussion

In this section, the results and observations presented in section 5.2 and 5.3 are discussed. The discussion is constructed as follows. First, the observations regarding the influence of different frame structure designs on steel part A and B are discussed. Second, the observations regarding the total number of unique configurations for all different frame designs are discussed. Lastly, the observations regarding the minimum, maximum, and average mass of steel parts A and B for all constructed cases are discussed.

5.4.1. Corresponding parameters

The parameters outlined in section 3.1.3 have determined the configurations for steel part A and B. The influences of the different frame designs on each parameter studied in analysis 1 and 2 are discussed below.

Fastener type

Analysis 1

The largest difference in the ratio between dowels and bolts in steel part B occurs in the LCA-members. According to the corresponding failure mechanisms, the larger bolts (16, 20 and 24 mm) fail due to failure mechanism F and I, which correspond with the single slotted-in steel plate and double slotted-in steel plate. These two failure mechanisms describe the failure mode of the embedment strength of the timber member. In general, this type of failure can be seen as a brittle failure, which reduces the ductile capacity of the joint. In this research project, the brittle failure mechanisms are excluded, as discussed in section 3.5. According to the equations E.6 and E.13 the failure mechanism F and I are determined by the member width and the diameter of the fastener. Since the LCA-members has a smaller width compared to the LHB-members, the LCA-member in combination with the larger diameters will reached faster the 'brittle' mechanism. Moreover, due to the additional rope effect, the

bolts can generate an additional capacity compared to dowels. This additional capacity only contributes to the 'ductile' failure mechanisms, the ones which fail based on the yielding of the fasteners, according to (NEN-EN-1995-1-1, 2004). This means that the 'brittle' failure mechanism is reached faster for bolts than for the dowels

In order to explain the ratio between lag screws and bolts in steel part A for joint 1 and 2, figure 5.21 illustrates the load distribution of the three constructed cases. Corresponding to this figure, the maximum moments and shear forces in the primary and secondary beam are shown in table 5.5.

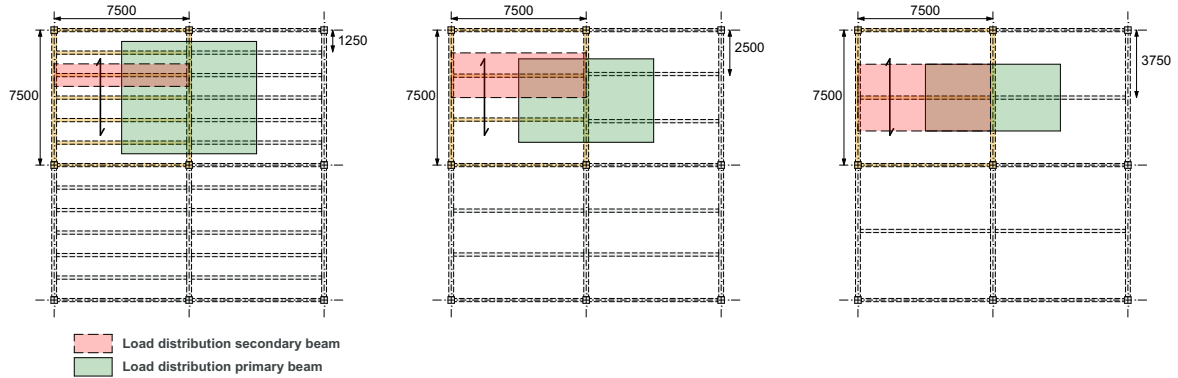


Figure 5.21: Load distribution secondary and primary beam

| Distance between secondary beams [m] | Secondary beam | | Primary beam | |
|--------------------------------------|----------------|---------------|----------------|---------------|
| | M_{Ed} [kNm] | V_{Ed} [kN] | M_{Ed} [kNm] | V_{Ed} [kN] |
| 1.25 | 76 | 41 | 454 | 203 |
| 2.50 | 149 | 79 | 404 | 163 |
| 3.75 | 222 | 119 | 452 | 123 |

Table 5.5: Maximum moments and shear forces in primary and secondary beam analysis 1

The figure and table illustrate that the primary beam with the smallest distance between the secondary beams transfers the highest shear forces, and the secondary beam with the largest distance between the secondary beams transfers the highest shear forces. This observation is reflected in the ratio between bolts and lag screws, illustrated in figure 5.2.

The following conclusions can be made. First, the ratio between lag screws and bolts in steel part A demonstrates a clear dominance of bolts in joint 1, wherein the highest loads occur. Important to mention is that this result is slightly biased, since the diameter of lag screws is limited to 16 mm, and bolts contain the additional diameters of 20 mm and 24 mm. Nevertheless, the data shows that the loading capacity of bolts is higher compared to lag screws. The main reason for this capacity difference is the additional capacity due to the rope effect, in which the withdrawal capacity of the lag screws is limited due to the available penetration length of the corresponding member.

Second, figure 5.2 demonstrates that all possible configurations that contain lag screws are available for all constructed cases except for the LHB-member in the constructed case with the largest distance between the secondary beams (3.75 m). From the table and the figure can be concluded that this secondary beam transfers the highest shear force, which results in a reduction of one for the number of possible configurations (lag screw - M8 - 2 column in fastener group). Finally, figure 5.2 illustrates that all possible configurations that contain bolts are available except for the LCA-members in joint 2. Similar to steel part B, the larger diameter (in this case the diameter 24 mm) reached the 'brittle' failure mechanism J for the members with small widths.

Analysis 2

The pattern observed in the ratio between dowels and bolts in steel part B in analysis 2 can be explained by the reasoning that is outlined above. Moreover, the enlargement of the grid sizes of the columns results in a reduction of possible configurations that contain lag screws. For grid size 8.75 m, there are no possible configurations containing lag screws. In the case of joint 2, the same pattern

is observed. The reduction in terms of the number of possible configurations can be explained based on the 'brittle' failure mechanism J being reached, as discussed before. Moreover, the distance between the secondary beams is constantly 1.25 m, and the difference in beam length does not result in a reduction of the number of possible configurations containing lag screws.

Diameter fastener

Analysis 1

The pattern that occurs at steel part B in the LCA-members in joint 1 and joint 2 and can be explained by the 'brittle' failure mechanisms can also be observed in the distribution between the different fasteners diameters. The diameters 12, 16, 20, and 24 mm are less present in the configurations of the LCA-members. Moreover, figure 5.4 illustrates that the diameter of 8 mm becomes more dominant in steel part A in joint 1. This pattern cannot be observed in joint 2. This can be explained as follows. The column width is generally determined by the primary beam with a maximum thickness of 240 mm, as discussed in section 3.1.4. As a result, the columns primarily have rectangular cross-sections, as seen in the standard cross-sections offered by the timber suppliers. Depending on the constructed case, the depth of the column varies. In order to limit significant column depths, the maximum width of the column was extended for the constructed cases that include high forces in the column. Table 5.6 illustrates the corresponding column sizes of each constructed case.

| | Analysis 1 | Analysis 2 |
|------------------|---------------------------|------------|
| Constructed case | Cross-section column [mm] | |
| 3.75x3.75 - 1.25 | | 240x240 |
| 5.00x5.00 - 1.25 | | 240x320 |
| 6.25x6.25 - 1.25 | | 240x520 |
| 7.50x7.50 - 1.25 | 280x640 | 280x640 |
| 7.50x7.50 - 2.50 | 280x640 | |
| 7.50x7.50 - 3.75 | 280x640 | |
| 8.75x8.75 - 1.25 | | 320x720 |

Table 5.6: Cross-section column for each constructed case

The generated configurations of steel part A in joint 1 demonstrate that no diameter, except for 8 mm, fits into a four column fastener group, due to the width of the corresponding column. In other words, the outer fasteners fall outside of the column, as illustrated in figure 5.22. Especially a four column fastener group in combination with a double slotted-in steel plate creates a wide steel part A. The enlargement of steel part A does not have an influence on joint 2, since the steel part is free to expand, as illustrated in figure 5.22. These results can be observed in the ratio between the diameters, illustrated in graph 5.4.

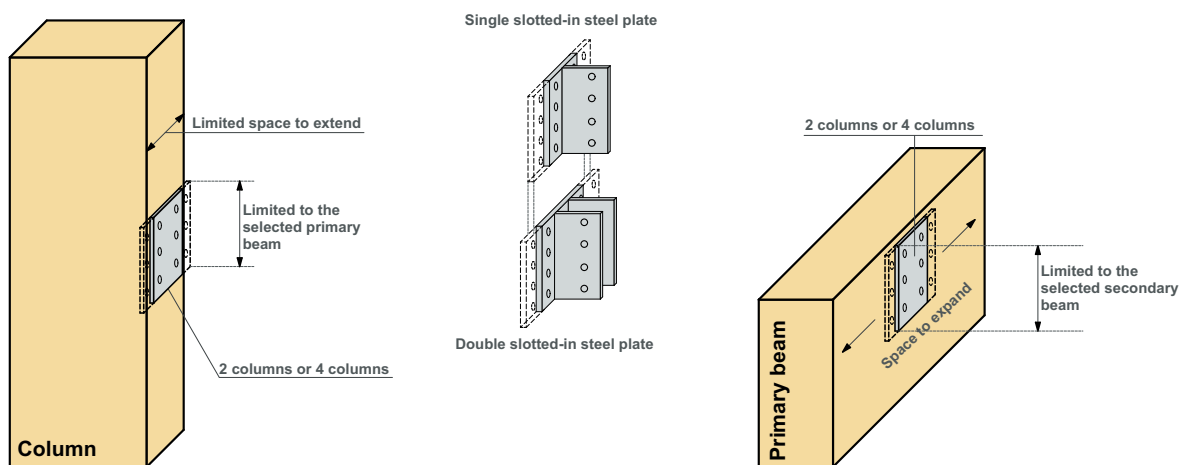


Figure 5.22: Limited space steel part A

Analysis 2

In analysis 2, the pattern that occurs at steel part B in the LCA-members in joint 1 and joint 2 - which can be explained by the 'brittle' failure mechanisms - is observed in the distribution between the different fastener diameters. Moreover, from graph 5.13 can be concluded that the larger diameters 20 and 24 mm cannot fit into the secondary LHB-members at grid size 3.75 m. For the LCA-member, solely 24 mm does not fit. This can be explained by the minimal distances between the fasteners and between the fasteners and the end of the member in combination with the small member height. Additionally, for the LHB-member, the number of possible configurations of the remaining diameters reduces as well, except for diameter 12 mm.

In steel part A, the effect of the limited column width has a similar effect on joint 1. Due to the large shear forces of the constructed cases 7.50 m and 8.75 m, the possible configurations of the LHB-members do not contain diameter 12 mm. The possible configurations of the remaining diameters are limited for both member categories due to the limited width of the column.

The options that are illustrated in figure 5.23 demonstrate ways to increase the number of possible configurations for steel part A in joint 1. The first option is increasing the column's width to ensure that the four columns layout of the fastener group fits. The second option is to release the height of steel part A, which is at the moment limited by the height of the corresponding primary beam. When enlarging steel part A upwards and/or downwards, the introduction of additional fasteners in the columns group is feasible. The third option is to slot in the steel plate(s) in the column as well. Graph 5.18 shows that the number of possible configurations is significantly higher for steel part B. The embedment strength in the column is higher, since the grain direction is parallel to the grain, as discussed in section 2.3.2. However, the effective number of fasteners (n_{ef}) needs to be considered for fasteners groups loaded parallel to the grain.

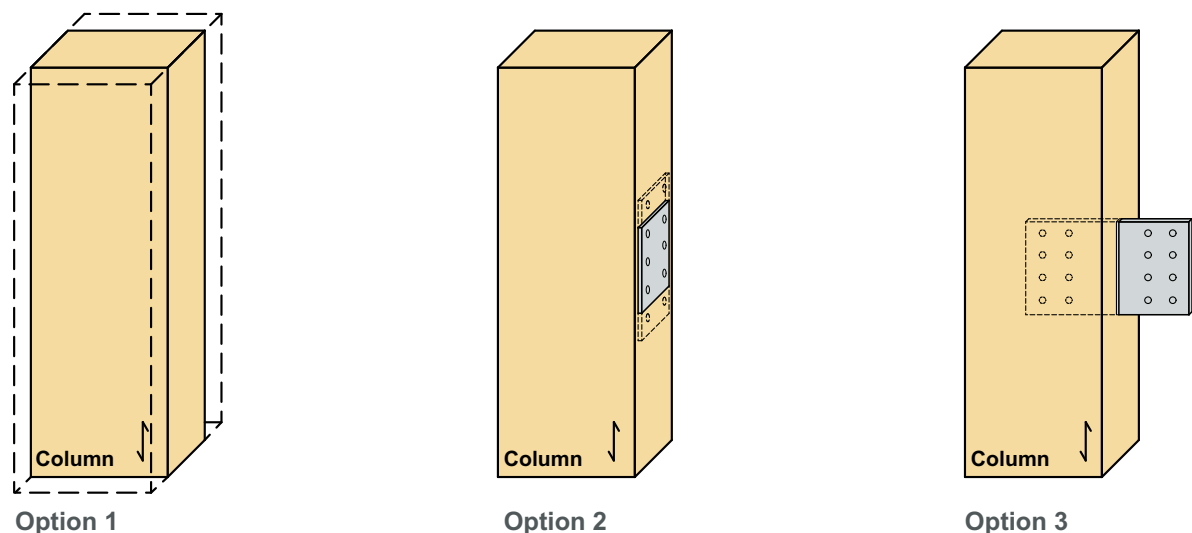


Figure 5.23: Options to enlarge the number of possible configurations for steel part A

Number of Columns in Fastener Group - Steel Part B

Analysis 1

The distribution between one column and two columns in the fastener group is approximately equally distributed for both joints, as illustrated in graph 5.5. From this observation can be concluded that the differences in distance between the secondary beams has hardly any influence on the number of columns in the fastener group. Moreover, the same pattern is observed regarding the 'brittle' failure mechanisms that occurs at steel part B in the LCA-members in joint 1 and joint 2.

Analysis 2

The ratio between one column and two columns in the fastener group for steel part B in analysis 2 is significantly different compared to analysis 1. From graph 5.16 can be concluded that, for the LHB-member, in grid sizes 3.75 m and 5.00 m significantly more configurations are generated that contain two columns in the fastener group. The smaller height of the member limits the possible configurations that include one column in the fastener group. For the remaining grid sizes, the member ratio between one column and two columns in the fastener group is equally distributed, as illustrated in graph 5.15. This can be explained by comparing the maximum shear forces and moment forces in the beam and assuming the reaction forces from the secondary beams on the primary beam as a distributed load, since the distance between the secondary beams is 1.25 m. In order to calculate the bending moment and the maximum shear force on a simple supported beam on two supports, loaded with a distributed load, the equation 5.1 can be applied.

$$\begin{aligned} V &= \frac{q}{2}L \\ M &= \frac{q}{8}L^2 \end{aligned} \quad (5.1)$$

Where:

| | | |
|-----|------------------|------|
| V | shear force | kN |
| M | bending moment | kNm |
| q | distributed load | kN/m |
| L | span | m |

The M/V ratio between moment and shear force increases linearly with the enlargement of the grid sizes. This means that the maximum moment increases faster than the maximum shear forces when enlarging the grid sizes. The smaller grid sizes, such as 3.75 m and 5.50 m, generate relatively high shear forces and a low bending moment compared to the remaining grid sizes. With a low bending moment, the height of the designed cross-section is relatively small, whereas the shear force is still relatively high. In that case, the height of the member is insufficient to transfer the shear force over one column group, and an additional column in the fastener group is required. Moreover, this effect can be observed as well between the LHB- and LCA-member within the 3.75 m grid size itself, as illustrated in graph 5.15

The shear forces are relatively low for the grid size 3.75 m compared to the larger grid sizes. Less complex connections such as joist hangers or steel brackets are connections types that are suitable for this grid size.

Number of Columns in Fastener Group - Steel Part A*Analysis 1*

The influence of the limited width of the columns in joint 1 is illustrated in graph 5.6. This graph demonstrates that there are only two unique configurations that contain four columns in the fastener group. Combining this graph with graph 5.2 and graph 5.4, one can conclude that the lag screw and bolt with a diameter of 8 mm satisfy for all constructed cases. Additionally, the number of unique configurations of the two columns in the fastener group increases with the enlargement of the distance between the secondary beams. This can be explained by the fact that the shear forces decrease in the primary beam when the distance between the secondary beams increases, as illustrated in graph 5.21 and table 5.1. Moreover, the width of steel part A in joint 2 is not limited, which can be observed in graph 5.6. The maximum number of configurations is possible, except for the LHB-member in joint 2 for the largest distance between the secondary beams. This beam needs to transfer the highest shear forces, as illustrated in table 5.5. Finally, for all constructed cases, the LHB-member generates for both column categories in the fastener group one configuration more than the LCA-member does. This can be linked to the larger diameter of 24 mm that reached the 'brittle' failure mechanism J for the members with small widths.

Analysis 2

The conclusions made regarding the observations for analysis 1 apply to analysis 2 as well. Additionally, from graph 5.6 in combination with graph 5.12 can be concluded that the only possible configuration that contains four columns in the fasteners group consists of bolts with a diameter of 8 mm.

Number of Slotted-in Steel Plates*Analysis 1*

The patterns found in graph 5.7 illustrate the effect of the 'brittle' failure mechanisms in the LCA-members, as previously discussed. Combining graph 5.7 with graph 5.3 and graph 5.1 illustrates that a member thickness of 140 mm starts to generate a 'brittle' failure mechanism in the following combinations. First, bolts with a diameter of 16 mm and larger, including a double-slotted in steel plate. Second, dowels with a diameter of 20 mm, including a double slotted-in steel plate. Third, bolts with a diameter of 24 mm, including a single slotted-in steel plate.

Analysis 2

The same conclusion can be made regarding the 'brittle' failure mechanism for LCA-members as the one that is made in analysis 1. Moreover, the double slotted-in steel plate in the LHB-member dominates the single slotted-in steel plate in joint 1 at grid size 3.75 m and 5.00 m. As mentioned in the paragraph about the M/V ratio, the members in these two grid sizes have relatively high shear forces and a low bending moment compared to the remaining grid sizes. In order to transfer the shear force, the parameter 'columns in the fastener group' shows that the majority of the configurations contains two columns in the fastener group. From graph 5.17 in combination with graph 5.13 can be concluded that the remaining configurations that contain one column in the fastener group need a double slotted-in steel plate to transfer the shear forces. The bolts and dowels with a diameter of 12 mm are only able to construct a configuration with one column in the fastener group and a single slotted-in steel plate for grid size 3.75 m. In the case of grid size 5.00 m, the 16 mm diameter bolts and dowels also allow for this configuration to be made.

5.4.2. Number of Unique Configurations Steel Part A and B

The number of unique configurations for steel part A and B helps one to understand whether the cross-sectional sizes of the member are dictated by the dimensional sizes of the laterally loaded dowel-type connection or the strength and stiffness requirements of the member itself.

Analysis 1

Graph 5.8 illustrates the number of unique configurations for each constructed case of analysis 1. From the graph can be concluded that there is always a configuration available that fits into the corresponding member. However, there is a difference in the number of unique configurations between the different steel parts for joint 1 and joint 2.

Joint 1

From the results can be concluded that the number of unique configurations for steel part A is significantly lower than those for steel part B. The column width has a huge impact therein, as discussed in section 5.4.1. Moreover, the number of unique configurations increases as the distance between the secondary beams increases for both member categories. This can be explained by the load transfer, which is illustrated in graph 5.21. Finally, there is a drop in the number of configurations visible, indicated with letter 'A' in graph 5.8. The smaller width of this member results in less possible configurations due to the 'brittle' failure mechanism that occurs in this member, as discussed in section 5.4.1.

Joint 2

From the graph can be concluded that the difference in distance between the secondary beams has no effect on steel part A for both member categories. Only a general reduction is visible, which is caused by the 'brittle' failure mechanisms. Moreover, the difference in distance between the secondary beams has less of an effect on the number of unique configurations of steel part B for both member categories. A small reduction can be seen for the higher loaded members. Finally, the effect of 'brittle' failure mechanisms is strongly visible between the LCA-members and the LHB-members in the number of unique

configurations.

Analysis 2

Graph 5.18 illustrates the number of unique configurations for each constructed case of analysis 2. From this graph can be concluded as well that there is always a configuration available that fits into the corresponding member. However, there is a difference in the number of unique configurations between the different steel parts for joint 1 and joint 2.

Joint 1

From the graph can be concluded that the number of possible configurations for steel part A in the LCA-member reduces linearly as the grid sizes increase. The combination of a limited column width and the increase of the shear force in the steel part leads to a reduction in number of unique configurations, as discussed in section 5.4.1. The number of unique configurations for steel part A is higher for the LCA-members than the LHB-members. This can be explained by the fact that the LCA-members are higher, which allows one to apply more fasteners in steel part A. The drop that is visible in the number of unique configurations for steel part B in the LCA-member, indicated with the letter 'A', demonstrates the effect of the 'brittle' failure mechanisms, as discussed in section 5.4.1. The number of unique configurations for steel part B in the LHB-member shows a drop between the grid size of 3.75 m and 5.00 m, indicated with the letter 'B'. This can be explained by the effect of a compact member in combination with a relatively high shear force, as discussed in section 5.4.1.

Joint 2

The different grid sizes have no effect on the number of possible configurations for steel part A for both member categories. This can be explained by the fact that the distance between the secondary beams in this analysis was constantly 1.25 m. Only the span differed, which resulted in relatively small differences between the shear forces in the joints. The number of unique configurations for steel part B in the LCA-members is equal for all constructed cases, except for grid size 3.75 m. The effect of a 'compact member' with relatively high shear forces can be found in this result. The drops ('A' and 'B') that are visible in the number of configurations for steel part B in the LHB-members are caused by the 'compact member' effect, as discussed in section 5.4.1, and the influence of the 'brittle' failure mechanism.

5.4.3. Steel Mass Ratio Steel Part A and B

In sections 5.2.3 and 5.3.3, the steel mass ratio of all unique configurations is analysed for steel part A and steel part B in both analysis 1 and 2. The graphs illustrate the steel mass of the lowest and highest configurations. Moreover, they show the average steel mass of all unique configurations.

From graph 5.9 and graph 5.10 can be concluded that the average steel mass of steel part A is higher compared to steel part B for all constructed cases, which means that steel part A needs more steel in order to transfer the same shear forces. Moreover, the average steel mass starts to converge for both steel parts as the distance between the secondary beams increases. This can be explained by the load distribution, as discussed in section 5.4.1. From graph 5.19 and graph 5.20 can also be concluded that the average steel mass of steel part A is higher than steel part B for all constructed cases, which means that steel part B is a more efficient steel part in terms material quantity.

From both analyses can be concluded that the difference between the lowest and highest configuration is significant. That means that the selected configuration can have a large influence on the total amount of steel applied to the timber structure. In order to add more value to the graphs 5.2.3 and 5.3.3, the lowest mass configurations are illustrated in the tables 5.1, 5.3, 5.2, 5.4. From 5.1 and 5.3 can be concluded that the configuration with the lowest steel mass for steel part A in all constructed cases primarily consists of lag screws with a diameter of 8 mm. This can be explained by the fact that, unlike bolts, lag screws do not have to penetrate the full width of a member in order to activate the fastener, as illustrated in figure 2.15. Especially in deep columns, the use of bolts leads to steel 'waste', which is needed in order to apply the fastener in a proper way. Therefore, the lag screws are the majority fastener type in steel part A when analysing the lowest steel mass configurations. In steel part B, the majority of the fasteners are dowels with a diameter of 8 mm in combination with a single slotted-in steel plate, as illustrated in table 5.10 and table 5.20. This can be explained by referring to the minimal distance between the fastener group and the end of the member, as discussed in section 2.4.5. Due

to the eccentricity moment, the fasteners close to the end of the member are specified as loaded end. According to table D.2 as shown in Appendix D, the distance increases with the enlargement of the diameter.

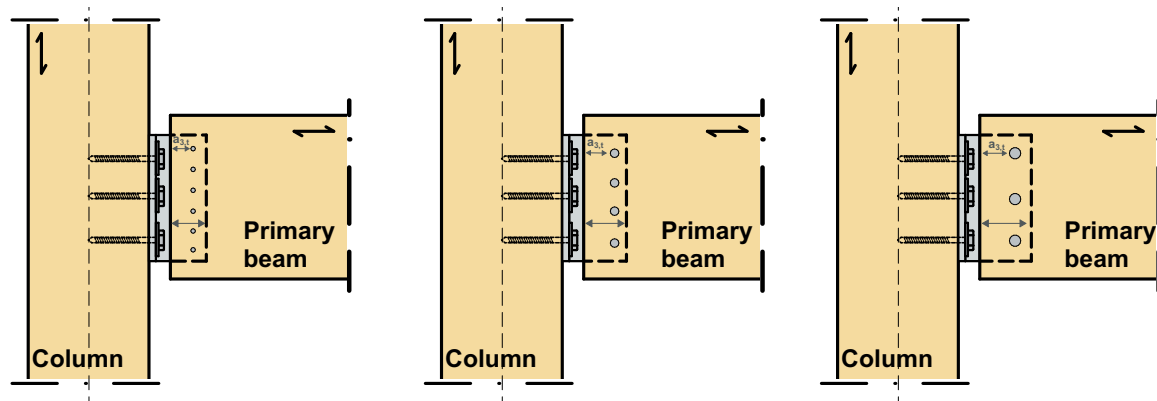


Figure 5.24: The different end distances between the fastener group and the member depending on the diameter fastener

As an illustration, a 8 mm dowel needs a minimal distance between the fastener and the end of the member of 80 mm. A dowel with a diameter of 24 mm needs a minimal distance of 168 mm. This means that the slotted-in steel plate(s) is/are integrated deeper into the member for the larger diameters in order to fulfill the minimal distance, as illustrated in figure 5.24. Since the slotted-in steel plate is integrated over the full height of the member, the extension of the steel plate(s) into the member has a large effect on the total steel mass of steel part B. Therefore, the dowels with a small diameter are the majority fastener type in steel part B, when examining the lowest steel mass.

This section has shown that the fasteners with a smaller diameter generate the configurations with the lowest steel mass. On the other hand, the number of fasteners applied in these configurations is significantly high compared to the configurations that consist of larger diameters. Based on other perspectives, such as manufacturing and site assembly, one can question whether a configuration with a large number of fasteners is efficient in terms of production and assembly time. Moreover, the complexity of the connection in terms of tolerance between the pre-drilled holes and the fasteners during the assembly can be quite difficult for connections that consist of a large number of fasteners. From those perspectives, the choice for a configuration that contains less fasteners and fasteners with a larger diameter can be imagined. In chapter 6 will be discussed how the use of the tool can help one to select the most 'efficient' configurations based on certain predefined criteria.

6

Conclusions and Recommendations

6.1. Conclusions

The importance of joints in timber structures is strongly emphasized in the existing literature. Yet, previous research that specifically examines the question of how important joints in timber structures really are is limited. The aim of this project was to provide insight into whether the cross-sectional sizes of the member are dictated by the dimensional sizes of the laterally loaded dowel-type connection or the strength and stiffness requirements of the member itself. The insight gained in this study adds knowledge to the existing literature that gives a new perspective on the importance of joints in timber structures. Moreover, the results of this study may help structural engineers to make well-argued decisions in determining the cross-section of timber members in a frame structure that take into account the effect of joints in the early design phase. Especially the tool that was constructed for this parametric study may be helpful for engineers. The following research question was formulated to guide this study:

"What is the dimensional interaction between laterally loaded dowel-type connections and structural members in timber frame structures?"

In order to answer this question, the effect of different distances between the secondary beams (analysis 1) and the effect of different grid sizes of the column in the frame structure (analysis 2) were studied. For each analysis, two member sizes were first selected based on the criteria 'lowest cross-sectional area' (LCA) and 'lowest height beam' (LHB). These two member sizes formed the starting point for generating different configurations of the laterally loaded dowel-type connections. The connection was separated into two steel parts, parts A and B, for the purpose of this research project. In all constructed cases, two joints were analysed - the joint between a primary beam and a column (joint 1) and the joint between two secondary beams and a primary beam (joint 2). In the sections below, the main outcomes of this research project are presented, focusing on the most significant reductions in the number of possible configurations. This is followed by an overall conclusion.

Column Width

Both analysis 1 and 2 highlighted that the number of possible configurations for steel part A in joint 1 reduces as the shear forces start to increase. In analysis 1, the increase in shear forces is caused by the smaller spans between the secondary beams. In analysis 2, the analysis in which the reduction was most clearly visible, the increase is caused by the larger grid sizes. In this analysis, the LHB-member in grid size 8.25 m with the highest shear force demonstrates that there are only 3 configurations that fulfill the load capacity. These configurations consist of the diameters 20 mm and 24 mm in combination with 2 columns in the fastener group. The remaining configurations need four columns in the fastener group, which do not fit on the predesigned column, except for the configurations that include a bolt with a diameter of 8 mm. This means that the column width has a significant impact on the number of possible configurations in combination with high shear forces. In order to increase the number of possible configurations for steel part A in joint 1, the adjustments that are illustrated in figure 5.23 may be considered by engineers. First, enlarging the column width allows the larger diameter to fit into a

four column fastener group. Second, extending steel part A upwards and/or downwards allows one to add vertical fasteners in the fastener group. The last presented adjustment is replacing steel part A with steel part B, which means a slotted-in steel connection in the column as well. In sum, high shear forces in combination with a small column width, wherein the majority of the diameters do not fit with four columns in the fastener group, caused a significant reduction in the number of possible configurations. This finding may increase the engineer's awareness regarding the relevance of selecting a column with a sufficient thickness for steel part A in joint 1 in the preliminary design phase.

Compact Member

In analysis 2, the effect of a 'compact' member was observed for steel part B in the LHB-member in joint 1 as well joint 2 for the grid size 3.75 m. The effect of a 'compact' member shows itself in a reduction in the number of possible configurations for this grid size. In this member, the moment-shear (M/V) ratio is smaller compared to the larger grid sizes, which increases linearly as the length of the span increases. The height of the LHB-member is small due to the relatively low bending moment, yet the shear forces are relatively high. In that case, the height of the member is insufficient to transfer the shear forces over one column group. An additional column in the fastener group or a double slotted-in steel plate is required for all examined diameters except for the 12 mm fastener. For the larger grid sizes, the M/V ratio increases rapidly, which means that the moment becomes more dominant compared to the shear forces. Therefore, the height of beams is sufficient to transfer the shear forces over one column in the fastener group. In sum, for grid size 3.75 m, a reduction in the number of possible configurations was found as a result of a 'compact' member. This finding shows that steel part B in the LHB-member uses additional steel - in terms of a second column in the fastener group and a double slotted-in steel plate - in order to fulfill the load capacity, except for the 12 mm fastener. Engineers who seek to avoid a large steel mass may want to consider this finding in their projects.

Brittle Failure Mechanisms

One of the design assumptions made in this research project was to exclude the 'brittle' failure mechanisms, wherein the embedment strength of the timber member fails. As a result, in analysis 1 and 2, the LCA-members generate less possible configurations for steel part B compared to the LHB-members. In steel part B, the following combinations generate 'brittle' failure mechanisms for the LCA-member with a thickness of 140 mm. First, bolts with a diameter of 16 mm and larger including a double-slotted in steel plate. Second, dowels with a diameter of 20 mm including a double slotted-in steel plate. Third, bolts with a diameter of 24 mm including a single slotted-in steel plate. The fact that the bolts generate the 'brittle' failure mechanism earlier is caused by the rope effect that adds additional load capacity to the bolts. This additional capacity contributes to the 'ductile' failure mechanisms, the ones which fail based on the yielding of the fasteners, according to NEN-EN-1995-1-1 (2004). This means that the 'brittle' failure mechanism is reached faster for bolts than for dowels in the LCA-member. In sum, given this study's findings, in order to avoid 'brittle' failure mechanisms, selecting the LHB-members instead of the LCA-members for steel part B can be advised.

Overall Conclusion

In this research project, the three aspects discussed above have caused the largest reduction in the number of unique configurations for all constructed cases examined in analysis 1 and 2. This finding suggests that the aspects small column widths combined with high shear forces, the effect of a 'compact' member on the steel mass for the LHB-member in grid size 3.75 m, and selecting the LHB-members instead of the LCA-members for steel part B may be relevant for engineers to take into account when designing the structural members. However, in this study, there was no constructed case in which the member needed to be redesigned in order to fit the connection. In other words, in terms of the dimensional interaction between the laterally loaded dowel-type connection and the structural members, one can conclude that the dimensional size of the structural member is dictated by the strength and stiffness requirements of the member itself. Before the start of this study, one of the imagined outcomes was the observation of certain turning points between the cross-sectional size being dictated by the member or dictated by the connection, forcing the engineer to redesign the member. The fact that these turning points did not appear in the data adds a new perspective to the existing literature regarding the importance of joints in timber structures.

Important to note is that, although a large number of parameters was incorporated into this study, not all potentially relevant parameters were taken into account. When incorporating factors such as the horizontal forces in the connection, the effect of shrinkage and swelling, the level of difficulty in terms of assembling the joints on site, and adjustments to guarantee a certain level of fire resistance, certain turning points in the dimensional interaction between joints and members may be found. Ultimately, the findings of this study are specific to timber frame structures that only transfer vertical loads and to the selected parameters.

Finally, beyond allowing for the dimensional interaction between joints and members to be studied, the different scenarios outlined in section 4.6.2 have shown that the tool constructed in this study is also valuable to practical engineering. The large amount of data that is generated by the tool allows the engineer to explore the different possible configurations in the process of designing joints. By connecting the output of the tool to the Design Explorer interface, the engineer has the opportunity to search through all the individual characteristics or a specific range and examine different possible connections in an efficient manner. One of the main contributions of this research project, therefore, lies in the tool itself.

6.2. Recommendations

This section presents a number of recommendations for further research in the field of timber joints based on this study's observations and conclusions.

Shrinkage and Swelling

The effect of swelling and shrinkage caused by varying moisture levels may lead to crack forming between the member and the connection components. These cracks may lead to strength reduction of the member and/or the joint. The cracks in the joint commonly run horizontally along the grains and start at the outer fasteners in the fastener group. The grains start to expand, yet are being held by the fasteners. The influence of swelling and shrinkage becomes larger as the height of the member increases. Two ways to reduce the effect of shrinkage and swelling in the joint for steel part B are illustrated in figure 6.1. First, providing the outer fasteners in the fastener group with vertically slotted holes. This adjustment has a substantial impact on the number of possible configurations, since the (outer) fasteners with the vertically slotted holes no longer contribute to the shear capacity. Instead, they only impact the horizontal force caused by the eccentricity moment. Second, limiting the fastener group to one position, for instance, at the bottom of the member, instead of dividing the fastener group over the entire height of the beam. By selecting this solution, the number of fasteners in the fastener group is reduced. In future research, these adjustments can be integrated into the tool that was constructed for this study, allowing for new analyses of the number of possible configurations to be achieved.

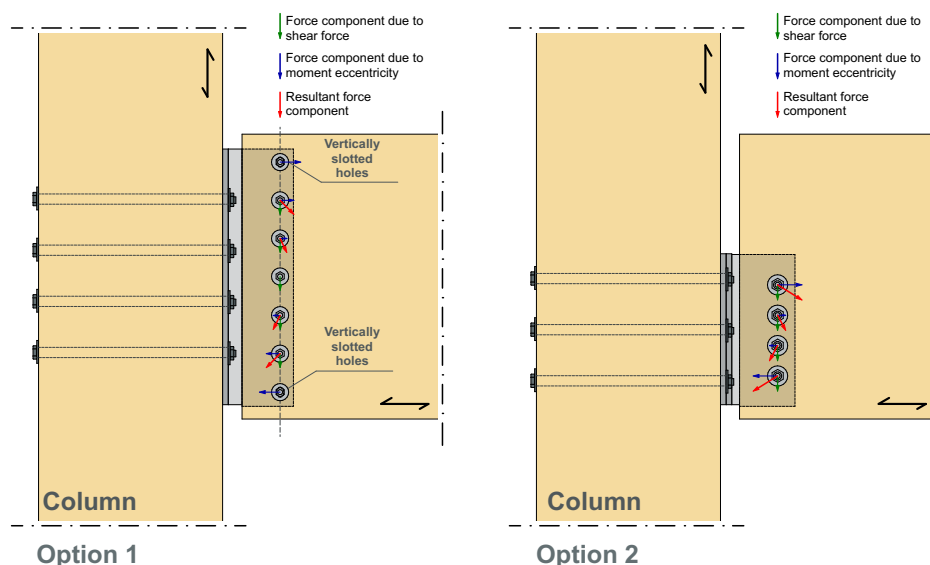


Figure 6.1: Options to reduce the effect of shrinkage and swelling

Tool

The tool constructed for this research project generates configurations based on a selected member in the frame structure. These configurations offer a large amount of data, such as the fastener type, the diameter of the fastener, number of slotted-in steel plates, and total steel mass. This data offers the engineer a set of possible configurations for a specific joint. The visualization interfaces of Design Explorer developed by Core studio, allow the engineer to search through all the individual characteristics or a specific range to examine different possible configurations in a efficient manner. Although the tool is already deemed valuable for the engineer, future research could further develop the tool and increase its value even more. To further increase the value of the tool for the engineer, one possible direction for future research would be to link certain weighting factors to specific parameters in order to incorporate the site assembly or production costs of each configuration into the tool.

Steel mass

In this research project, a set of first observations have been made regarding the steel mass ratio of each constructed case. The minimum, maximum, and average mass of all unique configurations for each constructed case were determined. The first results regarding the configurations with the lowest steel mass demonstrate that the configuration mainly consists of lag screws with a diameter of 8 mm for steel part A and dowels with a diameter of 8 mm for steel part B. The corresponding number of fasteners of these configurations is significantly high compared to the configurations that consist of larger diameters. Selecting a configuration based on its low steel mass may, therefore, have a negative impact on the feasibility of mounting the fastener. As already mentioned in the paragraph above, a formula consisting of different weighting factors may help the engineer to find the most 'efficient' configuration based on the predefined weighting factors. Incorporating steel mass as a weighting factor helps the engineer to select configurations that have a smaller environmental footprint in terms of the global structure.

Multiple connections

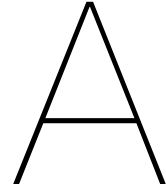
In order to limit the scope of this research, two joints were selected in the frame structure. The first was a single primary beam with a single column. The second joint was a joint between a primary beam and two secondary beams. In future research, a next step that can be made is constructing a joint with a minimal of three connections. The challenge with a joint that has more than two connections is that the fastener of each connection can be crossed by the fasteners of the other connections. Moreover, the adjustment of each fastener group can lead to a reduction in the number of fasteners, which can have an effect on the number of possible configurations. These factors are relevant to take into account for future research focusing on more than two connections in the joint.

References

- Apellániz, D. (2022). Parametric fem toolbox. <https://www.food4rhino.com/en/app/parametric-fem-toolbox>
- Blaß, H. (2003). Joints with dowel-type fasteners. In S. Thelandersson & H. Larsen (Eds.). John Wiley Sons.
- Blaß, H., & Sandhaas, C. (2017). Timber engineering - principles for design. KIT Scientific Publishing.
- Blass, H., Aune, P., Choo, B., Grolacher, R., Griffiths, D., Hilson, B., Racher, P., & Steck, G. (Eds.). (1995a). *Timber engineering step 1* (First). Centrum Hout.
- Blass, H., Aune, P., Choo, B., Grolacher, R., Griffiths, D., Hilson, B., Racher, P., & Steck, G. (Eds.). (1995b). *Timber engineering step 2* (First). Centrum Hout.
- Borgström, E. (Ed.). (2016). *Design of timber structures* (2:2016, Vol. 1). Swedish Wood.
- Claisse, P. A., & Davis, T. J. (1998). High performance jointing systems for timber. *Construction and Building Materials*, 12(8), 415–425. [https://doi.org/https://doi.org/10.1016/S0950-0618\(98\)00031-2](https://doi.org/https://doi.org/10.1016/S0950-0618(98)00031-2)
- COREStudio. (n.d.). Tool for exploring multi-dimensional parametric studies. <http://tt-acm.github.io/DesignExplorer/>
- DeGroot-Vroomshoop. (n.d.). Details and downloads. <https://gelijmde-houtconstructies.nl/gelijmde-houtconstructies/producten/specificaties/details-en-downloads/>
- Frühwald Hansson, E. (2011). Analysis of structural failures in timber structures: Typical causes for failure and failure modes [Modelling the Performance of Timber Structures]. *Engineering Structures*, 33(11), 2978–2982. <https://doi.org/https://doi.org/10.1016/j.engstruct.2011.02.045>
- Gečys, T., & Daniūnas, A. (2017). Rotational stiffness determination of the semi-rigid timber-steel connection. *Journal of Civil Engineering and Management*, 23, 1021–1028. <https://doi.org/10.3846/13923730.2017.1374305>
- Heko-spanten. (n.d.). Details archieven. <https://www.hekospanten.nl/download/details/>
- Jockwer, R., Caprio, D., & Jorissen, A. (2021). Evaluation of parameters influencing the load-deformation behaviour of connections with laterally loaded dowel-type fasteners. *Wood Material Science Engineering*, 1–14. <https://doi.org/10.1080/17480272.2021.1955297>
- Johansen, K. (1949). Theory of timber connections. *International Association for Bridge and Structural Engineering*, 9(9), 249–262.
- Kirkegaard, P., Sørensen, J., Čizmar, D., & Rajcic, V. (2011). System reliability of timber structures with ductile behaviour. *Engineering Structures*, 33, 3093–3098. <https://doi.org/10.1016/j.engstruct.2011.03.011>
- Kolb, J. (2008). *Systems in timber engineering: Loadbearing structures and component layers*. Walter de Gruyter.
- Masson-Delmotte, V., Zhai, P., Pirani, A., Connors, S., Péan, C., Berger, S., Caud, N., Chen, Y., Goldfarb, L., Gomis, M., Huang, M., Leitzell, K., Lonnoy, E., Matthews, J., Maycock, T., Waterfield, T., Yelekci, O., Yu, R., & Zhou, B. (2021). *The physical science basis. contribution of working group i to the sixth assessment report of the intergovernmental panel on climate change* [Summary for Policymakers]. Cambridge University Press.
- McLain, T. E. (1998). Connectors and fasteners: Research needs and goals. *Wood Engineering in the 21st Century: Research Needs and Goals*, 56–69.

- Metsä-Wood. (2016). Ich bin kerto. https://www.holz-boegner.de/fileadmin/user_upload/Partner_Boegner/03_Services/032_Entdecken_Planen/0323_Kataloge_Dokumente/Metsawood_Kerto.pdf
- NEN-EN-14080. (2013). *Timber structures - glued laminated timber and glued solid timber - requirements*. CEN.
- NEN-EN-1990. (2004). *Eurocode 0; basis of structural design*. CEN.
- NEN-EN-1991-1-1. (2004). *Eurocode 1; actions on structures - part 1-1: General actions - densities, self-weight-imposed loads for building*. CEN.
- NEN-EN-1993-1-1. (2006). *Eurocode 3; design of steel structures - part 1-1: General rules and rules for buildings*. CEN.
- NEN-EN-1995-1-1. (2004). *Eurocode 5; design of timber structures - part 1-1: General - common rules and rules for buildings*. CEN.
- NEN-EN-1995-1-1:concept. (20XX). *Eurocode 5; design of timber structures - part 1-1: General - common rules and rules for buildings*. CEN.
- NEN-EN-383. (2007). *Timber structures - test methods - determination of embedment strength and foundation values for dowel type fasteners*. CEN.
- Ong, C. (2015). 7 - glue-laminated timber (glulam). In M. P. Ansell (Ed.), *Wood composites* (pp. 123–140). Woodhead Publishing. <https://doi.org/https://doi.org/10.1016/B978-1-78242-454-3.00007-X>
- Ottenhaus, L., Jockwer, R., Drimmelen, D., & Crews, K. (2021). Designing timber connections for ductility – a review and discussion. *Construction and Building Materials*, 304, 124621. <https://doi.org/10.1016/j.conbuildmat.2021.124621>
- Pedersen, M. (2002). Dowel type timber connections. (Byg Rapport NO. R-039).
- Phong, T. (2020). Analysis and optimization of the bearing capacity of connecting wooden structures with application of dowel type self-drilling. *IOP Conference Series: Materials Science and Engineering*, 896, 012037. <https://doi.org/10.1088/1757-899X/896/1/012037>
- Rossi, S., Crocetti, R., Honfi, D., & Frühwald Hansson, E. (2016). Load-bearing capacity of ductile multiple shear steel-to-timber connections.
- Sawata, K., Sasaki, T., & Kanetaka, S. (2006). Estimation of shear strength of dowel-type timber connections with multiple slotted-in steel plates by european yield theory. *Journal of Wood Science*, 52, 496–502. <https://doi.org/10.1007/s10086-006-0800-9>
- Sjödin, J., & Johansson, C.-J. (2007). Influence of initial moisture induced stresses in multiple steel-to-timber dowel joints. *Holz als Roh- und Werkstoff*, 65, 71–77. <https://doi.org/10.1007/s00107-006-0136-6>
- Spreax. (n.d.). Convert your spreadsheet and increase engagement. <https://spreax.com/en>
- Stepinac, M., Cabrero, J. M., Ranasinghe, K., & Kleiber, M. (2018). Proposal for reorganization of the connections chapter of eurocode 5. *Engineering Structures*, 170, 135–145. <https://doi.org/https://doi.org/10.1016/j.engstruct.2018.05.058>
- Swedish-Wood. (n.d.). Moisture-related wood movement. <https://www.swedishwood.com/wood-facts/about-wood/wood-and-moisture/moisture-related-wood-movement/>
- Thelandersson, S., & Larsen, H. (Eds.). (2003). *Timber engineering* (First). John Wiley Sons.
- United Nations Environment Programme, G. A. f. B., & Construction. (2020). 2020 global status report for buildings and construction: Towards a zero-emissions, efficient and resilient buildings and construction sector - executive summary. <https://wedocs.unep.org/20.500.11822/34572>
- van der Lugt, P. (2020). *Tomorrow's timber: Towards the next building revolution*. MaterialDistrict.

Wettelijke afmetingen ontheffingen. (n.d.). <https://www.rdw.nl/zakelijk/branches/transporteurs/incidentele-ontheffing/wettelijke-afmetingen-ontheffingen>



Appendix Verification Members

Verification beams and columns

In this appendix the formulas are illustrated that are applied into the tool in order to verify the glued laminated members.

Shear Stress

The beams experience shear stress and should be validated by using the following formula as defined in NEN-EN-1991-1-1 (2004).

$$\tau_d = \frac{3}{2} \frac{V_d}{A} \leq f_{v,d} \quad (\text{A.1})$$

Where:

| | | |
|-----------|----------------------|-------------------|
| τ_d | Design shear stress | N/mm ² |
| $f_{v,d}$ | Design shear force | N |
| A | cross-sectional area | mm ² |

Bending Stress

The beams experience bending stress and should be validated by using the following formulas as defined in NEN-EN-1991-1-1 (2004). In this case the bending stress occurs only about the principle y-axis.

$$\frac{\sigma_{m,y,d}}{f_{m,y,d}} + k_m \frac{\sigma_{m,z,d}}{f_{m,z,d}} \leq 1 \quad (\text{A.2})$$

$$\frac{\sigma_{m,z,d}}{f_{m,z,d}} + k_m \frac{\sigma_{m,y,d}}{f_{m,y,d}} \leq 1 \quad (\text{A.3})$$

Where:

| | | |
|------------------|---|-------------------|
| $\sigma_{m,y,d}$ | Design bending stress about the principle y-axis | N/mm ² |
| $f_{m,y,d}$ | Design bending strength about the principle y-axis | N/mm ² |
| $\sigma_{m,z,d}$ | Design bending stress about the principle z-axis | N/mm ² |
| $f_{m,z,d}$ | Design bending strength about the principle z-axis | N/mm ² |
| f_m | factor considering re-distribution of bending stresses in a cross-section | - |

Combined Axial and Bending Stress

The columns in the frame structure experience axial stress combined with bending. In this case the bending is assumed as the shear force times the eccentricity between the center of the column and the edge of the column. The frame structure consists of different floor fields, which determined the load and unloaded situations for the imposed loads. The following formulas as defined in NEN-EN-1991-1-1 (2004) need to be considered.

$$\left(\frac{\sigma_{c,0,d}}{f_{c,0,d}}\right)^2 + k_m \frac{\sigma_{m,y,d}}{f_{m,y,d}} + \frac{\sigma_{m,z,d}}{f_{m,z,d}} \leq 1 \quad (\text{A.4})$$

$$\left(\frac{\sigma_{c,0,d}}{f_{c,0,d}}\right)^2 + \frac{\sigma_{m,y,d}}{f_{m,y,d}} + k_m \frac{\sigma_{m,z,d}}{f_{m,z,d}} \leq 1 \quad (\text{A.5})$$

Where:

| | | |
|------------------|---|-------------------|
| $\sigma_{c,0,d}$ | Design compressive stress along the grain | N/mm ² |
| $f_{c,0,d}$ | Design compressive strength along the grain | N/mm ² |
| $\sigma_{m,y,d}$ | Design bending stress about the principle y-axis | N/mm ² |
| $f_{m,y,d}$ | Design bending strength about the principle y-axis | N/mm ² |
| $\sigma_{m,z,d}$ | Design bending stress about the principle z-axis | N/mm ² |
| $f_{m,z,d}$ | Design bending strength about the principle z-axis | N/mm ² |
| k_m | factor considering re-distribution of bending stresses in a cross-section | - |

Member Stability

The columns in the frame structure are subjected to combined compression and bending. Hereby the following formulas formulated in NEN-EN-1991-1-1 (2004) need to be considered.

$$\frac{\sigma_{c,0,d}}{k_{c,y} f_{c,0,d}} + \frac{\sigma_{m,y,d}}{f_{m,y,d}} + k_m \frac{\sigma_{m,z,d}}{f_{m,z,d}} \leq 1 \quad (\text{A.6})$$

$$\frac{\sigma_{c,0,d}}{k_{c,z} f_{c,0,d}} + k_m \frac{\sigma_{m,y,d}}{f_{m,y,d}} + \frac{\sigma_{m,z,d}}{f_{m,z,d}} \leq 1 \quad (\text{A.7})$$

$$k_{c,y;z} = \frac{1}{k_{y;z} + \sqrt{k_{y;z}^2 - \lambda_{rel,y;z}^2}} \quad (\text{A.8})$$

$$k_{y;z} = 0.5(1 + \beta_c(\lambda_{rel,y;z} - 0.3) + \lambda_{rel,y;z}^2) \quad (\text{A.9})$$

$$\lambda_{rel,y;z} = \frac{\lambda_{y;z}}{\pi} \sqrt{\frac{f_{c,0,k}}{E_{0.05}}} \quad (\text{A.10})$$

$$\lambda_{y;z} = \frac{l_{eff,y;z}}{i_{y;z}} \quad (\text{A.11})$$

$$i_{y;z} = \frac{I_{y;z}}{A} \quad (\text{A.12})$$

Where:

| | | |
|---------------------|---|-------------------|
| $\sigma_{c,0,d}$ | Design compressive stress along the grain | N/mm ² |
| $f_{c,0,d}$ | Design compressive strength along the grain | N/mm ² |
| $\sigma_{m,y,d}$ | Design bending stress about the principle y-axis | N/mm ² |
| $f_{m,y,d}$ | Design bending strength about the principle y-axis | N/mm ² |
| $\sigma_{m,z,d}$ | Design bending stress about the principle z-axis | N/mm ² |
| $f_{m,z,d}$ | Design bending strength about the principle z-axis | N/mm ² |
| k_m | factor considering re-distribution of bending stresses in a cross-section | - |
| $k_{c,y;z}$ | Instability factor | - |
| $k_{y;z}$ | Instability factor | - |
| $\lambda_{rel,y;z}$ | Relative slenderness ratio corresponding to bending about y- and z-axis | - |
| $\lambda_{y;z}$ | Slenderness ratio corresponding to bending about y- and z-axis | - |
| $f_{c,0,k}$ | Characteristic compressive strength along the grain | N/mm ² |
| $E_{0.05}$ | Fifth percentile value of modulus of elasticity | N/mm ² |
| $l_{eff,y;z}$ | Effective length | mm |
| $I_{y;z}$ | Second moment of area about y- and z-axis | mm ⁴ |
| A | Cross-sectional area | mm ² |

B

Appendix Verification Connections

In this appendix the following formulas are applied into the tool in order to verify the laterally dowel type connections. The first equations described in this appendix are applicable for steel part A as well steel part B. Thereafter, the equations that are formulated are specific for steel part A and B. All described equations are according to the Eurocode 5 (NEN-EN-1991-1-1, 2004) and Eurocode 3 (NEN-EN-1993-1-1, 2006).

General

Embedment strength parallel to the grain

$$f_{h,0,k} = 0,082\rho_k d^{-0,3} \quad (\text{B.1})$$

$$f_{h,0,k} = 0,082(1 - 0,01d)\rho_k \quad (\text{B.2})$$

Where:

| | | |
|-------------|--|-------------------|
| $f_{h,0,k}$ | embedment strength parallel to the grain | N/mm ² |
| ρ_k | characteristic density wood | kg/m ³ |
| d | diameter fastener | mm |

Embedment strength under load direction

$$f_{h,\alpha,k} = \frac{f_{h,0,k}}{k_{90}\sin^2\alpha + \cos^2\alpha} \quad (\text{B.3})$$
$$k_{90} = 1,35 + 0,015d$$

Where:

| | | |
|------------------|--|-------------------|
| $f_{h,\alpha,k}$ | embedment strength under load direction in an angle to the grain | N/mm ² |
| k_{90} | softwood correction factor | - |
| α | angle of the load to the grain | rad or ° |

Yield moment fastener

$$M_{y,Rk} = 0,3f_u d^{2,6} \quad (\text{B.4})$$

Where:

| | | |
|------------|--|-------------------|
| $M_{y,Rk}$ | characteristic value of the yield moment | Nmm |
| f_u | ultimate steel strength | N/mm ² |
| d | diameter fastener | mm |

Effective number of fasteners N_{ef}

For fasteners group loaded parallel to the grain, the number of rows need to be calculated using the following effective number of fasteners.

$$n_{ef} = \min \left\{ \begin{array}{l} n \\ n^{0.94} \sqrt{\frac{a_1}{13d}} \end{array} \right. \quad (\text{B.5})$$

Where:

| | | |
|-------|--|----|
| a_1 | spacing between fasteners in the grain direction | mm |
| d | diameter fastener | mm |
| d | number of bolts in the row | - |

For fasteners groups loaded perpendicular to the grain, the effective number of fasteners should be taken as $n_{ef} = n$

Steel part A

Steel part A can be classified as a steel-to-timber connection according to NEN-EN-1991-1-1, 2004.

Failure mechanisms

- Thin steel plate in single shear: see table E.1
- Thick steel plate in single shear: see table E.2
- Thin steel plate in double shear: see table E.4
- Thick steel plate in double shear: see table E.5

Rope effect bolts - anchorage capacity of the washer

$$F_{ax,washer,Rk} = 3f_{c,90,k}A_{washer} \quad (\text{B.6})$$

Where:

| | | |
|-----------------|--|-------------------|
| $F_{ax,washer}$ | characteristic value of withdrawal capacity washer | N |
| $f_{c90,k}$ | charac. compressive strength perp. to the grain | N/mm ² |
| A_{washer} | area washer | mm ² |

Rope effect lag screws - withdrawal capacity

$$F_{ax,\alpha,Rk} = \frac{n_{ef} f_{ax,k} d l_{ef} k_d}{1,2 \cos^2 \alpha + \sin^2 \alpha} \quad (\text{B.7})$$

$$f_{ax,k} = 0,52d^{-0,5} l_{ef}^{-0,1} \rho_k^{0,8}$$

Where:

| | | |
|--------------------|--|-------------------|
| $F_{ax,\alpha,Rk}$ | char. withdrawal capacity of the connection at an angle to the grain | N |
| $f_{ax,k}$ | char. withdrawal strenght perp. to the grain | N/mm ² |
| n_{ef} | effective number of screws | - |
| d | outer diameter measured on the threaded part | mm |
| l_{ef} | penetration length of the threaded part | mm |
| ρ_k | characteristic density wood | kg/m ³ |
| α | the angle between screw shaft and the grain | rad or ° |

Fastener capacity - shear resistance

$$F_{v,Rd} = \frac{\alpha_v f_{ub} A_s}{\gamma_{M2}} \quad (\text{B.8})$$

Where:

| | | |
|---------------|---------------------------|-----------------|
| $F_{v,Rd}$ | Shear resistance | N |
| α_v | 0.6 for class 4.6 and 8.8 | - |
| A_s | tensile stress area | mm ² |
| γ_{M2} | partial safety factor | - |

Fastener capacity - tension resistance

$$F_{t,Rd} = \frac{k_2 f_{ub} A_s}{\gamma_{M2}} \quad (\text{B.9})$$

Where:

| | | |
|---------------|---------------------------|-------------------|
| $F_{t,Rd}$ | Tensile resistance | N |
| F_{ub} | Ultimate tensile strength | N/mm ² |
| k_2 | 0.9 | - |
| A_s | tensile stress area | mm ² |
| γ_{M2} | partial safety factor | - |

Steel part B

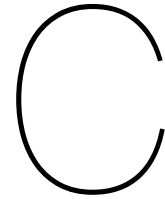
Steel part B can be classified as a steel-to-timber connection according to NEN-EN-1991-1-1, 2004.

Failure mechanisms

- Single slotted-in steel plate: see table E.3
- Double slotted-in steel plate: see table E.6

Rope effect bolts

See steel part A.



Appendix CLT-verification

In this appendix the CLT-panel is calculated based on the maximum span of 3.75 m studied in analysis 1. The calculation is separated into two parts. Part 1 contains the bending, shear, bearing pressure, and deflection verification by using CLT designer developed by holz.bau forschungs gmbh. Part 2 consist of a vibration calculation by using the simplified analytical method described in the "Vibration Design of Floors" guideline written by HIVOSS (Human Induced Vibrations of Steel Structures)

C.1. Part 1: Forces and Deflection



Center of Competence
holz.bau forschungs gmbh
Inffeldgasse 24, A-8010 Graz
support@cltdesigner.at

CLTdesigner
Version 8.3

Summary of results

| | |
|----------------------------|--|
| Project number: | 007 |
| Project: | Thesis Timber Joints |
| Structural element: | CLT-panel 5S-140-DL |
| Cross section: | KLH: 140mm 5s DL |
| Description: | Structural calculation of the CLT floor panel according to the largest span of 3.75 meter. |
| Date: | Dec 20, 2022 |
| Time: | 11:08:13 AM |
| Author: | Bieze |



Table of content

| | |
|--|----------|
| 1 General | 3 |
| 2 Structural system | 3 |
| 2.1 Supports | 3 |
| 3 Cross section | 3 |
| 3.1 Layer composition | 3 |
| 3.2 Material parameters | 4 |
| 3.3 Cross-sectional values | 4 |
| 4 Loads | 4 |
| 5 Specification concerning structural fire design | 5 |
| 6 Information concerning vibrations | 5 |
| 7 Results | 5 |
| 7.1 ULS | 5 |
| 7.1.1 Bending | 5 |
| 7.1.2 Shear | 6 |
| 7.1.3 Bearing pressure | 6 |
| 7.2 SLS | 6 |
| 7.2.1 Deflection | 6 |
| 8 Appendix | 7 |
| 8.1 Combinations | 7 |
| 8.2 Internal forces | 7 |
| 8.3 Deformations | 9 |
| 8.4 Supporting forces | 10 |
| 8.4.1 Characteristic supporting forces | 10 |
| 8.4.2 Design supporting forces | 10 |
| 8.5 Verification | 11 |
| 8.5.1 Bending | 11 |
| 8.5.2 Shear | 11 |
| 8.5.3 Bearing pressure | 12 |
| 8.5.4 Deformations | 12 |

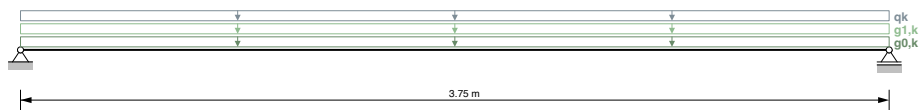


1 General

Service class 1

2 Structural system

Single span girder



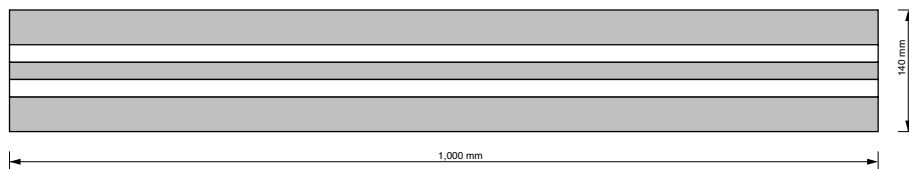
2.1 Supports

| Support | x | Width |
|---------|--------|--------|
| A | 0.0 m | 0.06 m |
| B | 3.75 m | 0.06 m |

3 Cross section

CLT-Product of the company KLH: 140mm 5s DL

5 layers (thickness: 140 mm)



3.1 Layer composition

| Layer | Thickness | Orientation | Material |
|-------|-----------|-------------|----------|
| # 1 | 40 mm | 0 | C24-KLH |
| # 2 | 20 mm | 90 | C24-KLH |



| | | | |
|-----|-------|----|---------|
| # 3 | 20 mm | 0 | C24-KLH |
| # 4 | 20 mm | 90 | C24-KLH |
| # 5 | 40 mm | 0 | C24-KLH |

Orientation 0 = top layer longitudinal to span; Orientation 90 = top layer perpendicular to span

3.2 Material parameters

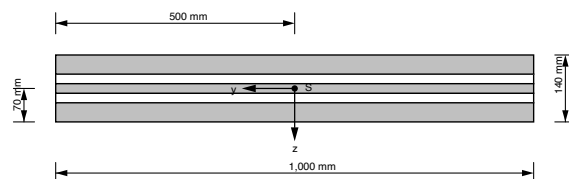
Partial safety factor $\gamma_M = 1.25$

System factor for CLT $k_{\text{sys}} = 1.1$

| Material parameters for | C24-KLH |
|---|-----------------------------|
| bending strength [N/mm ²] | $k_{\text{sys}} \cdot 24.0$ |
| tensile strength parallel [N/mm ²] | 16.5 |
| tensile strength perpendicular [N/mm ²] | 0.12 |
| compressive strength parallel [N/mm ²] | 24.0 |
| compressive strength perpendicular [N/mm ²] | 2.7 |
| shear strength [N/mm ²] | 2.7 |
| rolling shear strength [N/mm ²] | 1.2 |
| Youngs modulus parallel [N/mm ²] | 12,000.0 |
| 5%-quantile from Youngs modulus parallel [N/mm ²] | 10,000.0 |
| Youngs modulus perpendicular [N/mm ²] | 0.0 |
| shear modulus [N/mm ²] | 690.0 |
| rolling shear modulus [N/mm ²] | 50.0 |
| density [kg/m ³] | 350.0 |
| density mean value [kg/m ³] | 420.0 |

3.3 Cross-sectional values

| | |
|------------------|----------------------------|
| EA_{ef} | 1.2E9 N |
| EI_{ef} | 2.536E12 N·mm ² |
| GA_{ef} | 1.273E7 N |



4 Loads

| Field | $g_{0,k}$ | $g_{1,k}$ | q_k | Category | s_k | Altitude/Region | w_k |
|-------|-----------|-----------------------|-----------------------|----------|-------|-----------------|-------|
| 1 | 0.77 kN/m | 1.7 kN/m ² | 3.5 kN/m ² | B | | | |

**Partial safety factors:** $\gamma_G = 1.2$ $\gamma_Q = 1.5$ **Load position:**

Plate weight: Total

Permanent loads: Total

Imposed loads: Field-by-field

Snow: Field-by-field

Wind: Total

Combinations:

Combination factors: according to EN

Combinations of distributed and concentrated loads:

 q_k and Q_k will be considered as one load group s and S will be considered as one load group w_k and W_k will be considered as one load group**5 Specification concerning structural fire design**

No specifications are available

6 Information concerning vibrations

No specifications are available

7 Results

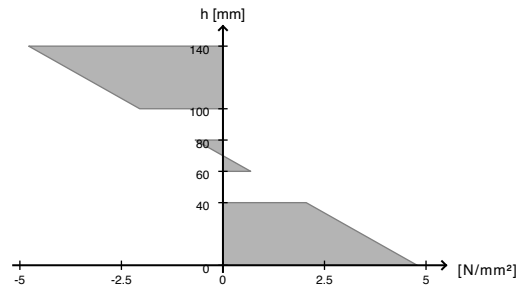
Referenced standards: EN 1995-1-1:2009, NEN EN 1995-1-1:2005/NB:2013

Underlying calculation method: Timoshenko

7.1 ULS**7.1.1 Bending**

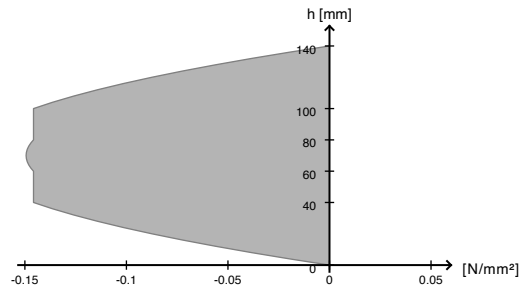


| | |
|-------------------------|---|
| Utilisation ratio | 28.3 % |
| k_{mod} | 0.8 |
| at x | 1.875 m |
| Ek | 2 |
| Fundamental combination | $1.20 \cdot g_{0,k} + 1.20 \cdot g_{1,k} + 1.50 \cdot 1.00 \cdot q_k$ |



7.1.2 Shear

| | |
|-------------------------|---|
| Utilisation ratio | 19.0 % |
| k_{mod} | 0.8 |
| at x | 3.75 m |
| Ek | 2 |
| Fundamental combination | $1.20 \cdot g_{0,k} + 1.20 \cdot g_{1,k} + 1.50 \cdot 1.00 \cdot q_k$ |



7.1.3 Bearing pressure

| | |
|-------------------------|---|
| Utilisation ratio | 11.1 % |
| k_{mod} | 0.8 |
| at x | 3.75 m |
| Ek | 2 |
| Fundamental combination | $1.20 \cdot g_{0,k} + 1.20 \cdot g_{1,k} + 1.50 \cdot 1.00 \cdot q_k$ |



7.2 SLS

7.2.1 Deflection

Limit values according to EN 1995-1-1

Instantaneous deformation $w_{inst} t = 0: l/500$ (6.9 mm, 91.8 %)



Final deformation $w_{net,fin} t = inf: l/250$ (10.1 mm, 67.6 %)

Final deformation $w_{fin} t = inf: l/250$ (10.1 mm, 67.6 %)

Limit values according to NEN EN 1995-1-1:2005/NB:2013

Instantaneous deformation $w_{inst} t = 0: l/300$ (6.9 mm, 55.1 %)

Final deformation $w_{net,fin} t = inf: l/250$ (10.1 mm, 67.6 %)

Final deformation $w_{fin} t = inf: l/250$ (10.1 mm, 67.6 %)

Final deformation $w_{net,fin} - w_{inst,G} t = inf: l/250$ (7.3 mm, 48.6 %)

| | |
|---|---------|
| Utilisation ratio | 91.8 % |
| w_{max} | 6.9 mm |
| k_{def} | 0.8 |
| at x | 1.875 m |
| E_k | 6 |
| Instantaneous deformation $w_{inst} t = 0$ ($l/500$) | |



8 Appendix

8.1 Combinations

| E_k | k_{mod} / k_{def} | Combination |
|---|---------------------|---|
| Fundamental combination | | |
| 1 | 0.6 | $1.20 \cdot g_{0,k} + 1.20 \cdot g_{1,k}$ |
| 2 | 0.8 | $1.20 \cdot g_{0,k} + 1.20 \cdot g_{1,k} + 1.50 \cdot 1.00 \cdot q_k$ |
| 3 | 0.6 | $g_{0,k} + g_{1,k}$ |
| 4 | 0.8 | $g_{0,k} + g_{1,k} + 1.50 \cdot 1.00 \cdot q_k$ |
| Accidental combination | | |
| SLS combinations according to EN 1995-1-1 | | |
| 6 | 0.8 | $g_{0,k} + g_{1,k} + 1.00 \cdot q_k$ |
| 7 | 0.8 | $g_{0,k} + (g_{0,k})_{creep} + g_{1,k} + (g_{1,k})_{creep} + 1.00 \cdot q_k + (0.30 \cdot q_k)_{creep}$ |
| 8 | 0.8 | $g_{0,k} + (g_{0,k})_{creep} + g_{1,k} + (g_{1,k})_{creep} + 1.00 \cdot q_k + (0.30 \cdot q_k)_{creep}$ |
| SLS combinations according to EN 1995-1-1:NA | | |
| 10 | 0.8 | $g_{0,k} + g_{1,k} + 1.00 \cdot q_k$ |
| 11 | 0.8 | $g_{0,k} + (g_{0,k})_{creep} + g_{1,k} + (g_{1,k})_{creep} + 1.00 \cdot q_k + (0.30 \cdot q_k)_{creep}$ |
| 12 | 0.8 | $g_{0,k} + (g_{0,k})_{creep} + g_{1,k} + (g_{1,k})_{creep} + 1.00 \cdot q_k + (0.30 \cdot q_k)_{creep}$ |
| 14 | 0.8 | $(g_{0,k})_{creep} + (g_{1,k})_{creep} + 1.00 \cdot q_k + (0.30 \cdot q_k)_{creep}$ |

8.2 Internal forces



Thesis Timber Joints
Detailed results

| Field | x | $M_{y,d}$ | $V_{z,d}$ |
|--|-------|-----------|-----------|
| | [m] | [kN·m] | [kN] |
| $Ek\ 1: 1.20 \cdot g_{0,k} + 1.20 \cdot g_{1,k}$ | | | |
| 1 | 0.0 | 0.0 | 5.557 |
| 1 | 0.375 | 1.876 | 4.446 |
| 1 | 0.75 | 3.335 | 3.335 |
| 1 | 1.125 | 4.377 | 2.223 |
| 1 | 1.5 | 5.002 | 1.111 |
| 1 | 1.875 | 5.21 | -0.0 |
| 1 | 2.25 | 5.002 | -1.112 |
| 1 | 2.625 | 4.377 | -2.223 |
| 1 | 3.0 | 3.335 | -3.335 |
| 1 | 3.375 | 1.876 | -4.446 |
| 1 | 3.75 | 0.0 | -5.558 |
| $Ek\ 2: 1.20 \cdot g_{0,k} + 1.20 \cdot g_{1,k} + 1.50 \cdot 1.00 \cdot q_k$ | | | |
| 1 | 0.0 | -0.0 | 15.401 |
| 1 | 0.375 | 5.198 | 12.321 |
| 1 | 0.75 | 9.241 | 9.241 |
| 1 | 1.125 | 12.128 | 6.161 |
| 1 | 1.5 | 13.861 | 3.08 |
| 1 | 1.875 | 14.439 | -0.0 |
| 1 | 2.25 | 13.861 | -3.08 |
| 1 | 2.625 | 12.128 | -6.161 |
| 1 | 3.0 | 9.241 | -9.241 |
| 1 | 3.375 | 5.198 | -12.321 |
| 1 | 3.75 | 0.0 | -15.401 |
| $Ek\ 3: g_{0,k} + g_{1,k}$ | | | |
| 1 | 0.0 | 0.0 | 4.631 |
| 1 | 0.375 | 1.563 | 3.705 |
| 1 | 0.75 | 2.779 | 2.779 |
| 1 | 1.125 | 3.647 | 1.853 |
| 1 | 1.5 | 4.168 | 0.926 |
| 1 | 1.875 | 4.342 | -0.0 |
| 1 | 2.25 | 4.168 | -0.926 |
| 1 | 2.625 | 3.647 | -1.853 |
| 1 | 3.0 | 2.779 | -2.779 |
| 1 | 3.375 | 1.563 | -3.705 |
| 1 | 3.75 | 0.0 | -4.631 |
| $Ek\ 4: g_{0,k} + g_{1,k} + 1.50 \cdot 1.00 \cdot q_k$ | | | |



| Field | x | $M_{y,d}$ | $V_{z,d}$ |
|-------|-------|-----------|-----------|
| | [m] | [kN·m] | [kN] |
| 1 | 0.0 | -0.0 | 14.475 |
| 1 | 0.375 | 4.885 | 11.58 |
| 1 | 0.75 | 8.685 | 8.685 |
| 1 | 1.125 | 11.399 | 5.79 |
| 1 | 1.5 | 13.028 | 2.895 |
| 1 | 1.875 | 13.57 | -0.0 |
| 1 | 2.25 | 13.028 | -2.895 |
| 1 | 2.625 | 11.399 | -5.79 |
| 1 | 3.0 | 8.685 | -8.685 |
| 1 | 3.375 | 4.885 | -11.58 |
| 1 | 3.75 | 0.0 | -14.475 |

8.3 Deformations

| Field | x | $w_{z,min}$ | $w_{z,max}$ |
|---------------------------|-------|-------------|-------------|
| | [m] | [mm] | [mm] |
| Load case group $g_{0,k}$ | | | |
| 1 | 0.0 | 0.00 | 0.00 |
| 1 | 0.375 | 0.28 | 0.28 |
| 1 | 0.75 | 0.53 | 0.53 |
| 1 | 1.125 | 0.73 | 0.73 |
| 1 | 1.5 | 0.85 | 0.85 |
| 1 | 1.875 | 0.89 | 0.89 |
| 1 | 2.25 | 0.85 | 0.85 |
| 1 | 2.625 | 0.73 | 0.73 |
| 1 | 3.0 | 0.53 | 0.53 |
| 1 | 3.375 | 0.28 | 0.28 |
| 1 | 3.75 | 0.00 | 0.00 |
| Load case group $g_{1,k}$ | | | |
| 1 | 0.0 | 0.00 | 0.00 |
| 1 | 0.375 | 0.63 | 0.63 |
| 1 | 0.75 | 1.18 | 1.18 |
| 1 | 1.125 | 1.60 | 1.60 |
| 1 | 1.5 | 1.87 | 1.87 |
| 1 | 1.875 | 1.96 | 1.96 |
| 1 | 2.25 | 1.87 | 1.87 |
| 1 | 2.625 | 1.60 | 1.60 |



| Field | x | $w_{z,min}$ | $w_{z,max}$ |
|-----------------------|-------|-------------|-------------|
| | [m] | [mm] | [mm] |
| 1 | 3.0 | 1.18 | 1.18 |
| 1 | 3.375 | 0.63 | 0.63 |
| 1 | 3.75 | 0.00 | 0.00 |
| Load case group q_k | | | |
| 1 | 0.0 | 0.00 | 0.00 |
| 1 | 0.375 | 0.00 | 1.29 |
| 1 | 0.75 | 0.00 | 2.42 |
| 1 | 1.125 | 0.00 | 3.30 |
| 1 | 1.5 | 0.00 | 3.85 |
| 1 | 1.875 | 0.00 | 4.04 |
| 1 | 2.25 | 0.00 | 3.85 |
| 1 | 2.625 | 0.00 | 3.30 |
| 1 | 3.0 | 0.00 | 2.42 |
| 1 | 3.375 | 0.00 | 1.29 |
| 1 | 3.75 | 0.00 | 0.00 |

8.4 Supporting forces

8.4.1 Characteristic supporting forces

| Load case group | Support | x | $F_{z,k,min}$ | $F_{z,k,max}$ |
|-----------------|---------|------|---------------|---------------|
| | | [m] | [kN] | [kN] |
| $g_{0,k}$ | A | 0.0 | 1.444 | 1.444 |
| | B | 3.75 | 1.444 | 1.444 |
| $g_{1,k}$ | A | 0.0 | 3.187 | 3.187 |
| | B | 3.75 | 3.188 | 3.188 |
| q_k | A | 0.0 | 0.0 | 6.562 |
| | B | 3.75 | 0.0 | 6.563 |

8.4.2 Design supporting forces

| Support | x | $F_{z,d,min}$ | E_k | $F_{z,d,max}$ | E_k |
|---------|------|---------------|-------|---------------|-------|
| | [m] | [kN] | | [kN] | |
| A | 0.0 | 4.631 | 3 | 15.401 | 2 |
| B | 3.75 | 4.631 | 3 | 15.401 | 2 |



8.5 Verification

8.5.1 Bending

| Field | x | Ek | k_{mod} | $M_{y,d}$ | $\sigma_{max,d}$ | $f_{m,d}$ | η |
|-------|-------|----|-----------|-----------|----------------------|----------------------|--------|
| | [m] | | [-] | [kN·m] | [N/mm ²] | [N/mm ²] | [%] |
| 1 | 0.0 | 4 | 0.8 | -0.00 | 0.00 | 16.90 | 0.0 |
| 1 | 0.375 | 2 | 0.8 | 5.20 | 1.72 | 16.90 | 10.2 |
| 1 | 0.75 | 2 | 0.8 | 9.24 | 3.06 | 16.90 | 18.1 |
| 1 | 1.125 | 2 | 0.8 | 12.13 | 4.02 | 16.90 | 23.8 |
| 1 | 1.5 | 2 | 0.8 | 13.86 | 4.59 | 16.90 | 27.2 |
| 1 | 1.875 | 2 | 0.8 | 14.44 | 4.78 | 16.90 | 28.3 |
| 1 | 2.25 | 2 | 0.8 | 13.86 | 4.59 | 16.90 | 27.2 |
| 1 | 2.625 | 2 | 0.8 | 12.13 | 4.02 | 16.90 | 23.8 |
| 1 | 3.0 | 2 | 0.8 | 9.24 | 3.06 | 16.90 | 18.1 |
| 1 | 3.375 | 2 | 0.8 | 5.20 | 1.72 | 16.90 | 10.2 |
| 1 | 3.75 | 2 | 0.8 | 0.00 | 0.00 | 16.90 | 0.0 |

8.5.2 Shear

| Field | x | Ek | k_{mod} | $V_{z,d}$ | $\tau_{v,d}$ | $f_{v,d}$ | η |
|-------|-------|----|-----------|-----------|----------------------|----------------------|--------|
| | | | | | $\tau_{r,d}$ | $f_{r,d}$ | |
| | [m] | | [-] | [kN] | [N/mm ²] | [N/mm ²] | [%] |
| 1 | 0.0 | 2 | 0.8 | 15.40 | 0.15 | 1.73 | 8.6 |
| | | | | | 0.15 | 0.77 | 19.0 |
| 1 | 0.375 | 2 | 0.8 | 12.32 | 0.12 | 1.73 | 6.9 |
| | | | | | 0.12 | 0.77 | 15.2 |
| 1 | 0.75 | 2 | 0.8 | 9.24 | 0.09 | 1.73 | 5.2 |
| | | | | | 0.09 | 0.77 | 11.4 |
| 1 | 1.125 | 2 | 0.8 | 6.16 | 0.06 | 1.73 | 3.5 |
| | | | | | 0.06 | 0.77 | 7.6 |
| 1 | 1.5 | 2 | 0.8 | 3.08 | 0.03 | 1.73 | 1.7 |
| | | | | | 0.03 | 0.77 | 3.8 |
| 1 | 1.875 | 2 | 0.8 | -0.00 | 0.00 | 1.73 | 0.0 |
| | | | | | 0.00 | 0.77 | 0.0 |
| 1 | 2.25 | 2 | 0.8 | -3.08 | 0.03 | 1.73 | 1.7 |
| | | | | | 0.03 | 0.77 | 3.8 |
| 1 | 2.625 | 2 | 0.8 | -6.16 | 0.06 | 1.73 | 3.5 |


Thesis Timber Joints
 Detailed results

| Field | x | Ek | k_{mod} | $V_{z,d}$ | $\tau_{v,d}$ | $f_{v,d}$ | η |
|-------|-------|----|-----------|-----------|----------------------|----------------------|--------|
| | [m] | | [-] | [kN] | [N/mm ²] | [N/mm ²] | [%] |
| | | | | | 0.06 | 0.77 | 7.6 |
| 1 | 3.0 | 2 | 0.8 | -9.24 | 0.09 | 1.73 | 5.2 |
| | | | | | 0.09 | 0.77 | 11.4 |
| 1 | 3.375 | 2 | 0.8 | -12.32 | 0.12 | 1.73 | 6.9 |
| | | | | | 0.12 | 0.77 | 15.2 |
| 1 | 3.75 | 2 | 0.8 | -15.40 | 0.15 | 1.73 | 8.6 |
| | | | | | 0.15 | 0.77 | 19.0 |

8.5.3 Bearing pressure

| Support | x | Ek | k_{mod} | F_d | A_{sec} | $k_{c,90}$ | $\sigma_{c,90,d}$ | $f_{c,90,d}$ | η |
|---------|------|----|-----------|-------|--------------------|------------|----------------------|----------------------|--------|
| | [m] | | [-] | [kN] | [mm ²] | [-] | [N/mm ²] | [N/mm ²] | [%] |
| A | 0.0 | 2 | 0.8 | 15.40 | 60,000 | 1.34 | 0.26 | 2.32 | 11.1 |
| B | 3.75 | 2 | 0.8 | 15.40 | 60,000 | 1.34 | 0.26 | 2.32 | 11.1 |

8.5.4 Deformations

| Field | x | Ek | k_{def} | w_{max} | w_{limit} | η |
|-------|-------|----|-----------|-----------|-------------|--------|
| | [m] | | | [mm] | [mm] | [%] |
| 1 | 0.0 | 6 | 0.8 | 0.00 | 7.50 | 0.0 |
| 1 | 0.375 | 6 | 0.8 | 2.20 | 7.50 | 29.3 |
| 1 | 0.75 | 6 | 0.8 | 4.13 | 7.50 | 55.0 |
| 1 | 1.125 | 6 | 0.8 | 5.62 | 7.50 | 74.9 |
| 1 | 1.5 | 6 | 0.8 | 6.56 | 7.50 | 87.5 |
| 1 | 1.875 | 6 | 0.8 | 6.89 | 7.50 | 91.8 |
| 1 | 2.25 | 6 | 0.8 | 6.56 | 7.50 | 87.5 |
| 1 | 2.625 | 6 | 0.8 | 5.62 | 7.50 | 74.9 |
| 1 | 3.0 | 6 | 0.8 | 4.13 | 7.50 | 55.0 |
| 1 | 3.375 | 6 | 0.8 | 2.20 | 7.50 | 29.3 |
| 1 | 3.75 | 6 | 0.8 | 0.00 | 7.50 | 0.0 |

C.2. Part 2: Vibration

Vibration Design of Floor according to Hivoss RFS2-CT-2007-00033

| | |
|-----------|----------------------------|
| Span (l) | 3,75 m |
| Width (b) | 1,20 m |
| E | 11000 N/mm ² |
| (EI) // l | 2331080 Nm ² /m |
| (EI) ⊥ l | 190913 Nm ² /m |

Total mass

| | | |
|-------------|------------------------|-------------------------------------|
| $g_{0,k}$ | 0,80 kN/m ² | |
| $g_{1,k}$ | 1,70 kN/m ² | |
| q_k | 3,50 kN/m ² | |
| M_{total} | 2,85 kN/m ² | ($g_{0,k}+g_{1,k}+10\%$ of q_k) |
| | 285 kg/m ² | |

First natural frequency of the orthotropic plate (assumed simply supported at all four edge)

$$f_1 = \frac{\pi}{2} \sqrt{\frac{EI_y}{m l^4}} \sqrt{1 + \left[2 \left(\frac{b}{l} \right)^2 + \left(\frac{b}{l} \right)^4 \right] \frac{EI_x}{EI_y}} \quad f_1 = 10,2 \text{ Hz}$$

Where:

| | |
|-------|---|
| μ | is the mass per m ² in kg/m ² , |
| l | is the length of the floor in m (in x-direction), |
| b | is the width of the floor in m (in y-direction), |
| E | is the Youngs-Modulus in N/m ² , |
| I_x | is the moment of inertia for bending about the x-axis in m ⁴ , |
| I_y | is the moment of inertia for bending about the y-axis in m ⁴ . |

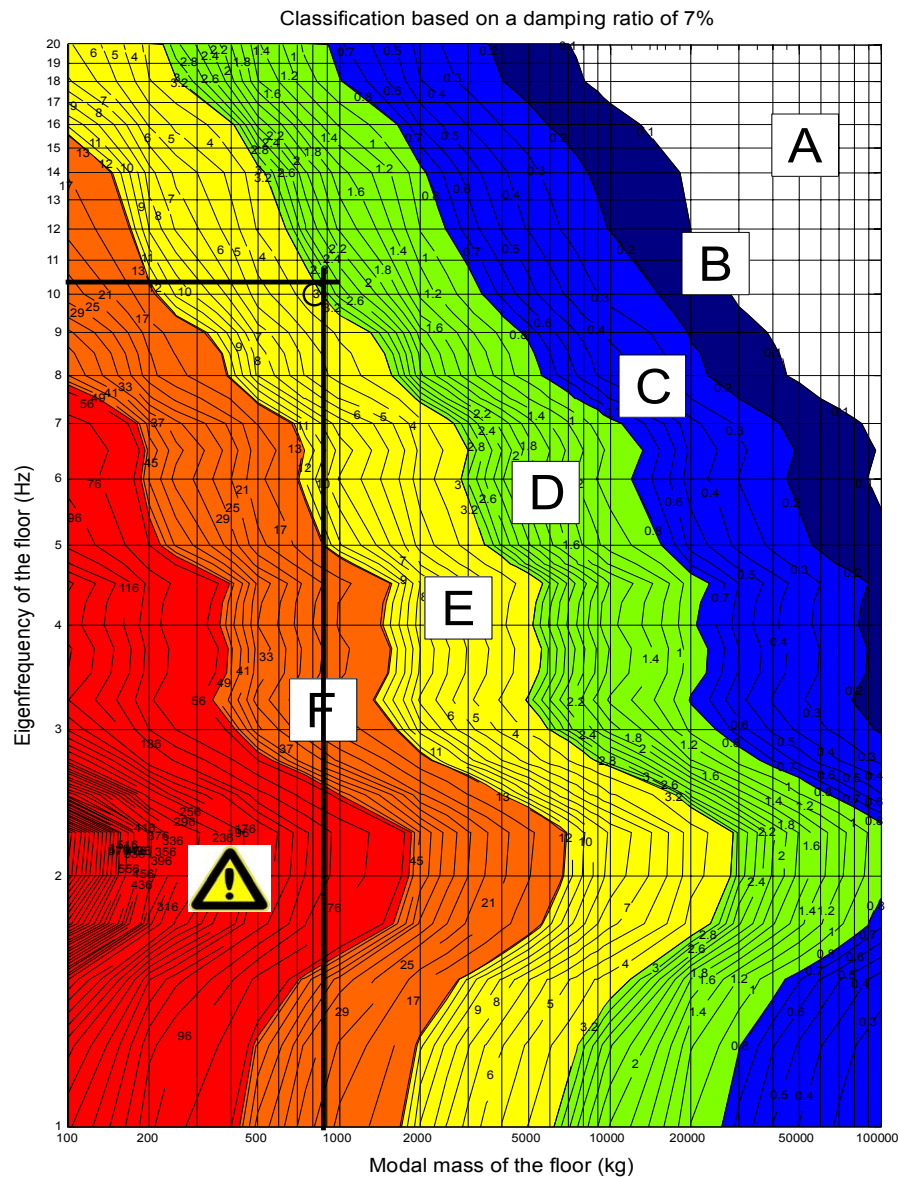
| | | |
|-------------|---------|---------------------------|
| b_{eff} | 3,125 m | (cooperating floor width) |
| Modalfactor | 0,25 | |
| M_{modal} | 835 kg | |

Damping ratio of timber according to table 3.

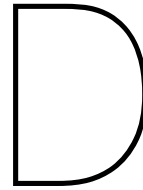
| | |
|----|-----|
| D1 | 6 % |
| D2 | 1 % |
| D3 | 0 % |
| D | 7 % |

Table 3: Determination of damping

| Type | Damping (% of critical damping) |
|---|---------------------------------|
| Structural Damping D_1 | |
| Wood | 6% |
| Concrete | 2% |
| Steel | 1% |
| Steel-concrete | 1% |
| Damping due to furniture D_2 | |
| Traditional office for 1 to 3 persons with separation walls | 2% |
| Paperless office | 0% |
| Open plan office. | 1% |
| Library | 1% |
| Houses | 1% |
| Schools | 0% |
| Gymnastic | 0% |
| Damping due to finishes D_3 | |
| Ceiling under the floor | 1% |
| Free floating floor | 0% |
| Swimming screed | 1% |
| Total Damping $D = D_1 + D_2 + D_3$ | |



The expected OS-RMS value is approx. 3 mm/s. Class D is classified as suitable for office buildings with a Lower Limit of 3.2 and the Upper Limit with 12.8. That means that the selected CLT 5S 140 DL slab fulfills the vibrations requirements.



Appendix Minimum Values of Spacing and Edge and End Distances

In this research project, the following minimum values of spacing and edge and end distance of bolts, lag screws and dowels have been used according to NEN-EN-1991-1-1 (2004).

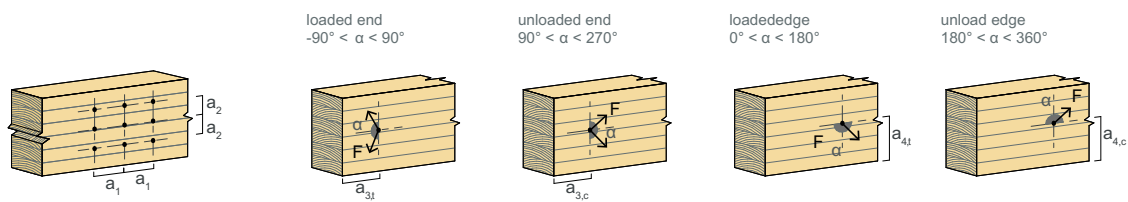


Figure D.1: Minimal spacing, end and edge distance fasteners

Bolts and Lag Screws

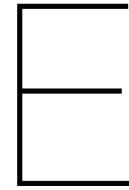
| | | |
|--------------------------------|--|------------------------------------|
| a_1 (parallel to grain) | $0^\circ \leq \alpha \leq 360^\circ$ | $(4 + \cos \alpha) d$ |
| a_2 (perpendicular to grain) | $0^\circ \leq \alpha \leq 360^\circ$ | $4 d$ |
| $a_{3,t}$ (loaded end) | $-90^\circ \leq \alpha \leq 90^\circ$ | $\max (7 d; 80 \text{ mm})$ |
| $a_{3,c}$ (unloaded end) | $90^\circ \leq \alpha < 150^\circ$ | $\max [(1 + 6 \sin \alpha) d; 4d]$ |
| | $150^\circ \leq \alpha < 210^\circ$ | $4 d$ |
| | $210^\circ \leq \alpha \leq 270^\circ$ | $\max [(1 + 6 \sin \alpha) d; 4d]$ |
| $a_{4,t}$ (loaded edge) | $0^\circ \leq \alpha \leq 180^\circ$ | $\max [(2 + 2 \sin \alpha) d; 3d]$ |
| $a_{4,c}$ (unloaded edge) | $180^\circ \leq \alpha \leq 360^\circ$ | $3 d$ |

Figure D.2: Minimal values for spacing and edge and end distances for bolts and lag screws

Dowels

| | | |
|--------------------------------|--|-------------------------------------|
| a_1 (parallel to grain) | $0^\circ \leq \alpha \leq 360^\circ$ | $(3 + 2 \cos \alpha) d$ |
| a_2 (perpendicular to grain) | $0^\circ \leq \alpha \leq 360^\circ$ | $3 d$ |
| $a_{3,t}$ (loaded end) | $-90^\circ \leq \alpha \leq 90^\circ$ | $\max(7 d; 80 \text{ mm})$ |
| $a_{3,c}$ (unloaded end) | $90^\circ \leq \alpha < 150^\circ$ | $\max(a_{3,t} \sin \alpha) d; 3d$ |
| | $150^\circ \leq \alpha < 210^\circ$ | $3 d$ |
| | $210^\circ \leq \alpha \leq 270^\circ$ | $\max(a_{3,t} \sin \alpha) d; 3d$ |
| $a_{4,t}$ (loaded edge) | $0^\circ \leq \alpha \leq 180^\circ$ | $\max(2 + 2 \sin \alpha d; 3d)$ |
| $a_{4,c}$ (unloaded edge) | $180^\circ \leq \alpha \leq 360^\circ$ | $3 d$ |

Figure D.3: Minimal values for spacing and edge and end distances for dowels



Appendix Failure Mechanisms Steel-to-timber Connections

Single shear steel-to-timber joints with $t_{steel} \leq 0,5d$

| | |
|--|--|
| | $F_{V,Rk} = 0,4f_{h,k}t_1d[a](E.1)$ |
| | $F_{V,Rk} = 1,15\sqrt{2M_{y,Rk}f_{h,k}d} + \frac{F_{ax,Rk}}{4} [k](E.2)$ |

Table E.1: Failure mechanisms of single shear steel-to-timber joints with $t_{steel} \leq 0,5d$

Single shear steel-to-timber joints with $t_{steel} \geq d$

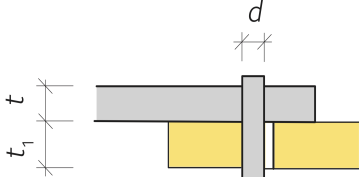
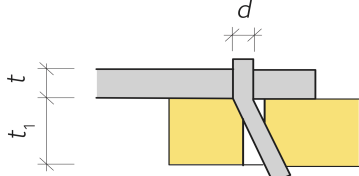
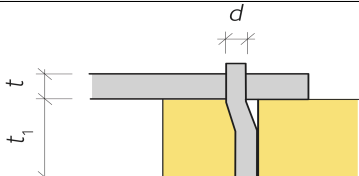
| | |
|---|--|
|  | $F_{V,Rk} = f_{h,1,k} t_1 d [c] \text{ (E.3)}$ |
|  | $F_{V,Rk} = f_{h,1,k} t_1 d \left(\sqrt{2 + \frac{4M_{y,Rk}}{f_{h,1,k} t_1 d^2}} - 1 \right) + \frac{F_{ax,Rk}}{4} [d] \text{ (E.4)}$ |
|  | $F_{V,Rk} = 2,3 \sqrt{M_{y,Rk} f_{h,1,k} d} + \frac{F_{ax,Rk}}{4} [e] \text{ (E.5)}$ |

Table E.2: Failure mechanisms of single shear steel-to-timber joints with $t_{steel} \geq d$
Slotted-in steel plates

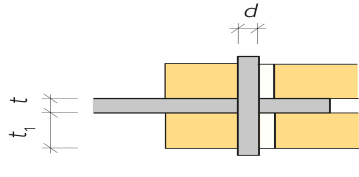
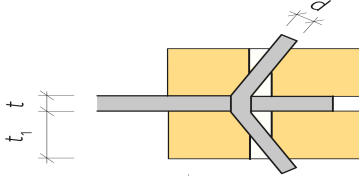
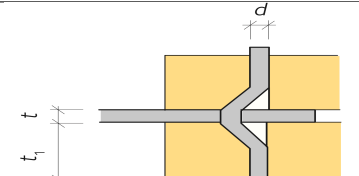
| | |
|---|--|
|  | $F_{V,Rk} = f_{h,1,k} t_1 d [f] \text{ (E.6)}$ |
|  | $F_{V,Rk} = f_{h,1,k} t_1 d \left(\sqrt{2 + \frac{4M_{y,Rk}}{f_{h,1,k} t_1 d^2}} - 1 \right) + \frac{F_{ax,Rk}}{4} [g] \text{ (E.7)}$ |
|  | $F_{V,Rk} = 2,3 \sqrt{M_{y,Rk} f_{h,1,k} d} + \frac{F_{ax,Rk}}{4} [h] \text{ (E.8)}$ |

Table E.3: Failure mechanisms slotted-in steel plates

Double shear steel-to-timber joints with $t_{steel} \leq 0,5d$

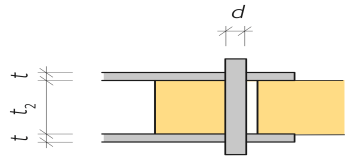
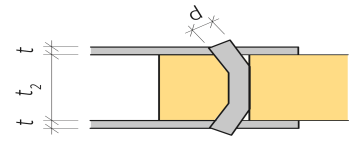
| | |
|---|---|
|  | $F_{V,Rk} = 0,5f_{h,2,k}t_2d[j](E.9)$ |
|  | $F_{V,Rk} = 1,15\sqrt{2M_{y,Rk}f_{h,2,k}d} + \frac{F_{ax,Rk}}{4} [k](E.10)$ |

Table E.4: Failure mechanisms of double shear steel-to-timber joints with $t_{steel} \leq 0,5d$

Double shear steel-to-timber joints with $t_{steel} \geq d$

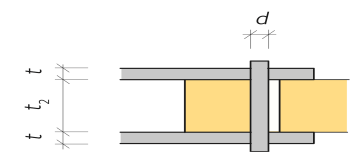
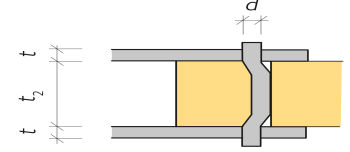
| | |
|--|---|
|  | $F_{V,Rk} = 0,5f_{h,2,k}t_2d[l](E.11)$ |
|  | $F_{V,Rk} = 2,3\sqrt{M_{y,Rk}f_{h,2,k}d} + \frac{F_{ax,Rk}}{4} [m](E.12)$ |

Table E.5: Failure mechanisms of double shear steel-to-timber joints with $t_{steel} \geq d$

Double slotted-in steel plates

Where:

| | | |
|-------------|--|-----|
| $F_{V,Rk}$ | characteristic load-carrying capacity per shear plane per fastener | N |
| $f_{h,k}$ | embedment strength in the timber member | |
| t_1 | the smaller of the thickness of the timber member or the penetration depth | mm |
| t_2 | thickness of the timber middle member | mm |
| d | diameter fastener | mm |
| $M_{y,Rk}$ | characteristic value of the yield moment | Nmm |
| $F_{ax,Rk}$ | characteristic withdrawal capacity of the fastener | N |

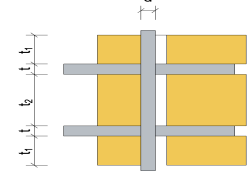
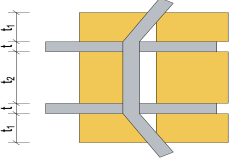
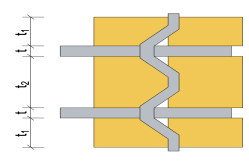
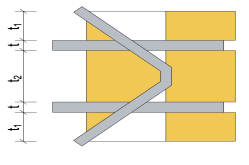
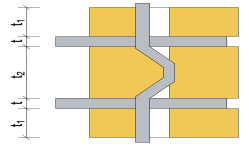
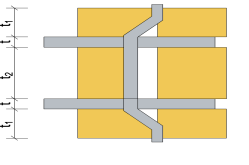
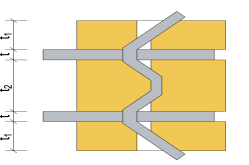
| | |
|---|--|
|  | $F_{V,Rk} = f_{h,k} d \frac{1}{4} (2t_1 + t_2) \quad (\text{E.13})$ |
|  | $F_{V,Rk} = f_{h,k} d \left(-\frac{1}{2}t_1 + \frac{t_2}{4} + \sqrt{\frac{1}{2}t_1^2 + \frac{M_{y,Rk}}{df_{h,k}}} \right) \quad (\text{E.14})$ |
|  | $F_{V,Rk} = \sqrt{4M_{y,Rk}f_{h,k}d} \quad (\text{E.15})$ |
|  | $F_{V,Rk} = f_{h,k} d \left(\frac{1}{2}t_1 + \frac{1}{2}\sqrt{t_1^2 + \frac{2M_{y,Rk}}{df_{h,k}}} \right) \quad (\text{E.16})$ |
|  | $F_{V,Rk} = f_{h,k} d \left(\sqrt{\frac{M_{y,Rk}}{df_{h,1,k}}} + \frac{1}{2}t_1 \right) \quad (\text{E.17})$ |
|  | $F_{V,Rk} = f_{h,k} d \left(\sqrt{\frac{M_{y,Rk}}{df_{h,1,k}}} + \frac{1}{4}t_2 \right) \quad (\text{E.18})$ |
|  | $F_{V,Rk} = f_{h,k} d \left(-\frac{1}{2}t_1 + \sqrt{\frac{1}{2}t_1^2 + \frac{M_{y,Rk}}{df_{h,k}}} + \sqrt{\frac{M_{y,Rk}}{df_{h,k}}} \right) \quad (\text{E.19})$ |

Table E.6: Failure mechanisms double slotted-in steel plates (Pedersen, 2002)



Appendix Database Tool

The following figures present the database that provides the tool from data.

| NB_NEN-EN 1990, A1.4.3(3) | | |
|--|------------------------------------|------------------------|
| Configuration floor or roof | Permissible additional deformation | Loading cor |
| Floor bearing crack sensitive separation wall | 0,002 | frequency (6.15b) |
| Remaining floors and roofs loaded intensify by persons | 0,003 | frequency (6.15b) |
| Remaining roofs | 0,004 | characteristic (6.14b) |

| NB_NEN-EN 1990, A1.4.3(4) | | |
|--|-------------------------------|--------|
| Appearance floor or roof | Permissible final deformation | Kolom1 |
| The appearance of the structure is important | 0,004 | |
| The appearance of the structure is not important | | |

Tables NEN-EN 1995

| NEN-EN 1995-1-1, 2.3.1.3 | |
|--------------------------|--|
| Service class | |
| 1 | |
| 2 | |
| 3 | |

| NEN-EN 338 & NEN-EN 14080 | | | |
|------------------------------------|------------------------|-----------------------|--|
| Materials | Material | Standard | |
| Sawn timber softwood | Solid timber | NEN-EN 338, table 1 | |
| Combined Glued Laminated Timber | Glued Laminated Timber | NEN-EN 14080, table 4 | |
| Homogeneous Glued Laminated Timber | Glued Laminated Timber | NEN-EN 14080, table 5 | |

| NEN-EN 338 & NEN-EN 14080 | | | |
|---------------------------|------------|----------------------|---------------------------|
| Material qualities | Row number | Sawn timber softwood | Combined Glue Homogeneous |
| | 1 | C18 | GL 20c GL 20h |
| | 2 | C20 | GL 22c GL 22h |
| | 3 | C22 | GL 24c GL 24h |
| | 4 | C24 | GL 26c GL 26h |
| | 5 | C27 | GL 28c GL 28h |
| | 6 | | GL 30c GL 30h |
| | 7 | | GL 32c GL 32h |

| NEN-EN 1995-1-1, 2.4.1, table 2.3 | | |
|-----------------------------------|----------------------------|----------|
| Materials | Partial factors γ_m | Kolom1 |
| Solid timber | 1,30 | EN 14081 |
| Glued Laminated Timber | 1,25 | EN 14080 |
| Connections | 1,30 | |

| NEN-EN 1995-1-1, 3.1.3, tabel 3.1 | | K_{mod} | | | | | | |
|-----------------------------------|----------|---------------|---------------|-----------|------------|------------|------------|-----------------------------------|
| K_{mod} | Standard | Service class | Permanent aci | Long term | Medium ter | Short term | Instantane | Standard2 |
| Solid timber | EN 14081 | 1 | 0,60 | 0,70 | 0,80 | 0,90 | 1,10 | Solid timber-EN 14081-1 |
| Solid timber | EN 14081 | 2 | 0,60 | 0,70 | 0,80 | 0,90 | 1,10 | Solid timber-EN 14081-2 |
| Solid timber | EN 14081 | 3 | 0,50 | 0,55 | 0,65 | 0,70 | 0,90 | Solid timber-EN 14081-3 |
| Glued Laminated Timber | EN 14080 | 1 | 0,60 | 0,70 | 0,80 | 0,90 | 1,10 | Glued Laminated Timber-EN 14080-1 |
| Glued Laminated Timber | EN 14080 | 2 | 0,60 | 0,70 | 0,80 | 0,90 | 1,10 | Glued Laminated Timber-EN 14080-2 |
| Glued Laminated Timber | EN 14080 | 3 | 0,50 | 0,55 | 0,65 | 0,70 | 0,90 | Glued Laminated Timber-EN 14080-3 |

| NEN-EN 1995-1-1, 3.4, tabel 3.2 | | K_{def} | |
|---------------------------------|---------------|-----------|--|
| Standard | Service class | Kdef2 | Standard2 |
| Solid timber | EN 14081 | 1 | 0,60 Solid timber-EN 14081-1 |
| Solid timber | EN 14081 | 2 | 0,80 Solid timber-EN 14081-2 |
| Solid timber | EN 14081 | 3 | 2,00 Solid timber-EN 14081-3 |
| Glued Laminated Timber | EN 14080 | 1 | 0,60 Glued Laminated Timber-EN 14080-1 |
| Glued Laminated Timber | EN 14080 | 2 | 0,80 Glued Laminated Timber-EN 14080-2 |
| Glued Laminated Timber | EN 14080 | 3 | 2,00 Glued Laminated Timber-EN 14080-3 |

Figure F.1: Tables NEN-1990 and 1995

Combined strength table NEN-EN 338 / NEN-EN 14080

| Strength class | Strength classes for softwood based on edgewise bending tests - strength, stiffness and density values | | | | | | | Rolling shear |
|------------------------------|--|------------------|-------------------|----------------------|---------------------------|-------------|-------------|---------------|
| | Bending | Tension parallel | Tension parallel2 | Compression parallel | Compression perpendicular | Shear | | |
| NEN-EN 338, table 1 | | | | | | | | |
| | $f_{m,k}$ | $f_{t,0,k}$ | $f_{t,90,k}$ | $f_{c,0,k}$ | $f_{c,90,k}$ | $f_{v,k}$ | - | |
| C18 | 18,0 | 10,0 | 0,4 | 18,0 | 2,2 | 3,4 | - | |
| C20 | 20,0 | 11,5 | 0,4 | 19,0 | 2,3 | 3,6 | - | |
| C22 | 22,0 | 13,0 | 0,4 | 20,0 | 2,4 | 3,8 | - | |
| C24 | 24,0 | 14,5 | 0,4 | 21,0 | 2,5 | 4,0 | - | |
| C27 | 27,0 | 16,5 | 0,4 | 22,0 | 2,5 | 4,0 | - | |
| NEN-EN 14080, table 4 | | | | | | | | |
| | $f_{m,k}$ | $f_{t,0,k}$ | $f_{t,90,k}$ | $f_{c,0,k}$ | $f_{c,90,k}$ | $f_{v,0,k}$ | $f_{r,0,k}$ | |
| GL 20c | 20,0 | 15,0 | 0,5 | 18,5 | 2,5 | 3,5 | 1,2 | |
| GL 22c | 22,0 | 16,0 | 0,5 | 20,0 | 2,5 | 3,5 | 1,2 | |
| GL 24c | 24,0 | 17,0 | 0,5 | 21,5 | 2,5 | 3,5 | 1,2 | |
| GL 26c | 26,0 | 19,0 | 0,5 | 23,5 | 2,5 | 3,5 | 1,2 | |
| GL 28c | 28,0 | 19,5 | 0,5 | 24,0 | 2,5 | 3,5 | 1,2 | |
| GL 30c | 30,0 | 19,5 | 0,5 | 24,5 | 2,5 | 3,5 | 1,2 | |
| GL 32c | 32,0 | 19,5 | 0,5 | 24,5 | 2,5 | 3,5 | 1,2 | |
| NEN-EN 14080, table 5 | | | | | | | | |
| | $f_{m,k}$ | $f_{t,0,k}$ | $f_{t,90,k}$ | $f_{c,0,k}$ | $f_{c,90,k}$ | $f_{v,0,k}$ | $f_{r,0,k}$ | |
| GL 20h | 20,0 | 16,0 | 0,5 | 20,0 | 2,5 | 3,5 | 1,2 | |
| GL 22h | 22,0 | 17,6 | 0,5 | 22,0 | 2,5 | 3,5 | 1,2 | |
| GL 24h | 24,0 | 19,2 | 0,5 | 24,0 | 2,5 | 3,5 | 1,2 | |
| GL 26h | 26,0 | 20,8 | 0,5 | 26,0 | 2,5 | 3,5 | 1,2 | |
| GL 28h | 28,0 | 22,3 | 0,5 | 28,0 | 2,5 | 3,5 | 1,2 | |
| GL 30h | 30,0 | 24,0 | 0,5 | 30,0 | 2,5 | 3,5 | 1,2 | |
| GL 32h | 32,0 | 25,6 | 0,5 | 32,0 | 2,5 | 3,5 | 1,2 | |

| Mean modulus of elasticity parallel | 5 percent modulus of elasticity parallel | Mean modulus of elasticity perpendicular | 5 percent modulus of elasticity perpendicular | Mean shear modulus | 5 percent of shear modulus | Mean rolling shear modulus | 5 percent rolling shear modulus | Mean density | 5 percent density |
|-------------------------------------|--|--|---|--------------------|----------------------------|----------------------------|---------------------------------|-----------------|-------------------|
| $E_{m,0,mean}$ | $E_{m,0,k}$ | $E_{m,90,mean}$ | - | G_{mean} | G_k | - | - | ρ_{mean} | ρ_k |
| 9000 | 6000 | 300 | - | 560 | 380 | - | - | 380 | 320 |
| 9500 | 6400 | 320 | - | 590 | 400 | - | - | 400 | 330 |
| 10000 | 6700 | 330 | - | 630 | 420 | - | - | 410 | 340 |
| 11000 | 7400 | 370 | - | 690 | 460 | - | - | 420 | 350 |
| 11500 | 7700 | 380 | - | 720 | 480 | - | - | 430 | 360 |
| $E_{m,0,mean}$ | $E_{0,0,05}$ | $E_{90,0,mean}$ | $E_{90,0,05}$ | $G_{g,mean}$ | $G_{g,05}$ | $G_{r,g,mean}$ | $G_{r,g,05}$ | $\rho_{g,mean}$ | $\rho_{g,k}$ |
| 10400 | 8600 | 300 | 250 | 650 | 540 | 65 | 54 | 390 | 355 |
| 10400 | 8600 | 300 | 250 | 650 | 540 | 65 | 54 | 390 | 355 |
| 11000 | 9100 | 300 | 250 | 650 | 540 | 65 | 54 | 400 | 365 |
| 12000 | 10000 | 300 | 250 | 650 | 540 | 65 | 54 | 420 | 385 |
| 12500 | 10400 | 300 | 250 | 650 | 540 | 65 | 54 | 420 | 390 |
| 13000 | 10800 | 300 | 250 | 650 | 540 | 65 | 54 | 430 | 390 |
| 13500 | 11200 | 300 | 250 | 650 | 540 | 65 | 54 | 440 | 400 |
| $E_{m,0,mean}$ | $E_{0,0,05}$ | $E_{90,0,mean}$ | $E_{90,0,05}$ | $G_{a,mean}$ | $G_{a,05}$ | $G_{r,a,mean}$ | $G_{r,a,05}$ | $\rho_{a,mean}$ | $\rho_{a,k}$ |
| 8400 | 7000 | 300 | 250 | 650 | 540 | 65 | 54 | 370 | 340 |
| 10500 | 8800 | 300 | 250 | 650 | 540 | 65 | 54 | 410 | 370 |
| 11500 | 9600 | 300 | 250 | 650 | 540 | 65 | 54 | 420 | 385 |
| 12100 | 10100 | 300 | 250 | 650 | 540 | 65 | 54 | 445 | 405 |
| 12600 | 10500 | 300 | 250 | 650 | 540 | 65 | 54 | 460 | 425 |
| 13600 | 11300 | 300 | 250 | 650 | 540 | 65 | 54 | 480 | 430 |
| 14200 | 11800 | 300 | 250 | 650 | 540 | 65 | 54 | 490 | 440 |

Figure F.2: Tabels NEN-1990 and 1995

